HIFI AOT Observing Mode Release and Performance Notes

Abstract

This document summarizes the performances of the HIFI Observing Modes leading up to and following their formal commissioning and release for scheduling. The results are based on analysis of AOT test mode observations and engineering tests carried out over the Performance Verification and Routine Phases on redundant HIFI subsystems.

Document approval

Prepared by: P. Morris

Checked by: M. Olberg, V. Ossenkopf

Authorized by: P. Roelfsema, R. Shipman

Distribution

   ESA

                                 Herschel Science Centre

   HIFI steering committee

                                 F. Helmich
                                 P. Roelfsema
                                 R. Shipman
                                 T. Phillips
                                 E. Caux
                                 J. Stutzki
                                 X. Tielens

   HIFI Project Office

                                 F. Flederus

   HIFI Calibration Group

   HIFI ICC

Revision history

Version	Date	Changes	Author
Draft	24/02/2010	First version for DBS mode readiness review with HSC.	PM
1.0	08/03/2010	Updates and revisions with HIFI ICC inputs	PM
1.1	05/04/2010	Merged DBS and Point non-DBS mode release notes	PM
1.2	07/04/2010	Integrated inputs from calibration team: A. Boogert, C. Borys, W. Jellema, C. McCoey, F. Herpin, J. Braine, S. Lord, V. Ossenkopf, M. Olberg, D. Teyssier, C. Risacher, I. Avruch	PM
2.0	10/04/2010	Minor edits, updates to noise figure M. Olberg, Tsys figures D. Teyssier. Release version to HSC.	PM
3.0	08/09/2011	Revision of document from "Release Notes" to reflect many performance results updates, all sections cleaned up, some structural re-organization, many ICC inputs: I. Avruch, S. Beaulieu, A. Boogert, C. Borys, J. Braine, C. McCoey, M. Olberg, V. Ossenkopf, D. Teyssier.	PM

Contents

Reference Documents

1. "In-Orbit Performance of Herschel-HIFI", Roelfsema, P., et al., 2011 A&A, in press.
2. HIFI AOT Release Notes, version 2.0 (April 2010), HIFI-ICC 2010/009.
3. HIFI PV Calibration Data Release Explanatory Note, HIFI-ICC v1.0 (03 May 2011)
4. HIFI User Reference Manual (HIFI-URM), latest version linked into
5. Higgins, R., "Advanced Optical Calibration of the Herschel HIFI Heterodyne Spectrometer", 2011 PhD Thesis, NUI Maynooth, Chapter 3 (http://bit.ly/thesisRonanHiggins)
6. "Calibration Impact of HIFI Optical Standing Waves", Technical Note SRON-G/HIFI/TR/2011-0xx.
7. HIFI Observer's Manual, HERSCHEL-HSC-DOC-0784 (version 2.4 for OT2)
8. The stability of spectroscopic instruments: a unified Allan variance computation scheme", Ossenkopf, V., 2008 A&A 479, 915

Documents listed above may be downloaded from
http://herschel.esac.esa.int/twiki/bin/view/Public/HifiCalibrationWeb

1. Scope

This document summarizes the performances of all HIFI Observing Modes which have been offered in HSpot, with the goal of providing the Astronomer with essential information about the manner in which observations have been carried out in conjunction with performances which have been learned about the real instrument and telescope, and on the resulting data qualities which may be relevant to scientific interpretations.

Instrument performance items which directly affect the data quality of certain modes or all modes are discussed but the reader may find more information on specific topics on HIFI's Calibration Web (http://herschel.esac.esa.int/twiki/bin/view/Public/HifiCalibrationWeb), which includes a link to this document and the HIFI Inflight Performance paper in A&A (RD-1). Data qualities are also subject to the state of calibrations, pipeline processing and interactive analysis methods; the environments and versions of these are included with the Observing Mode performance descriptions.

This document incorporates information which was written into the HIFI AOT Release Notes (RD-2), as well as HIFI Information Notes on the HSC's website concerning key calibration updates and specific effects in the Observing Modes that the User should be aware of (see the above link to the HIFI Calibration Web). The AOT Release Notes were written in association with the Observing Mode release timeline of AORs to the HSC's scheduling pool, and should be considered superseded by the current document.

A brief Release Note accompanying the public release to the HSA of calibration observations carried out with the standard (non-engineering) modes for AOT commissioning and performance characterizations is found in RD-3.

The intended audience of this document is the HIFI Astronomical User Community.

2. Introduction

As a consequence of the interruption to AOT testing at an early stage following the Single Event Upset (SEU) experienced by HIFI on August 3rd 2009 (OD 81) and the necessity to switch to redundant-side electronics, the nominal AOT commissioning strategy was revised from an essentially parallel scheme of Observing Mode validation to one which serially emphasized the most requested modes in the Key Programmes, under the spectre of a potentially limited instrument lifetime and sudden termination of operations. This would accelerate the release of the modes according to their subscription. Some iterations between the HIFI PI, the HIFI Proejct Scientist, KP PIs, and the AOT test team were required in

Table 1: AOT mode summary. Numbers refer to the group of modes that were reviewed and released together for science scheduling, discussed in Sec. 4.

Reference scheme	AOT		
	Single Point	*Mapping[c]*	*Spectral Scanning*
Position Switch	2	OTF: 3	N/A
Dual Beam Switch[a]	1	DBS Raster: 1	1
Frequency Switch[b]	2	OTF: 3	2
Load Chop[b]	2	OTF: 3	2

Notes:
  a. The Dual Beam Switch (DBS) modes with all three AOTs are available in either a normal or fast chop rate, and with optional continuum stabilization.
  b. Frequency Switch (Frequency Switch) and Load Chop (Load Chop) modes with all three AOTs have the option for a position-switched sky reference measurement for optimum standing wave correction.
  c. Maps with either DBS/FastDBS or On-the-Fly modes are available with Nyquist or lower sampling.

conjunction with the formulation of the HIFI Priority Science Programs (PSPs) and an accelerated re-commissioning phase (aka COP-II) to establish hardware status and fundamental operating procedures which had not been completed prior to the August 2009 SEU.   A positive note was added by access to more suitable celestial sources such as Orion and the Galactic Center and other prolific and heavily subscribed KP targets when AOT testing resumed in February 2010. However, the benefit of short-term feedback loops to help identify unexpected features or unresolved operations which are common between modes had to be missed in the serial validation scheme as an acceptable risk in favour of achieving highest priority (PSP-I/II) science observations.

After the initial release of all Observing Modes requested in the KPs (summarized in Table 1), the HIFI-ICC continues to characterize performances into the Routine Phase, incorporating experience with instrument purity and stability, updates to the calibrations of the mixer beams, characterization of the standing waves and their effects on observations by mode, and maturing software systems. For the remainder of this document, we attempt to concisely summarize these evaluations in the framework of the AOTs.

Table 1 provides an overview of the HIFI AOTs and modes of observing along with initial release group number.

3. Mode Release Summary

Observing Modes were released in groups following initial validations and readiness reviews by the HIFI ICC and between the HIFI ICC and the HSC. A summary of the releases along with caveats or conditions on mode usage which have been recommended to HIFI Users follows below in this section. The background for the caveats is discussed in later sections.

Referring to the group numbers in Table 1:

1. DBS Observing Modes, all AOTs.

   DBS observing modes have been released in each of the Point, Mapping, and Spectral Scan AOTs for carrying out observations starting February 28, 2010 (effective OD 291).   The prioritization of the DBS modes to be released together first has been driven by subscription by the HIFI PSPs and maturation of the modes over various ground-based and COP-I (first light) and PV-I test campaigns. However, additional validations and revisions to the DBS Raster spectral mapping modes were later carried out in conjunction with OTF map readiness testing.

   ● Results from comparing performances of the normal (or slow) chop DBS with FastDBS modes indicate that the latter generally perform better with respect to correction for electrical standing waves in Bands 6 and 7. This will be explained further below.   The recommendation is to use FastDBS in the HEB bands.

   ● Prior to OD 419, DBS/FastDBS mapping observations which requested Nyquist sampling use a definition in which the spacing between sample points is 0.5 times the Half Power Beam Width (HPBW/2.0). After OD 419, the Nyquist spacing was changed to HPBW/2.4.

   ● AORs which use DBS/FastDBS-Cross mapping modes have been on hold over much of the science phase of the mission due to a complex command timing issue in the interactions between the AOT logic and instrument onboard software that can manifest itself in the pipeline as an asyncronicity of the ON/OFF phases, turning emission lines into absorption lines or vice versa. The data quality is generally unaffected, and the problem is not systematic, however identification of affected observations and a workaround of the phase switch in the pipeline are not straightforward. Due to this maintenance issue and relatively low subscription, the modes are no longer offered in HSpot after version 6.0 in OT1 or OT2.

2. Point AOT with Position Switch, Frequency Switch and Load Chop.
   Spectral Scan AOT with Frequency Switch and Load Chop.

   Remaining Point AOT observing modes, namely Position Switch, Frequency Switch and Load Chop, as well as the Spectral Scans using Frequency Switch and Load Chop, have been released for scheduling AORs using these modes starting April 29, 2010 (effective on OD 330).

   ● The Frequency Switch mode is available in all LO bands with the Point AOT, but it is discouraged in Bands 6 and 7 due to indications of poor stability, mainly in difficulty of stabilizing the LOs at the frequency throw in reasonable times under

the constraint of generally very short Allan times, and occasional unstable pairings of the reference measurements after retuning when mixer currents are drifting without invoking long wait times. The lack of stabilization can be manifest in data terms of baseline shapes or drifts, ripples, and artefacts that may not be treatable in interactive data processing, such that S/N goals set by the User in HSpot can ever be achieved, and may thus compromise the intended science goals.   The general recommendation is to use the Load Chop mode in the HEB bands, when the DBS modes cannot be used due to source size.

- In Spectral Scans the Frequency Switch mode has been discontinued in Bands 6 and 7, due to the stability problems mentioned above. Invoking longer wait times is technically possible but makes the mode too inefficient to be usable.

- The Frequency Switch and Load Chop modes are recommended to be used only with the sky reference option to obtain a spectrum at a User-selected line-free region (within 2 degrees of the science target) for standing wave correction in the pipeline. This is especially true for the diplexer SIS Bands 3 and 4 and HEB Bands 6 and 7, in which the standing waves are not accurately fit by one or two sine waves of constant amplitude and period.   Only if the User expects very strong lines and is not concerned by the standing wave pattern in the surrounding baseline, or expects to be able to fit out the standing waves in IA when the lines are narrow, should the "no reference" option be considered.

3. <u>OTF modes (normal, Frequency Switch, Load Chop) of the Mapping AOT.</u>

   The OTF mapping modes have been released on July 28, 2010 (effective on OD 441), which includes standard OTF (with position switch) and OTF using Frequency Switch or Load Chop.

   - OTF with Frequency Switch in Bands 6 and 7 is discontinued in HSpot for reasons of poor stability as described above. The exception for OTF with Frequency Switching is over a range of LO frequencies 1890 – 1898 GHz which has been optimized for stability and purity in the area of the C^+ 1900.54 GHz line.

   - As with the Point and Spectral Scan AOTs which use the Frequency Switch or Load Chop modes, the reference sky option to obtain a (preferably) line-free spectrum for optimum standing wave correction in the pipeline is recommended with OTF maps that use these modes. This is especially true for the diplexer SIS Bands 3 and 4 and HEB Bands 6 and 7 (where permitted with Frequency Switch in HSpot), in which the standing waves are not accurately fit by one or two sine waves of constant amplitude and period.   Only if the User expects very strong lines (peaking well above the amplitude of the HEB waves; see Sec. 7.2) and is not concerned by the standing wave pattern in the surrounding baseline, or expects to be able to fit out the standing waves in IA when the lines are narrow compared to the period of the ripple (see Sec. 7.2), should the "no reference" option be considered. It is difficult to provide strict criteria since these depend on the how the observation has been carried out (in terms of baseline noise requirements) but generally a line less than several K peak intensity and broader than ~50 MHz FWHM in Band 6 or 7 may be swamped by either of the 300 MHz electrical or (generally weaker) 98 GHz optical standing waves.

- Prior to OD 419, OTF mapping observations which requested Nyquist sampling with any mode use a definition in which the spacing between sample points is 0.5 times the Half Power Beam Width (HPBW/2.0). After OD 419, the Nyquist spacing was changed to HPBW/2.4.

- Due to a form of timing "jitter" between instrument and telescope pointing commands, all OTF maps are subject to a "zig-zag" pattern of the scan legs. The size of the effect depends on several factors such as requested sampling, readout times and telescope scan speed, and may not be very noticeable in many observations. One additional readout along the scan legs is added after OD 419 to compensate for this effect so that Users obtain the expected sampling up to the requested map dimensions.

4. General Caveats and Conditions on All Observing Modes

4.1 Spectral Purity

There are several frequencies in HIFI where the Local Oscillator has been shown to produce more than one frequency. In these cases, an observed spectrum will have some or all of the features from a different unknown (and possibly unstable) other frequency. When this is the case the mixer gain at the desired frequency will be unknown and it will not usually be possible to calibrate the flux accurately. Most of the impure regions were fixed in the ILT, TV/TB and CoP test campaigns; however, several frequencies remain to be addressed or cannot be addressed due to hardware safety considerations. The known impure frequencies include:

- **Band 1a**: For data taken before OD474, LO frequencies above 550 GHz (extreme upper end of tuning range).

- **Band 2a**: LO frequencies above 714 GHz (extreme upper end of tuning range).

- **Band 3b**: LO frequencies near (±1 GHz) 941 and 952 GHz.

- **Band 4b**: LO frequencies above 1114 GHz (extreme upper end of tuning range).

- **Band 5a**: LO frequencies near (±2 GHz) 1135 GHz. For data taken before OD642, there is also a known issue around (±2 GHz) 1206 GHz.

- **Band 5b**: LO frequencies below 1236 GHz and around (±1 GHz) 1255 GHz.

- **Band 7a:** LO frequencies between 1755 and 1759 GHz.

- **Band7b:** Currently there are no known remaining purity issues, but Users should be aware that tunings at LO frequencies above 1899.8 GHz suffer from a sensitivity degradation by about a factor 2 (due to unavoidable mixer over-pumping). For most sources, this should be far enough for tunings targeting the C+ line, where robust tuning is now achieved in most cases. Users should however be aware that the tuning success in the upper end of band 7b can be influenced by the chain

thermalization history, and the exact targeted LO frequency. So there could still be observations that will not benefit from the best sensitivity, usually rendering the scientific data very difficult to exploit.

The scheduling implications are summarized as follows:

- Spectral Scans in Bands 3b, 4b and 5a may be carried out as planned, and Users are recommended to inspect and possibly discard the spectra taken at the unruly LO frequencies. This will imply some noise degradation after the spectrum deconvolution.

- For Spectral Scans in Band 7a, the User is advised to split the frequency coverage into at least two AORs which avoid the impure areas. As a consequence there will be a slight penalty due to the slew time tax charged at each AOR, and the (temporary) degradation of the achieved noise at the edges of the deconvolved spectra due to a coarser redundancy. Once the LO purity has been satisfactorily established, the excluded regions can be scanned if needed. Presently this means that LO tunings only over the following ranges are advised:

    o   Band 7a: [1701.2 – 1755] and [1759 – 1793.8] GHz

    [Note: Several SDP and PSP1 AORs in Band 7a have been carried out over the impure ranges, prior to the preparation of this Release Note].

- For observations in Band 7b requesting LO frequencies > 1899.8 GHz, there are currently no scheduling restrictions, but Users must be aware of the lower performances that can result from the tuning issues described above.

- For single frequencies (in AORs using the Point and Map AOTs) whenever possible, the main lines of interest should be moved into the image bands if the new LO frequency falls in an area not affected by purity issues. Otherwise, it is probably wise to put the observations on hold until the chain is fixed in the targeted frequency area. [Note: this will not have been possible for the very early SDP and PSP1 AORs which had to be scheduled prior to the preparation of this Release Note].

4.2 HIFI tuning ranges

In addition to certain known impure frequencies (see Sec. 4.1), the various HIFI LO chains have frequency ranges over which they cannot provide adequate output power to sufficiently pump the mixers. The receiver noise temperature is very high in these ranges. Unlike the purity issues, however, there is little improvement to be expected on the short term so these areas must be considered as regions of low performance, over the spectral coverage currently achievable by HIFI.

While the border between sensitive and non-sensitive ranges is not abrupt and the noise degradation is often gradual, the band edges are defined and set in HSpot to avoid frequencies where the mixers are not even marginally pumped. Between the formal (HSpot) band limits, Users are able to recognize LO frequencies which offer lower performances from the output of time estimation in HSpot: at the requested LO frequency (Point and Map AOTs), the noise temperature is quoted in the Message window. The effect of higher noise temperature is to increase the observing time at a

fixed noise goal (entered by the User), or conversely to reduce the S/N ratio at a fixed observing time goal. It is always worthwhile for the User to attempt to find a setting which minimizes the noise, where some flexibility is allowed in the IF placement of the spectral line(s) of interest. Note that most system temperatures have been measured to a granularity of ~2 GHz, and therefore only significant differences may be noticed when changing the LO frequency that switches the target line(s) from one image band to the other.

The plots below illustrate the overall distribution of the receiver noise temperatures as measured in flight. All temperatures are the median DSB receiver temperatures over the full WBS bandwidth, in K. Frequencies are in GHz.

As can be seen from the plots, there are two types of poor sensitivity ranges:

- Those with a marginally, but still pumped mixer. They show up as receiver temperatures of the order of 2-3 times the average temperatures. Those frequency areas are considered in the range offered in HSpot, and will be scanned through during spectral scan, usually with an integration time doubled compared with other frequencies.
- Those where the mixer cannot be pump at all. Such ranges at band edges have been cut off from the HSpot front-end frequency ranges so that no time is spent observing at those frequencies. When those holes occur in the middle of a band, they are still offered to the User, and will be scanned through during spectral scan, usually with an integration time doubled compared with other frequencies. However, at those frequencies, the data may have to be discarded for an optimum SSB deconvolution. Only Bands 1a, 4a, 4b and 6a are concerned by this situation. *It should also be noted that there can be sensitivity issues at the upper end of 7b (above 1899.8 GHz).* See the discussion of this in Sec. 4.

Sensitivity changes at the upper end of Band 1a:

As explained below in Sec. 4.3.1.1, an extensive engineering campaign has achieved the suppression of spurs almost everywhere in Band 1a. As a consequence, the sensitivity at the upper end of this band has slightly changed. In particular, the receiver noise temperature below 551.9 GHz has now improved and is better or similar to that at the lower end of band 1b (see plots below). Above this frequency (and up to 553.4 GHz), the sensitivity has degraded compared to what it was before. This leads to the following recommendations:

- Users targeting the ortho-water line at 556.9 GHz may want to consider Band 1a rather than band 1b (which was the recommended band when strong spurs were present in this frequency range) whenever it makes sense for their science. Users should however bear in mind that for target noise lower than typically a few tens of mK, Band 1b should be preferred (in terms of sensitivity at least) when the LO frequency is above 551.9 GHz. For higher noise RMS, the difference in time estimate for the two bands is negligible.
- The new receiver noise distribution over Band 1a has an influence on time and noise estimates for Full Spectral scans in that band. On the one hand the so-called reference frequency, providing the system noise temperature used to compute the noise RMS at each frequency step, will change and move to one featuring a better sensitivity. On the other hand, the number of frequencies considered to deserve double integration due to lower sensitivity has increased

(typically at the upper end of the band). Overall, the two effects counter-balance each other but depending on the redundancy and noise goals, the time estimates of Full Spectral Scans in band 1a may increase or decrease. One way for User to avoid any increase is to truncate the upper end to 551.9 GHz, which is the frequency at which the receiver noise temperature starts to significantly increase.
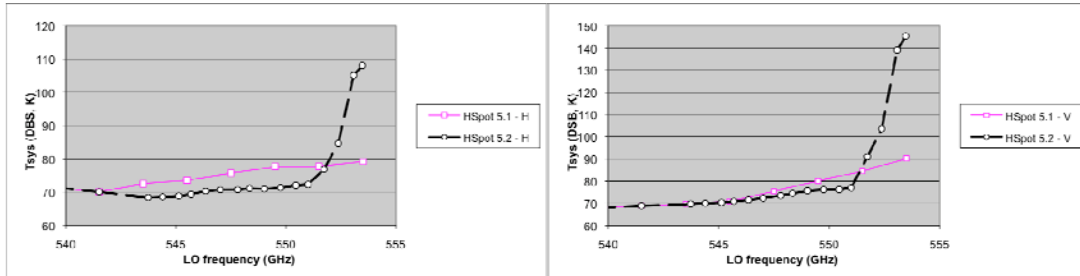

Figure 1: New DSB receiver temperature at the upper end of Band 1a (used in HSpot 5.2), compared to the earlier temperature curves (used in HSpot 5.1 and earlier).

Additionally, Users should be warned that the tunings in the 530-540 GHz LO frequency range of Band 1a are not completely reproducible, depending on the band thermalization history as well as which LO frequencies was tuned prior to observations in this range. This means that Users planning to perform partial Spectral Scans starting at a frequency close to this range should contact the helpdesk to check the current situation.
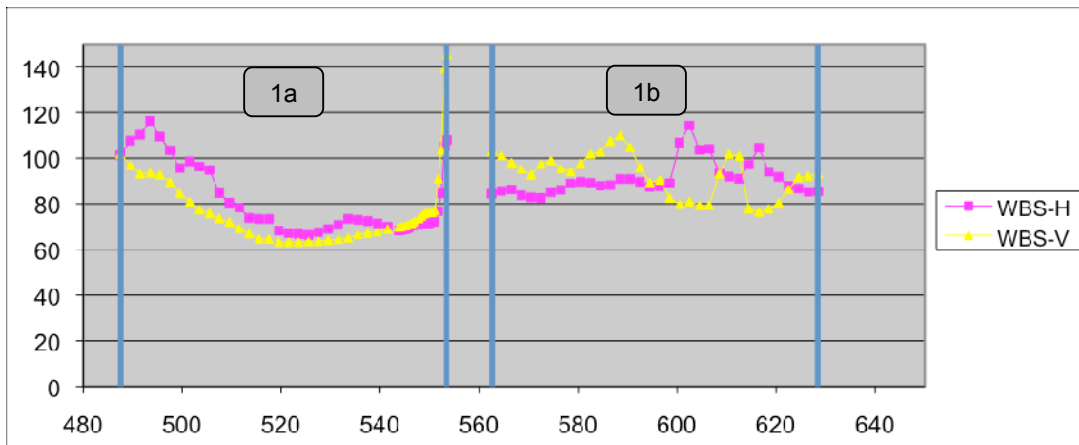

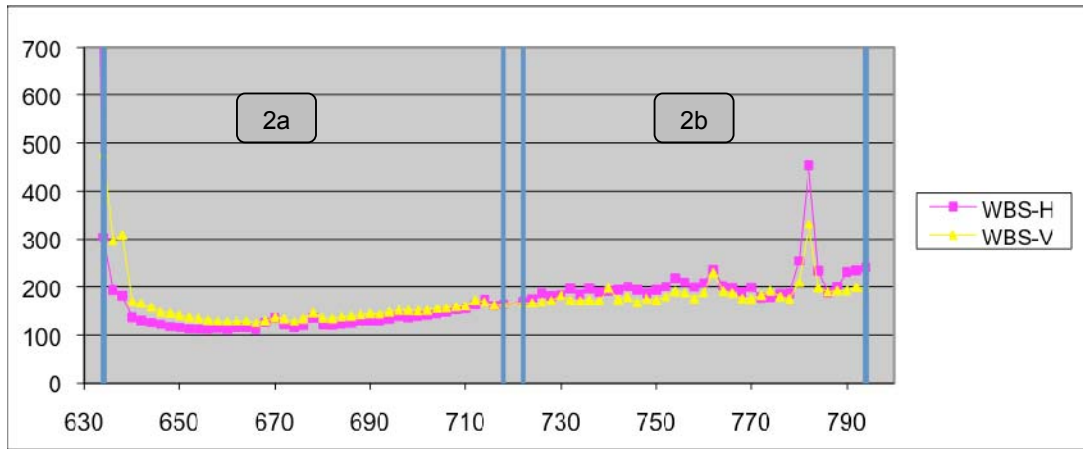*Figure 2: Band 1a/1b DSB receiver temperature distribution.*

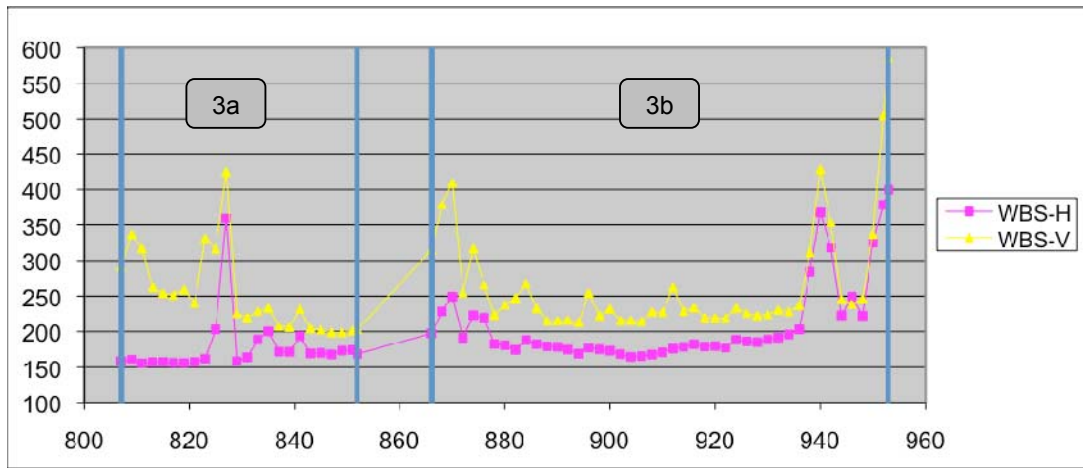*Figure 3: Band 2a/2b DSB receiver temperature distribution.*

Figure 4: Band 3a/3b DSB receiver temperature distribution.
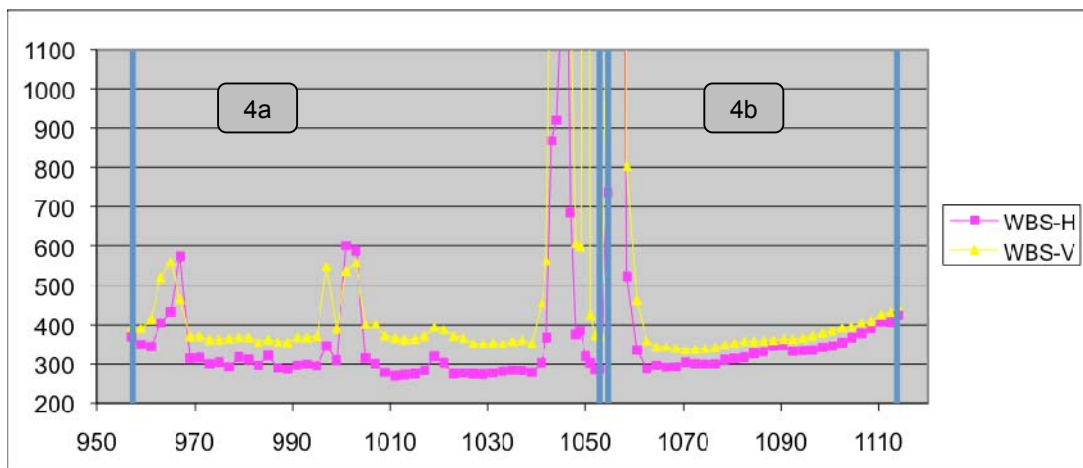

Figure 5: Band 4a/4b DSB receiver temperature distribution.
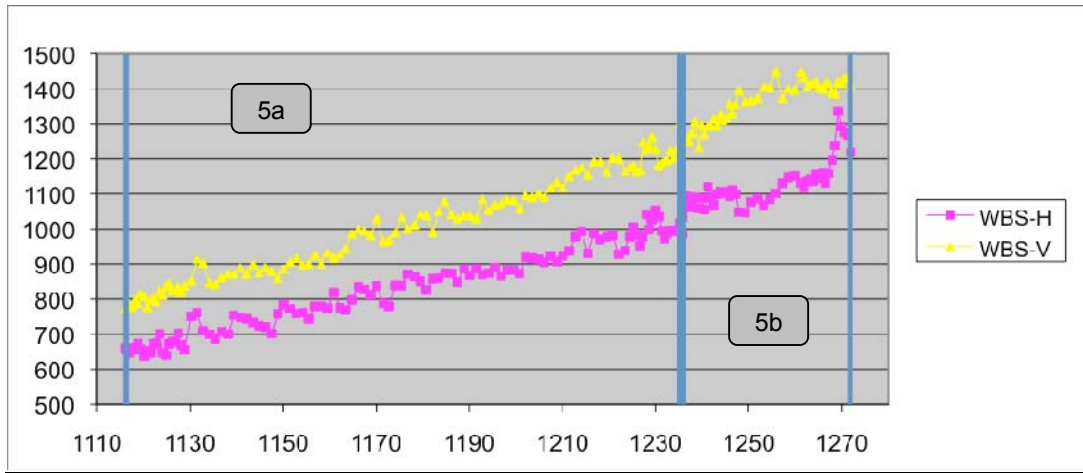
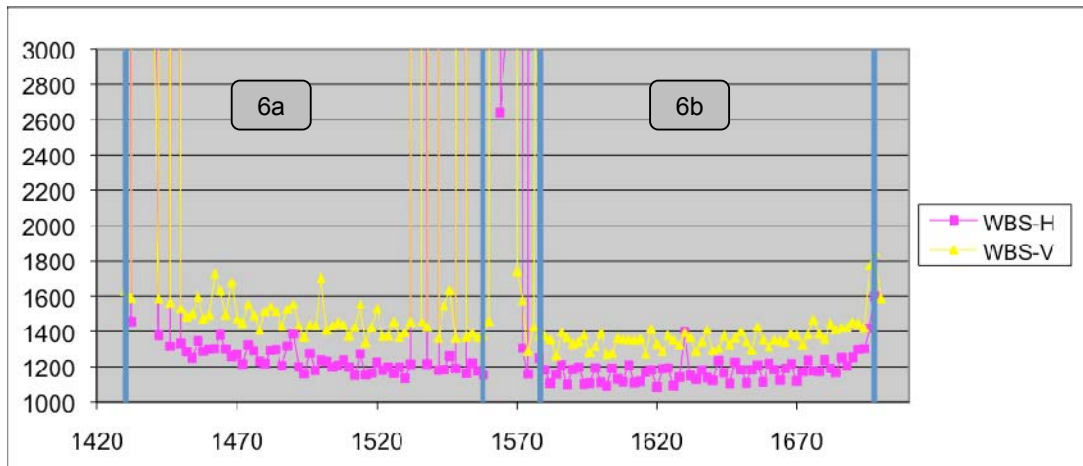*Figure 6: Band 5a/5b DSB receiver temperature distribution.*

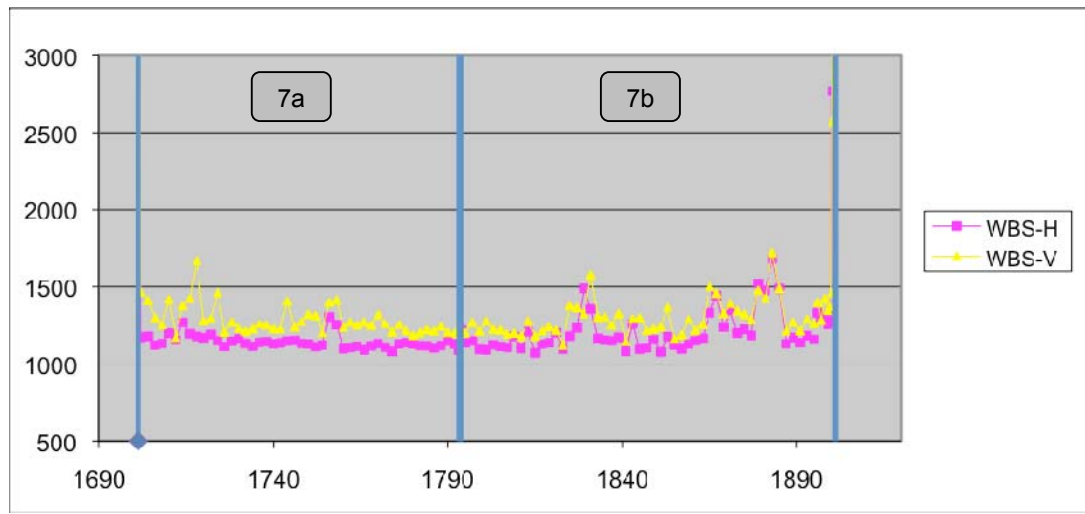*Figure 7: Band 6a/6b DSB receiver temperature distribution.*

Figure 8: Band 7a/7b DSB receiver temperature distribution.

4.3 Spurious Responses in HIFI

HIFI, like all heterodyne receivers, can respond to signal from unwanted frequencies, resulting in 'spurs' in the science data. There may be several causes of the spurs in the different bands and at different frequencies but often due to oscillations in one or more of the multipliers. When they can be tracked down and their severity assessed, corrective measures to multiplier bias settings (for example) can and have been taken. The effort to clean up the spurs is driven by the most problematic cases, such as where they can dramatically affect data quality around key spectral lines, but in general not all frequencies covered by HIFI can be cleansed due to the costs in manpower and observing time to carry out the engineering tests and implement reliable changes to the operation of the hardware.   This furthermore means that the AOTs will generally perform differently at frequencies where attenuations have occurred to the signal mixing process and resulting system temperatures, naturally producing a different balance between observing efficiencies and noise performances with the objective to arrive at overall improved quality of the calibrated science data.

Since spurs can significantly degrade the quality of spectra, and it has been prudent to track and catalogue these features in all HIFI data taken since pre-launch. This catalogue has been implemented in HSpot so Users can be warned if they tune the LO near the position of known spurs; see the example in Figure 9.
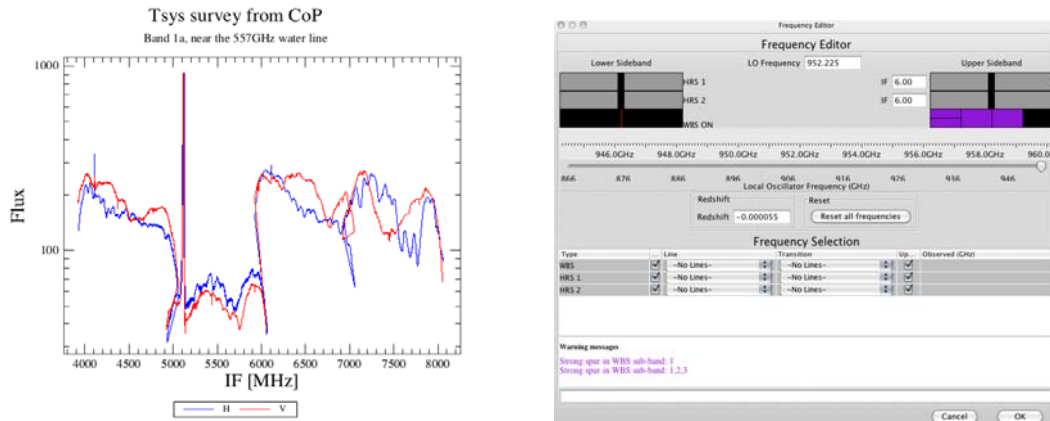
Figure 9: Data spurs and visualization in the HSpot observation planning system. On the left is the spectrum from the CoP Tsys survey of the Band 1a spur affecting observations of the H2O 110 – 101 557 GHz line through OD 495. On the right is the warning system for unruly LO frequencies, which has been implemented in HSpot since version 5.0 (in this example for spurs at the upper end of Band 4a).

4.3.1   Analysis of spurious responses in WBS data

In general spur positions and strengths have remained similar between the prime and redundant electronic sides, and across more than two years of data acquisition stretching back to pre-launch test activities and then on the redundant side.

The spurs that caused the enough concern to put primary emphasis on finding corrective settings for the instrument, have been the ones near important water lines in Bands 1a and 4b and other significant lines or over substantial impure portions of certain sub-bands such as 5b. As there is a time dependency of how data have been affected, a summary of the main spurs and current status follows.

4.3.1.1   Spurs in Band 1a

In data taken through OD 495, a strong spur has existed blueward of 548.7 GHz. This spur is very strong, saturating the detector and rendering the entire 4GHz passband generally unusable. Figure 9 shows the appearance of the spur in the hot and cold loads, which propagates into the science data following bandpass calibration in the pipeline. Unfortunately it can directly impact observations of the 557 GHz water line to the point of severely compromising the spectral profile and noise performances. There are very narrow (~500MHz) regions in LO tunings where the spur seems well behaved and a relatively clean spectrum is expected from observations which requested tunings in that narrow range; see the example in Figure 10. However it was not clear how stable this 'safe zone' was over time, and the HIFI ICC recommended that Users try to use the lower sideband of Band 1b if possible, until efforts to remove the spur could be implemented.

After an extensive engineering effort, hardware settings for Band 1a were adjusted to suppress this strong spur (effective OD 496) without causing an appreciable degradation of the system temperature. Some tradeoff was nonetheless expected, and a compromise has been made over the last ~2 GHz at the upper end of the band where

17

Tsys has increased in order to mitigate the strong spur; see Figure 1.   The sensitivity is better or similar than that in Band 1b for LO frequencies up to 551.9 GHz.

It should also be noted that a mild artifact remains at 542.378 GHz that occasionally impacts data in the first subband. We have recommended that Users wishing to use Band 1a with an LO tuning higher than 540 GHz contact the helpdesk if in doubt about the quality of the data in that range.

After removal of the strong spur, Users who used to Band 1b in order to observe the 557 GHz water line have been invited to reconsider using Band 1a if it makes sense for their program. For tunings above 551.9 GHz, the time penalty in using Band 1a rather than Band 1b depends on the requested noise level, but typically there is no significant difference down to noise RMS of some tens of mK.
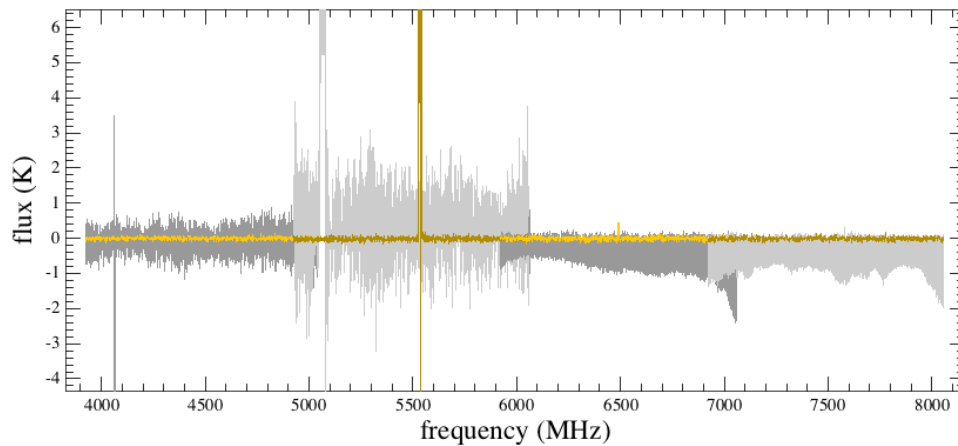
Figure 10: Spectra taken from 2 different LO tunings in Band 1a, prior to cleanup of the spur. The grey plot is from a tuning of 549.3 GHz and the spur wipes out not only subband 2 data in which it resides, but the entire spectra due to the crosstalk. At 550.4 GHz however (yellow trace), the spectrum is well behaved aside from the spur in the second subband.

4.3.1.2   Spurs in Band 4b

Through OD81, the H_2O $1_{11} - 0_{00}$ 1113 GHz line could be potentially corrupted by a spur that appeared between LO tunings of 1090 GHz and 1108 GHz. However unlike the 1a spur, this one was very weak and sometimes disappears altogether, likely due to changes in instrument temperature. An example is shown in Figure 11. The position of the spur in the IF as a function of LO is fit well by the following formula:
$$IF = 5064.9 - 44.3x - 0.6x^2$$

where $x = LO - 1090.498$ GHz

After OD81 the spur was effectively erased by adjustments to the multiplier settings, and thus the spur will be present only in early AOT calibration data that have been released to the public.

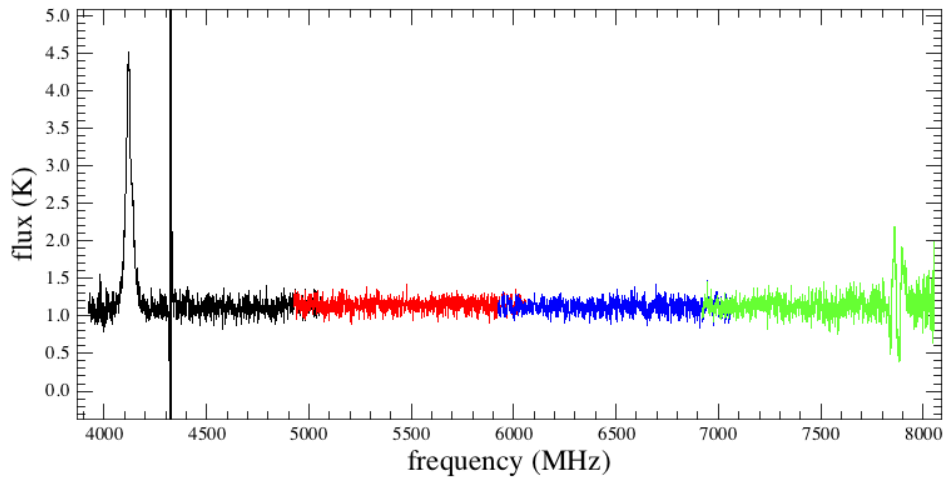*Figure 11: Though band 4b spurs are strong compared to real lines, they are very narrow and do not seem to affect the integrity of the spectra around them. This spectra was taken during PV at an LO setting of 1105.6 GHz.*

4.3.1.3   Spurs in Bands 5a and 5b

Bands 5a and especially 5b were known to be affected by spurs and spurious response since ground based testing, but could not be tested with different settings of the instrument before launch (since neither use diplexers). AORs which requested observations in 5b were on hold until corrective actions could be taken, involving several iterations on the multiplier biases and power settings. As of OD 595, and as mentioned in Sec. 4.1, spurs in Band 5a remain at LO frequencies near 1135 (±2 GHz) GHz. For data taken before OD 642, there is also a known issue around 1206 (±2 GHz) GHz. Currently in Band 5b which was released on OD 595, LO frequencies below 1236 GHz and around (±1 GHz) 1255 GHz can be affected by spurs.

4.3.1.4   Spurs in Band 7b

Efforts to purify the 1866 – 1888 GHz range and stabilize LO tuning in the vicinity of the C^+ 1900.5 GHz line have been successfully accomplished. The purifications took effect in OD 355 (prior to which the calibration errors may be much higher for data taken at LO tunings in the 1866 – 1888 GHz range). Robust LO tuning for C^+ observations took effect in OD377, prior to which not all data meet expected noise and spectral qualities due to higher system temperatures and distorted baselines.

There is one remaining region 1829 – 1838 GHz in Band 7b which remains to be cleansed of a peculiar spur that appears as a "kink" in Tsys data and is free-running (unstable in frequency), and has the potential to ruin observations of the OH line at 1837.837 GHz.   It is not easily detected by a spur detection routine used in the HIFI pipeline since it does not occur in single load spectra.   See Figure 12 for an example. Engineering tests to remove this instability are on-going.
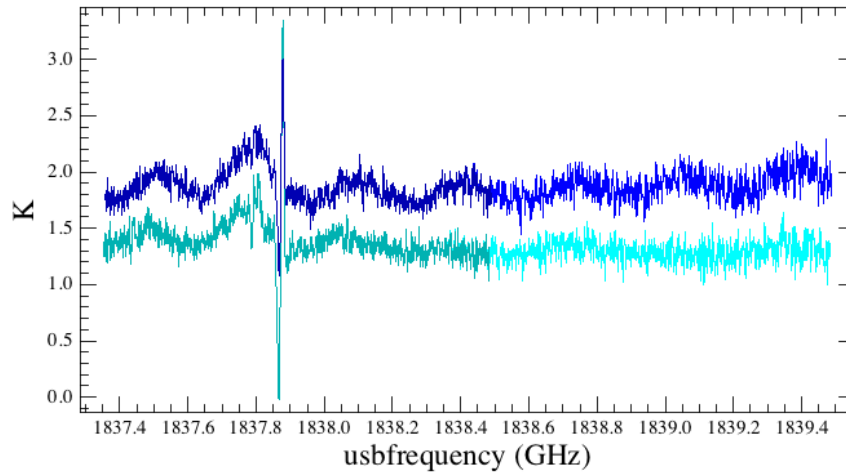
Figure 12: System temperature data from WBS-H (dark blue) and -V (light blue).

4.3.1.5   Spurs across other bands

For an inventory of problematic frequencies that include spurs, impurities, IF saturations, and poor LO settling, the User is referred to RD-3 (which is associated to the release of calibration observations which may be affected). The unruly frequencies in RD-3 are not all generally constant in time, but can apply to specific periods of time as a consequence of efforts to purify and stabilize specific frequency ranges. The latest list of problematic frequencies which should be used for observation planning and AOR updating can be accessed in HSpot.

At this writing, an approximate current inventory of the most problematic frequencies is provided below.   Note that the ranges could be as much as 2GHz wider on each side of a spur due to the resolution of the surveys from which these were determined. Users who need LO tunings for their science or have already acquired data in any of the affected ranges are encouraged to contact the helpdesk(s) for advice.

- 1a: Strong spur at 540.929 GHz
- 1b: Strong spur at 583.5-587.5
- 2a: Weak spurs at 692.0, 708.0-719.0 GHz.
- 2b: Strong spurs between 761.0-771.0 GHz and 775.0-787.0 GHz
- 3a: weak spur at 841.0 GHz.
- 3b: strong spur 951-954 GHz, saturated 867.6-877.0 and instabilities from 881.0-953.0
- 4a: no spurs, saturation/instability from 957.0-959.1 and 964.6-968.0 and 973-1008.0
- 4b: Settling issue 1050.9 and 1088.0. Spur from 1096.2-1100.1 and also within 1GHz of 10039.1
- 5a: weak spur and instability near 1134.5 GHz
- 5b: impurities near 1235.5 and 1135.0 GHz
- 6a: Instabilities exist at many LO tunings in this band
- 6b: Instability near 1700.0 GHz
- 7a: Instabilities exist at many LO tunings in this band
- 7b: Saturation near 1809.0 GHz, and a weak spur near 1831.5 and 1835.8 GHz
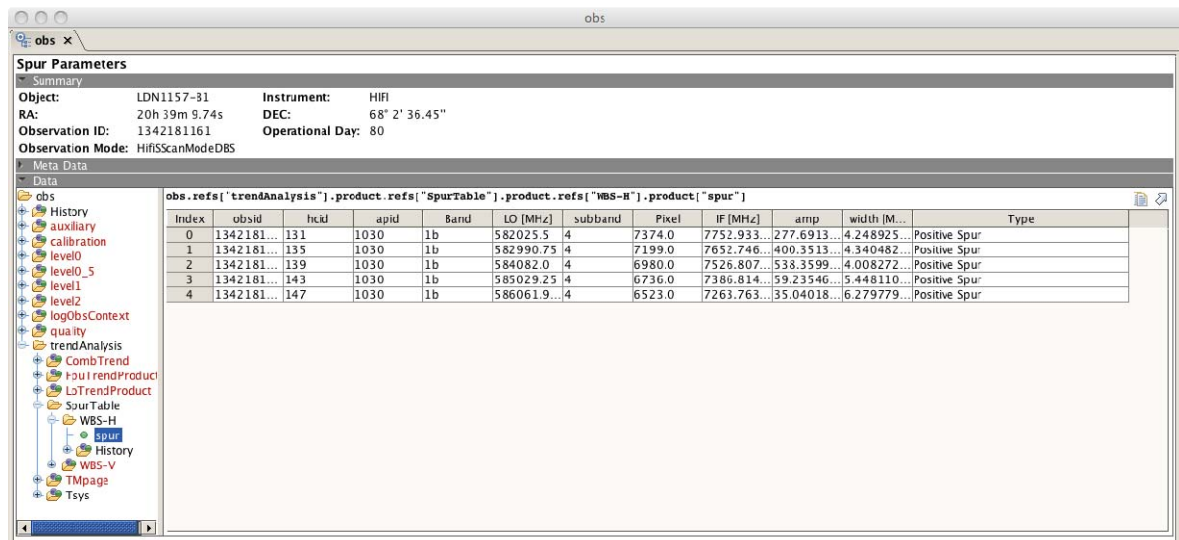
4.3.2   Spurious response in HRS

Spurs in WBS data do not correspond to spurs in HRS. While the investigation of HRS spurs has not yet been as detailed as in WBS, it is already clear that the spur in 1a for instance does not impact the HRS at all. Because spurs are most readily found in spectral surveys, and since HRS science data are only occasionally generated in spectral surveys, a full catalogueue of HRS spurs has been slower to generate. Nonetheless, spurs are routinely checked for in HRS data (in the cold load measurements) as part of the HIFI pipeline starting with HIPE 8.0, and are indicated in the LoTrendProduct for each observation (see Section 4.3.3).

4.3.3   Treating spurs in software

Two spur checking algorithms are used in the standard HIFI pipeline. The first compares the LO tuning of the observation against the master list of spurs and flags the entire spectrum as suspect if the tuning is in the range of an historically problematic area. This flag is not used in the pipeline, but serves only to warn the user that an issue may exist. For spectral surveys, the deconvolution tool can be told to honor it, and spectra will be ignored if so. The main spur finder actively inspects the data and looks at the loads to find spurious responses. If it does, it flags the channels as bad (refer to the chapter on "Flags in HIFI Data" in the HIFI Users Manual for flagging definitions) and adds an entry to the spur table found in the observation context. Specifically this can be called as a variable in HIPE as

obs.refs["trendAnalysis"].product.refs["SpurTable"].product.refs["WBS-H"].product["spur"], and this table can be viewed with the Dataset Viewer. An example is shown in Figure 13. This flag *is* used by the software to mask out the spur.

Figure 13: The Spur Table generated in the HIFI pipeline, associated with WBS-H data from an arbitrary Spectral Scan.

Generally speaking, the spur finder detects all spurs of moderate strength and above. For those that may be missed, one can either re-run the pipeline with more sensitive

spur finder parameters, or flag the channels manually using software within HIPE. Weak spurs in the loads can sometimes appear very strong in the final spectra. This occurs when slight deviations in the ordinarily smooth load spectra results in the loads being nearly the same intensity. The calibration equation has a step that involves dividing spectra by the difference of the hot and cold load, and when the difference is very small, the spectra will appear to be corrupted. In these cases, one can attempt to clean the load spectra, or flag it as bad if the affected region is not required.

For advice on data cleaning and spur management, the User is encouraged to contact one of the helpdesks (HSC or NHSC).   Some interactive scripting has been in development and provided with examples in the DP workshops, and at least advice if not updated versions of the scripts may be given to Users whose data would benefit.

5. Noise performances

Baseline noise properties are a key measure of how well the assumptions about instrument performance which go into time estimation in HSpot for each Observing Mode are matched with the real instrument.   This in turn establishes how well the goal signal-to-noise requirements set by the HIFI User are met, with strong dependencies on pipeline processing and certain higher level data reduction steps (such as data cleaning and sideband deconvolution of spectral scans). Below we summarize the measured noise performances vs those predicted in HSpot for the various modes, and point out effects which the User may find helpful when evaluating the quality of their data. The observations which are represented in the plots below are not filtered for [a small number] of AOT tests which used modes or AOR configurations in an un-recommended way as part of the definition or refinement the guidelines for best usage of the Observing Modes and sometimes exhibit not unexpectedly lower data quality.

The RMS noises have been measured taking into account the correct bandwidths (resolutions) as set in HSpot, the two polarizations (assumed to be combined), and the double-sideband format of HIFI data out of the pipeline. The measurements were performed a manner consistent with the mathematical tools currently available in HIPE, such as one might find with the statistics tool in the spectral tools package. For a large number of observations the RMS measurements have been scripted (getRMS.py) and occasionally the spectral content of the observations can influence the results (an example will be shown below). In general, Users should identify line-free regions of the baseline and smooth to the requested upper and lower resolutions when measuring and comparing noise values.

A final note concerns observations which have used Frequency Switch or Load Chop modes. It was noticed that data quality would be improved by switching the order of the frequency calibration and reference subtraction steps (see Figure 14) to best remove the spikes in WBS-V data caused by imperfections on the CCD, and this has been implemented starting HIPE 6.0. Thus noise measures of observations using these modes in the figures in Sections 5.3 and 5.4 (generated prior to HIPE 6.0) may be on the pessimistic side in some cases.
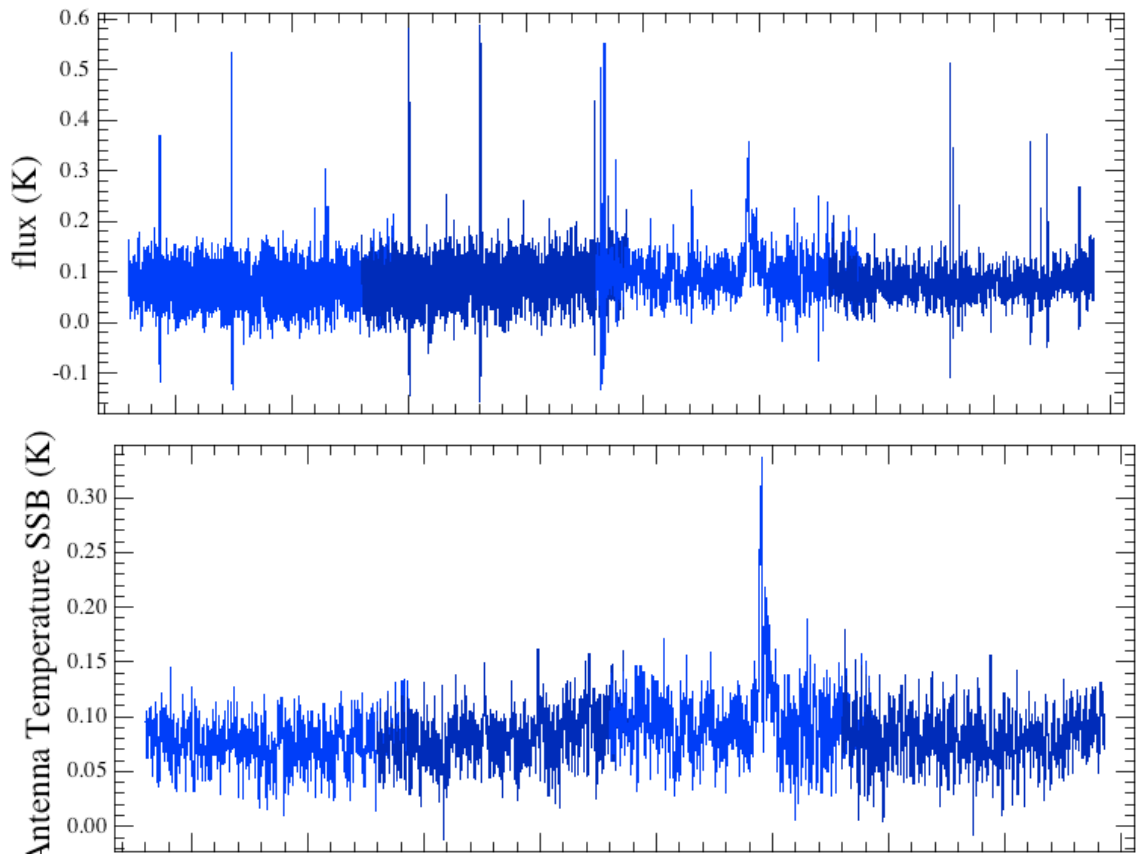
Figure 14: WBS-V data showing calibrated data before (top) and after (bottom) changing the order of the frequency calibration and reference subtraction in the pipeline.

5.1 Composition

The observations analyzed for *Figure 16* and Figure *17* come from AOT checkout tests in PV-2 using the standard observing modes which could be planned in HSpot under the operational version of the AOT logic, calibration or configuration tables, and instrument operating procedures. Many observations taken in AOT checkout are part of a block, for example to evaluate the efficiency and calibration accuracy tradeoffs in certain bands with FastDBS versus normal DBS mode with overlapping ranges of chop rates, with and without continuum timing. Such blocks of tests in principle yield recommended optimum AOR setups or practices for different observing scenarios which are summarized in the HIFI Observer's Manual (RD-7), meaning that some observations could be expected to have lower than predicted data qualities when available parameter space is tested around the edges so to speak. The noise measurements are nonetheless shown at their face value.

5.2 Comparing Measured vs Predicted Noise: the "Uplink-Downlink Connection"

An important aspect that Users should be aware of when comparing the data qualities to expected performances is that accurate comparisons depend on several pieces of information from the time estimation output parameters, such as the noise reference

frequency and the noise predictions which were generated in HSpot which used the version of the AOT logic and calibration or configuration tables that were operational at the time the observation was scheduled and carried out. The AOT logic and tables and instrument operating procedures are part of the Calibration Uplink System (CUS) that also encompasses telescope operations, which becomes part of the Mission Configuration (MC) to safely and efficiently run the instrument and spacecraft. The MC is routinely updated for changes to the operating procedures of any of the observatory's subsystems, including the instrument AOT and engineering CUS, the Mission Planning System and Proposal Handling System which HSpot falls under, and in HIFI's case the Java sequencer engine used during time estimation to minimize an observing cost function. Any new version of the MC which is linked into HSpot does not always but can affect time estimation. An AOR which was scheduled early in the mission can have different observing times and predicted noise levels in more recent versions of HSpot. Common cases for this arise from changes to sensitivity tables following engineering tests to purify signal over certain frequency ranges, or updates to stability parameters.

Thus the User has to be able to compare measured noise to what has been predicted from HSpot at the time the AOR was scheduled, requiring that the noise parameters which are given in the Messages after time estimation are stored and merged with the associated data products created in the HSC's SPG. Due to architectural constraints of the uplink system, this has not been possible for observations until Cycle 47 (starting OD 834). For those observations, the User may access the relevant parameters from the Observation Request table of the Uplink Product with each observation's data products. An example is shown in *Figure 15*.
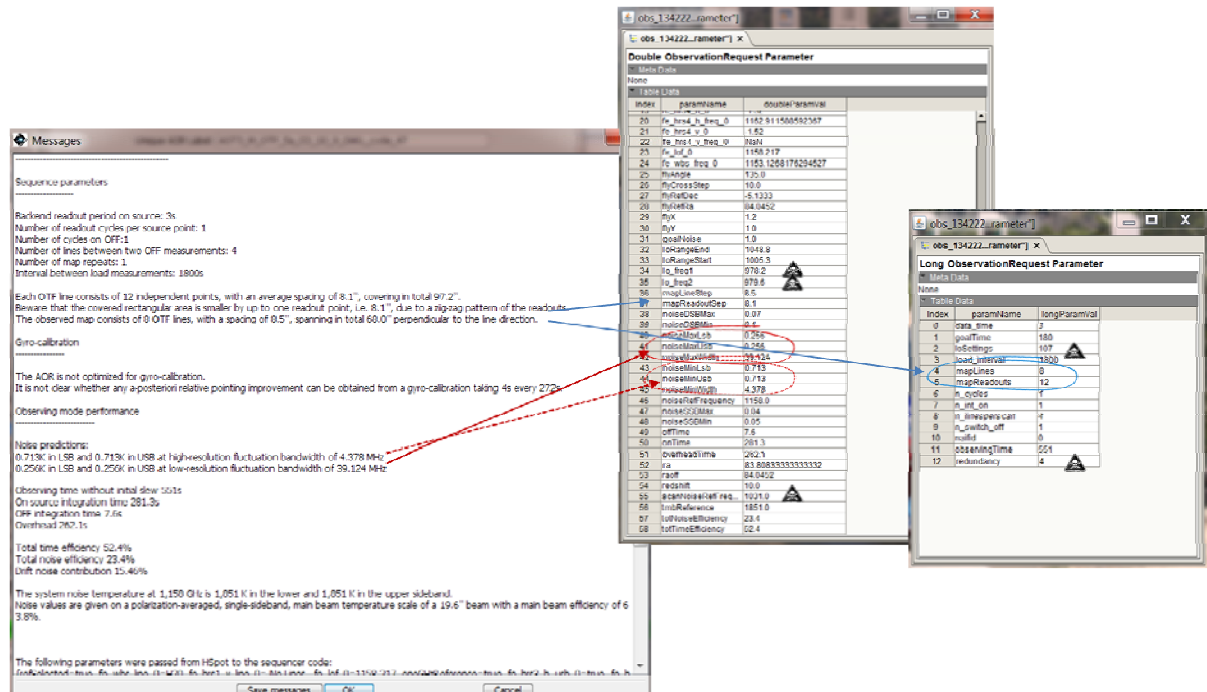
Figure 15:   Illustration of Message output from HSpot time estimation and corresponding parameters in ObsRequestData tables as part of the ObsContext Uplink Product (see text). This is from an OTF map and a few examples of the map layout and noise predictions parameters are shown. There are also parameters which should be ignored, in this example the parameters refer to Spectral Scans defaults. It is expected that the extraneous parameters will be removed by HIPE 8.

Table 2: Noise and observing performance parameters, generated from HSpot time estimation output and transferred to observation data products (see text). The parameters in this table are provided for _all AORs_, independent of Observing Mode.

Description	Parameter	Unit
Predicted SSB Noise USB at minimum bandwidth	noiseMinUsb	K
Predicted SSB Noise USB at maximum bandwidth	noiseMaxUsb	K
Predicted SSB Noise LSB at minimum bandwidth	noiseMinLsb	K
Predicted SSB Noise LSB at maximum bandwidth	noiseMaxLsb	K
PredictedSSB Noise mimimum bandwidth	noiseMinWidth	MHz
Predicted SSB Noise maximum bandwidth	noiseMaxWidth	MHz
Temperature (main beam) at noise reference frequency	TmbReference	K
Noise reference frequency	noiseRefFrequency	GHz
Observing time	observingTime	s
On source time	onTime	s
Off source time	offTime	s
Overhead	overheadTime	s
Total time efficiency[1]	totTimeEfficiency	%
Total noise efficiency[1]	totNoiseEfficiency	%
Drift noise contribution[2]	driftNoiseContrib	%

1. The observing time and noise efficiencies are with respect to an "ideal" instrument, i.e. using the radiometric equation applicable to each observing mode.
2. Drift noise contribution is with respect to the total noise including the radiometric component.

A caveat on the obsRequestData table is that it contains not only those parameters which describe the expected noise performances, layout on the sky [for spectral maps] and other reference information as given in HSpot according to the observing mode for the specific observation being examined, but a superset of parameters that describe configurations and predicted performances for *all* observing mode setups. Only those parameters relevant to the data which are associated with the AOR and its observing mode have been updated while the rest have default values, however it is not obvious to the User how to distinguish those (tables are provided below) and the ICC intends to filter the invalid and potentially misleading parameters, starting in HIPE 8.0. It is also intended to modify the format of the obsRequestData table so that parameter units and descriptors may be included.

A list of selected parameters are provided in this section, describing configuration, noise predictions, and observing efficiencies that are reported on an observation basis in the HSpot time estimation Messages. Each parameter may be browsed in the

25

obsRequestData tables by data type (boolean, string, long, integer, and double) in the uplinkProduct. Table 2 lists noise and observing efficiency parameters which are common to all observations, Table 3 through Table *5* through list parameters which are specific to the requested observing mode.

Table 3: Configuration parameters from HSpot time estimation for DBS and Fast DBS modes.

Description	Parameter	Unit	Applicable DBS Modes
Chop frequency	dbsChopFrequency	Hz	All DBS modes
Chop phase length	dbsChopPhase	s	All DBS modes
Number of map lines	rasterMapLines		DBS Raster maps only
Map line spacing	rasterMapLineSep	arcsec	DBS Raster maps only
Number of readouts per line	rasterMapReadouts		DBS Raster maps only
Line readout spacing	rasterLineReadoutSep	arcsec	DBS Raster maps only

Table 4: Configuration parameters from HSpot time estimation for all OTF Mapping modes.

Description	Parameter	Unit
Number of map lines	otfMapLines	
Map line spacing	otfMapLineSep	arcsec
Number of readouts per line	otfMapReadouts	
Line readout spacing	otfLineReadoutSep	arcsec

.

Table 5: Configuration parameters from HSpot time estimation for all Spectral Scan modes.

Description	Parameter	Unit
HRS in parallel	hrsParMode	"wide", "low", "high", or "none"
Number LO settings	loSettings	
Actutal LO range start	loRangeStart	GHz
Actutal LO range end	loRangeEnd	GHz
Noise reference frequency in scan range	scanNoiseRefFreq	GHz

Observations taken prior to OD 834 do not contain the full set of AOR performance description parameters in the Uplink Product. The HIFI ICC is researching solutions to "back-fill" the data products with the various time estimation message parameters synchronized to the operational MC at the time of scheduling, possibly storing these in the HIFI calibration tree. The solution is not likely to appear in HIPE until version 9 or 10. In the meantime the User can obtain approximate predictions from running time estimation for the AORs of interest with latest version of HSpot. Users who access data from the public archive can download the associated AORs of interest in HSpot with the "File" → "View Accepted Proposal" application. Help can be obtained from the HSC or NHSC helpdesk.

5.3 Fixed LO observations

HSpot provides noise estimates on a single sideband (SSB) main-beam brightness scale for combined H and V polarization spectra. Observations carried out in PV-2 were analysed in order to verify these predictions, which drive observing time at goal and maximum spectral resolutions entered in HSpot by the User. The 1 GHz reference option has almost always been used in the noise predictions, which means that the baseline in only one WBS sub-band is considered for stability instead of the full IF, to take standing waves within that 1 GHz window into account. This is recommended for most observing situations except, when lines are very broad (such as from external galaxies or fast outflows).

5.3.1 Point AOT Modes

Figure 16 and Figure *17* show the ratios of observed over predicted noise, at the goal and maximum spectral resolutions (entered in the AORs).

![HiFi ICC SRON logo]

**HIFI Observing Modes
Performance Notes**

Doc.: ICC/2010-009
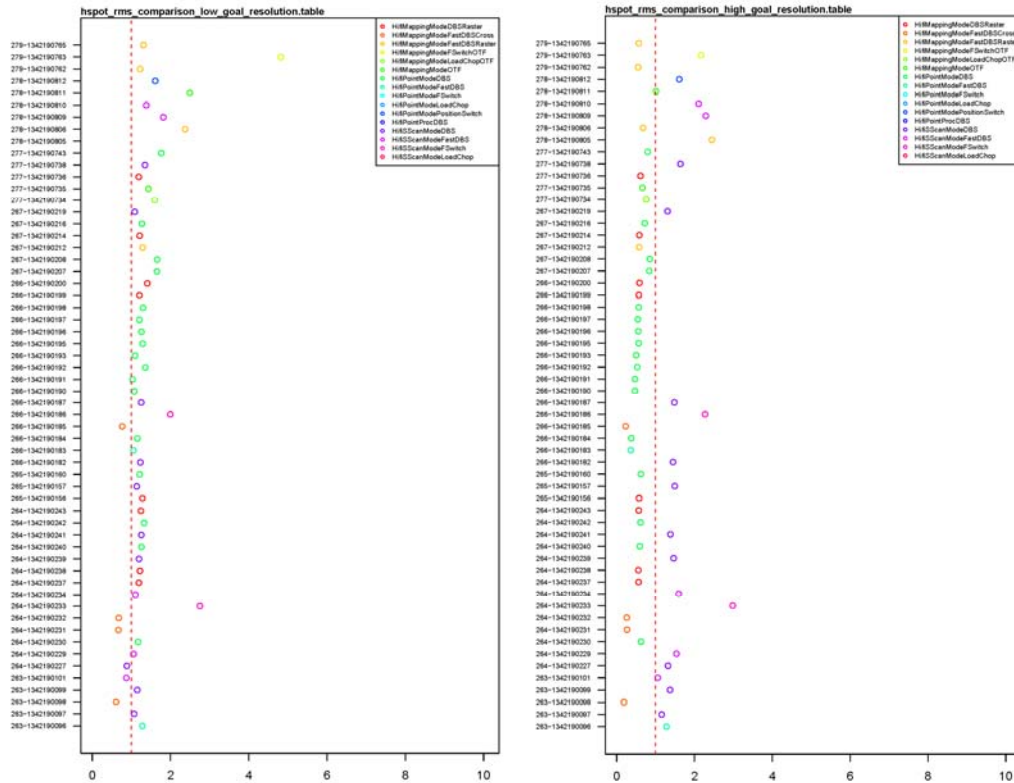Date: 24/09/2011
Issue: Version 3.0

Figure 16: Ratios of measured to predicted (HSpot) noise for observations carried out in PV-2 through February 25, 2010, with data smoothed to the goal low resolution (left) and high resolution (right). Y axis labels indicate OD-Obsid.
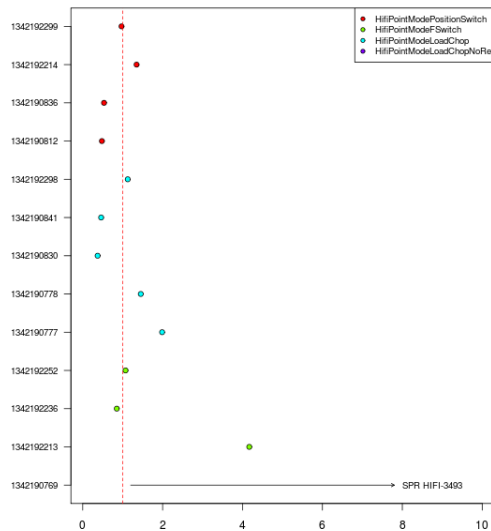

Figure 17: Ratios of measured to predicted (HSpot) noise for all non-DBS Point AOT observations carried out in PV-2 through March 17, 2010, with data smoothed to the goal high resolution. The plot represents 13 of 16 scheduled observations, where three were not carried out successfully due to a Single Event Upset on OD305, later recovered during Routine Phase calibration time. The largest outlier (1342190769) is a PointFrequency Switch observation in Band 7b with extremely poor baseline quality, prior to optimizations to increase instrument stability over many frequencies in Bands 6 and 7.

In Figure 17 the outlier Point Frequency Switch observation (1342192213) represents a limitation to measure the baseline RMS noise when the spectrum is rich and complex, making the definition of a mask for the measurements difficult; see Figure 18. Therefore this case does not represent a performance issue, however we have to keep such cases in mind when comparing auto-generated RMS measures of the baseline to the HSpot predictions if (for example) this becomes part of the HIFI pipeline as a trend parameter.
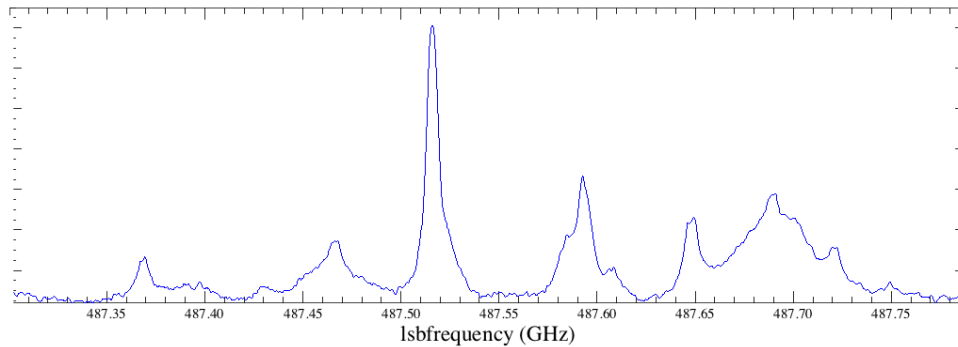

Figure 18: Obsid 1342192213, a Point Frequency Switch observation (unfolded) in Band 1a.

5.3.2 Spectral Maps

5.3.2.1 Noise conventions

On a scan-by-scan basis the DBS and FastDBS Raster mapping modes do not exhibit any remarkable differences with the corresponding Point AOT modes. However the noise levels in both OTF and Raster maps indicated in Figure 16 are simplified in order to make the inter-mode comparisons, in that they represent averages across the entire map as if they were spatially a single point observation. Thus they generally appear to show lower noise in the data than expected from the HSpot estimations. One contributing reason for this is that the noise in the time estimation output is computed on a map point basis, and does not take into account neighbouring readout points (signal beam convolution). Thus the actual noise will be somewhat better than expected, and is sampling dependent: a Nyquist-sampled map will show a relative improvement of ~18% compared to a Half-Beam sampled map of a region with a relatively flat brightness distribution. There will be attenuating factors in reality such as edge effects especially in smaller maps, and drifts or residual standing waves which we address below.

In general, for best comparison to HSpot predictions, the User should measure the noise in spectra extracted from individual map points of data gridded into spectral cubes where the number of pixels are precisely set according to the actual number of scan lines (otfMapLines or rasterMapLines in Tables Table *3* and Table *4*) and the number of readouts per line (otfMapReadouts or rasterMapReadouts) that were carried out. Alternatively one can use the spectra in the Level 2 HTPs prior to gridding, remembering to combine the right number of datasets at each sky point according to the supersample factor and number of map cycles. Averaging these together will yield a crude way to compare to the HSpot predictions. In either approach, the resulting RMS values should be on the optimistic side of the HSpot values if the form of the data (DSB, single

29

polarization) and measurement bandwidths are factored in consistent with the HSpot calculations.   Based on the nominal results the User can then decide if regridding the data to higher samplings (smaller pixels) can be afforded.

5.3.2.2   Baseline drift and standing wave effects

While spectral maps can be thought of as a connected series of single point observations, the timing of the telescope manoeuvres and cycling of calibration measurements (internal and on the sky) over typically longer total observing times makes the data more sensitive to system stability. Stability is represented by total power and spectroscopic Allan times (RD-8) measured at selected frequencies on the ground and in flight, and the real instrument may depart from the adopted values which drive the calibration loops. This is mostly expected in the total power mode of standard OTF maps, where LO thermalization after switch-on is more important than in the chopped modes, and especially in the HEB bands where Allan times are anyway very short. Below we show what a typical "ugly" case might look like at the end of the Level 2 pipeline before gridding to a spectral cube, from a standard OTF map of C+ in Band 7b.
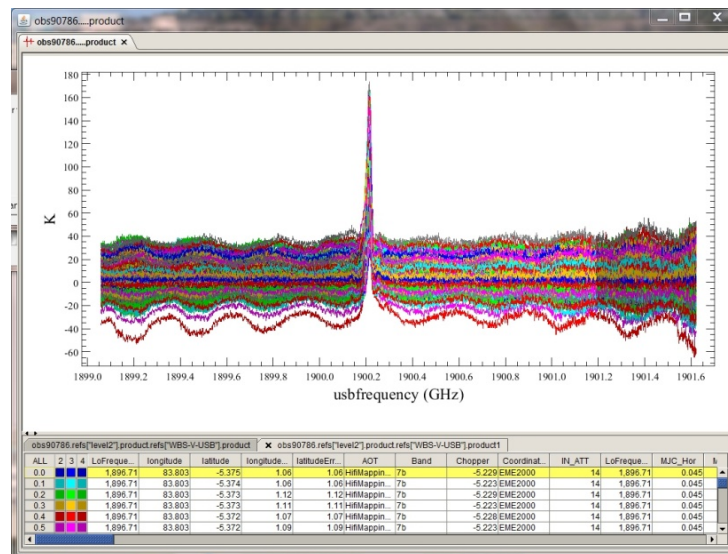

Figure 19: Level 2 WBS-H HTP of all spectrum datasets from a standard OTF map at 1897 GHz. The spectra exhibit the effects of baseline drift and residual standing waves which were not effectively calibrated out in the pipeline.

The spectral cube will show detrimental effects from convolving residual instrument artefacts of the substantial drift and ripples exemplified in Figure 19, if left uncorrected. The use of an internal switching mode may mitigate some of the baseline drift, which can be important to establishing variable source continuum levels across the map. The Load Chop is recommended in Bands 6 and 7, where test observations may show similar extrema of drift levels and standing wave amplitudes in individual spectra but overall a lower RMS of all spectrum baselines around a nominal (drift-free average continuum) level. On the other hand, exceptionally low stability of Frequency Switching in OTF maps compels the ICC to forbid this mode in Bands 6 and 7, except over a range of most stabilized frequencies around the C+ line (see Section 3).

If continuum levels are not important, then the User can remove the drifty baselines and residual standing waves in two steps in HIPE (fitBasline and fitHifiFringe) or in a single step (fitHifiFringe), depending on different levels of desired control in the fitting and outputs offered by these tools.   While the removal of the baselines alone is probably good enough to compute a reasonably distortion-free line intensity map of the main component in Figure 19, which is reasonably narrow compared to the 300 MHz standing wave, removing the standing wave is also needed to characterize the many lower amplitude velocity components on the line wings, which vary across this particular map.
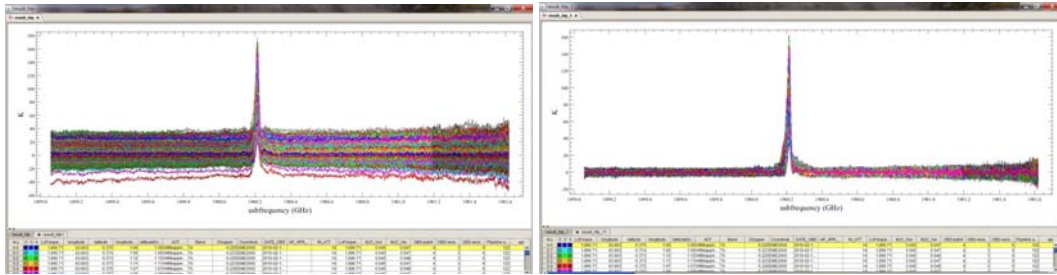

Figure 20: Data shown in Figure 19 after removal of the residual fringes (left) and then the baselines (right) in HIPE. The resulting data yield the best quality line intensity and velocity maps and P-V diagram, but all continuum levels entangled with baseline drift have been removed.

As mentioned above, the reasons for the residual baseline drifts and standing waves at the end of the pipeline are largely due to a mismatch between adopted Allan times driving the calibration loops and real instrument behaviour over the course of the observation, and these are most important in non-DBS modes and in the bands or at frequencies where stability is lower.   An interesting aspect about this is that the amplitude of the residual waves scales with the baseline offset, and sometimes the phase is generally opposite between positive and negative offset datasets. Typically the datasets with the most negative offsets (relative to a nominal level) have the highest amplitude ripples. This is shown in the examples of Figure 21.
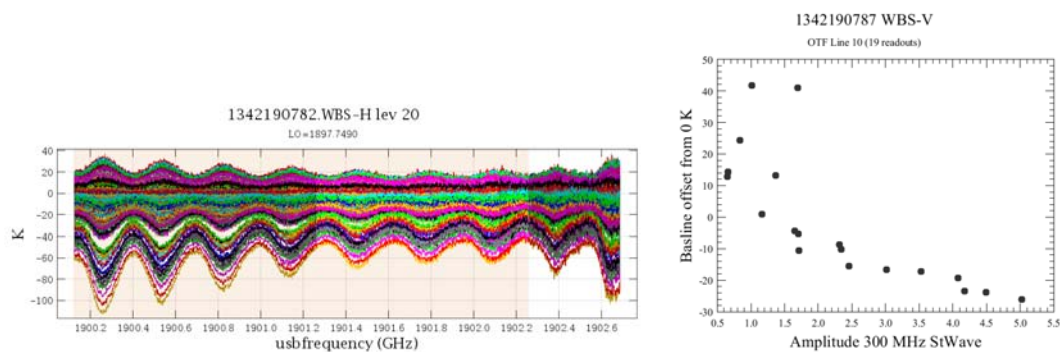
Figure 21: Level 2 spectral datasets from two similar OTF map observations, showing the increasing amplitude of the residual standing waves with the size of the baseline drift. In these examples the data also tend to show the highest amplitude ripples at negative baseline offsets, but this is not always the case.

The examples shown in Figure 19 through Figure *21* are among some of the most extreme cases to illustrate our points; most HIFI spectral maps exhibit these residual

effects to a much lower level, often not to any significant level with a *general* trend towards best data quality in the DBS Raster maps, and increasing quality from HEB diplexer Bands 6 and 7 to SIS diplexer Bands 3 and 4 to SIS beam splitter Bands 1 and 2.

Standing waves in other modes are discussed in Section 7.

5.3.2.3   *OTF map "striping"*

The behaviour described in the preceding paragraphs may lead the User to wonder how it might manifest as kind of "striping" in affected HIFI OTF maps, similar to the elongated artefacts along the scanning direction of some maps obtained on ground-based telescope. These mostly arise from the imperfect correction of the receiver instability due to the atmospheric contribution of the overall signal. The common practice is then to take maps along two perpendicular scanning directions, and combine them with more or less sophisticated algorithm (e.g. the PLAIT technique developed by Emerson et al. 1992). For HIFI, such a contribution does not exist, so that it is expected that the only residual spurious spatial structures would arise from the imperfect cancellation (in the ON-OFF calibration) of instabilities due to the receiver drifts, such as standing waves or other band-pass distortion, e.g. at the IF edges of diplexer bands. There is also a spatial zig-zagging of OTF map scan legs (discussed below) that may be present and might contribute to the appearance of a kind of alternating signal pattern in the map.

In order to quantify this effect, we have looked at several cases, both in SIS and HEB bands, for maps taken along various scanning directions. The net result is that **line peak intensity, or integrated line intensity maps in a more general way**, **are not noticeably affected by the striping effects when a proper baseline correction is performed**. In most of the checked cases, removing the possible continuum present in the spectra is good enough to clean the artefact spatial structures, but it is of course always better to also take care of standing waves residuals.

On the other hand, we have noted that **continuum maps may suffer from residual striping**, especially in the HEB bands where the continuum stability is fairly poor. This effect can be mitigated for some particular stable frequencies on the SIS bands, but from a general perspective, we do not recommend to use the OTF mode if the science goal requires an accurate recovery of the continuum spatial emission. The case we illustrated is in Figure 19 where real source continuum emission levels are distorted by uncorrected drift.   If continuum levels are important to the science case, the alternative would be to use the DBS raster mode, together with the Fast-Chop and/or Continuum-optimisation options selected. Since this mode is less time-efficient than the OTF, especially for large maps, another alternative would be to perform OTF maps along two perpendicular scanning directions. However, the HIFI ICC has not yet looked into this option in great detail (first needing to identify good cases), and dedicated tools to optimally combine such maps (e.g. the PLAIT algorithm) have not yet been tested for HIFI in HIPE. In HIPE 8 it is planned to release a simple version of this, which simply combines Level 2 HTPs as the input to the HIFI doGridding algorithm to convolve the signal according to specified beam parameters and create a single output spectral cube.

The following examples illustrate typical maps obtained in strong spectral lines in the OTF mode. They show the spatial distribution of the brightness temperature, distinguishing between 1) single channel maps ("line peaks"), 2) integrated intensity

maps ("integrated line"), and 3) "continuum" maps, i.e. integrated intensity maps in regions of the spectra with no line emission. For cases 1) and 2), one checks the results before and after removal of the continuum level (here, a simple 1st order polynomial fit to the baseline). In the examples below, the data are pipelined up to level2, then exported to and regridded in Class.

- **Example 1:** Perpendicular maps taken in the ^{12}CO (8-7) line in DR21.

The plots below illustrate the distribution of the emission for the various spectral slices described above. The continuum map corresponds to the integrated intensity between 100 and 200 km/s, while the integrated line map covers the range between -50 and +46 km/s. The line peak is taken at -5 km/s. All velocities are with respect to that of the rest frequency of CO (8-7). The blue dot represent the positions associated to each readout prior to regridding (i.e. in the Level 2 products). The plot in Figure 22 illustrates those areas on top of the averaged spectra over the whole map. An individual spectrum is also shown to illustrate the typical baseline shape in a map readout.
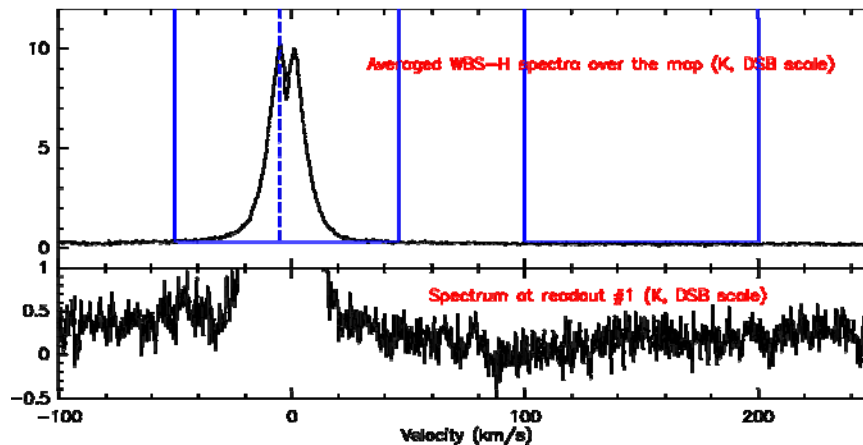

Figure 22: Top: averaged WBS-H spectrum over the full map taken at PA=0. The two blue areas indicate the respective velocity ranges for the integrated line and continuum maps. The dashed line shows the velocity for the line peak map. Bottom: blow-up of the baseline shape for one individual spectrum.
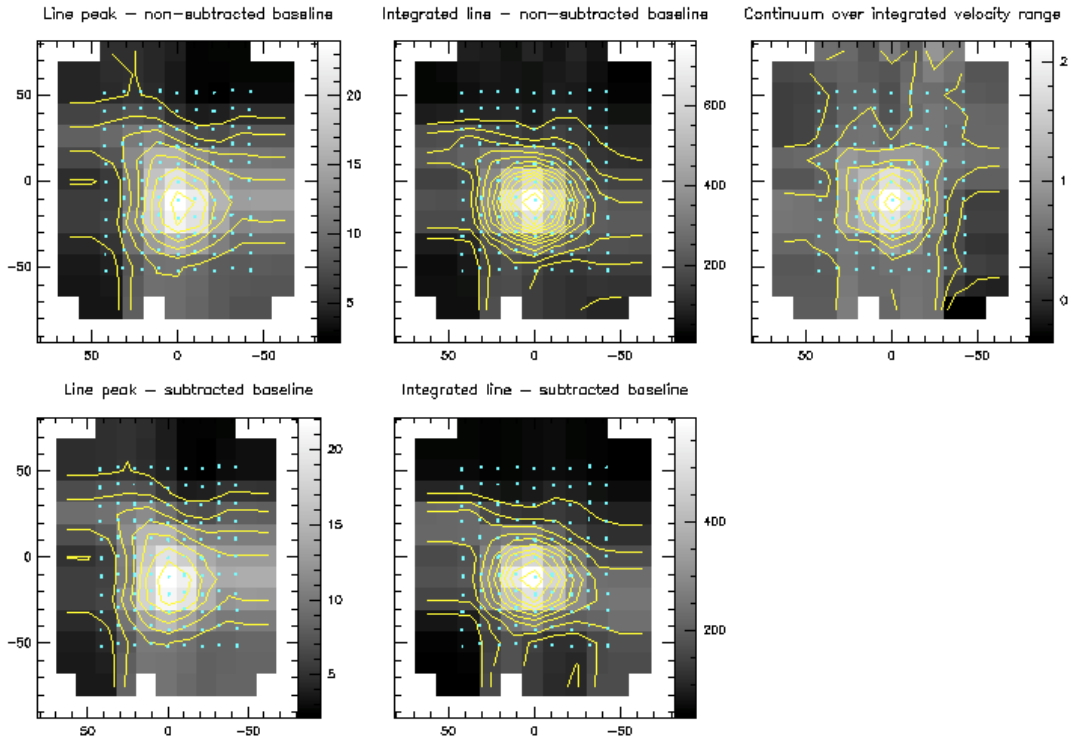
Figure 23: Map taken with the scanning direction along the Declination axis (PA = 0). Left: Line peak map with and without baseline continuum subtracted, Middle: integrated intensity maps with and without baseline continuum subtracted, Right: Continuum map. Contours from 5 to 25 K in steps of 2.5 K (line peak maps), 100 to 700 K km/s in steps of 50 K km/s (integrated intensity maps), and 0 to 3 K km/s in steps of 0.25 K km/s (continuum).
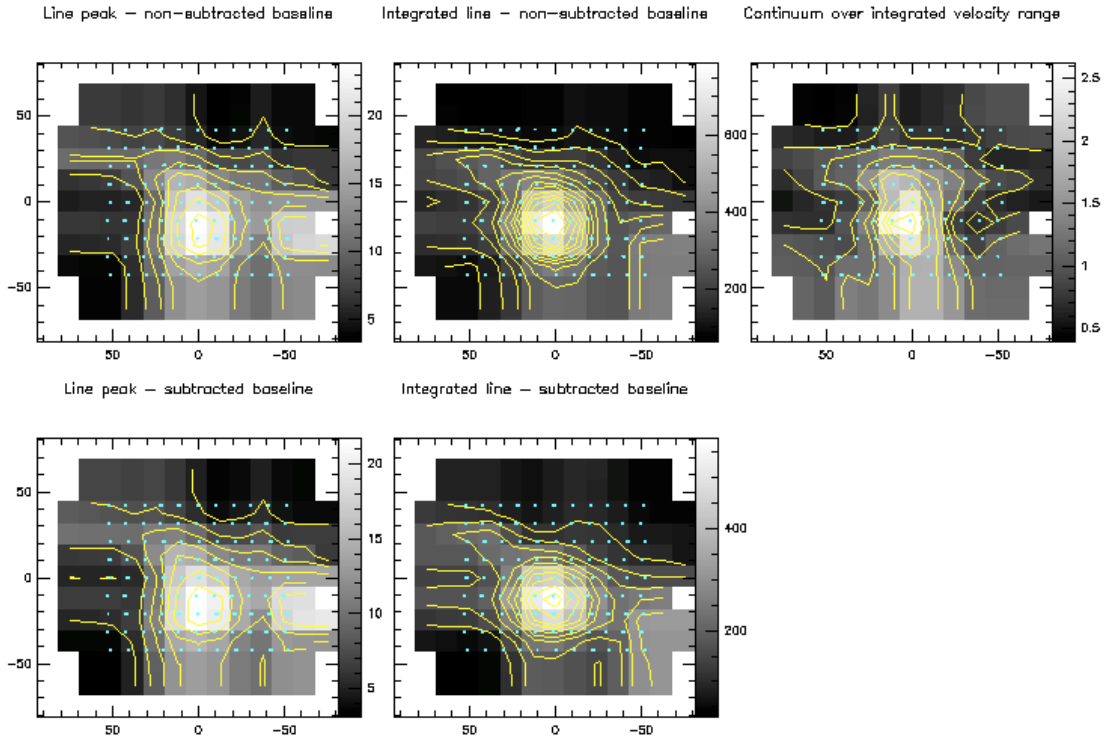
Figure 24: Same as Figure 23 for the map taken along the R.A. axis (PA=90). Contour levels are the same.

One can probably argue that there are some elongated structures along the respective scanning directions in the lowest contours of the continuum maps. In the line and integrated intensity maps, peak structure is fairly circular. The source extend in the CO line seems to be a bit larger than the map size, so that it is not easily possible to interpret the spatial structures at the map edges (beside the additional fact that the Class regridding considers pixels well outside of the covered positions). There is an extended structure towards the North-East of the map. This structure is seen in both coverages so that it is likely real and not a result of striping residuals. This is confirmed when looking at the same data projected onto a common grid (see Figure 25).
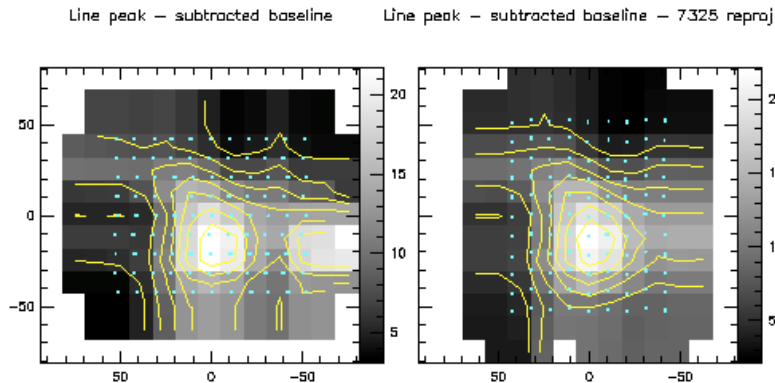

Figure 25: Line peak map with baseline corrected, shown for the two orthogonal coverages, projected into a common grid (that of the left map). Left: OTF map with PA=90, Right: OTF map with PA=0.

- **Example 2:** OTF map taken in the C+ line in the Orion region.

The plots below illustrate the distribution of the emission in a similar fashion as in the previous case. The map is taken with a scanning direction along the R.A. axis. The continuum map corresponds to the integrated intensity between -200 and -100 km/s, while the integrated line map covers the range between 4 and 17 km/s. The line peak is taken at 9 km/s. All velocities are with respect to that of the rest frequency of C+.
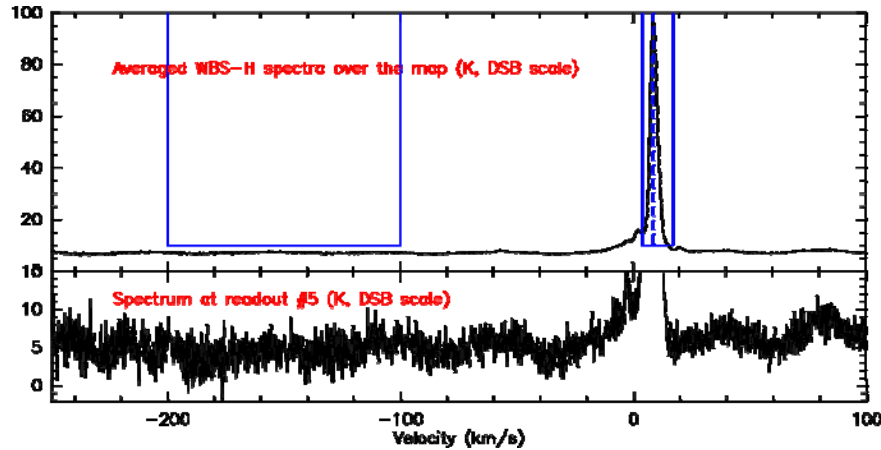

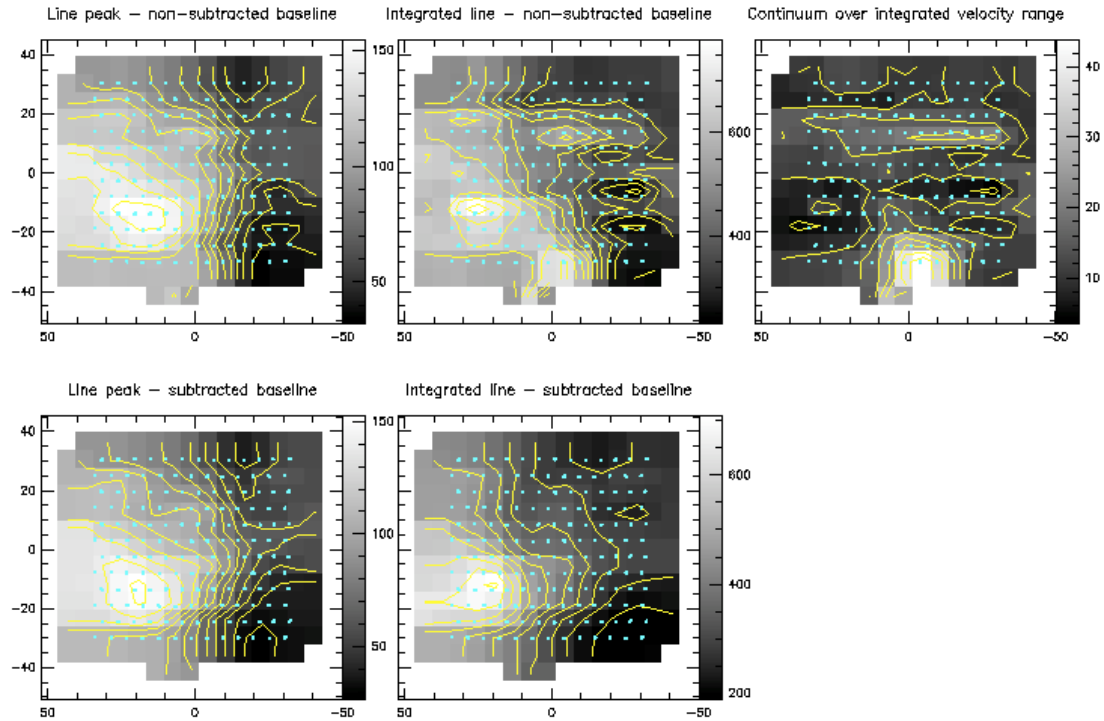*Figure 26: Same as Figure 22 for the C+ map.*

Figure 27: Same as Figure 23 for the C+ map. Contours from 30 to 150 K in steps of 10 K (line peak maps), 200 to 800 K km/s in steps of 50 K km/s (integrated intensity maps), and 0 to 50 K km/s in steps of 5 K km/s (continuum).

In this case, there is a strong continuum emission present over the covered area. The continuum map clearly shows residual striping effects, which in some fashion contaminate the integrated line intensity line when no continuum removal is applied. Removing the continuum substantially corrects from those artefacts.

Summarizing, striping becomes most noticeable in OTF maps at frequencies which are of generally low stability, primarily in the HEB bands, or else where measurements are made over spectral ranges that are known to suffer band-pass distortions as at the IF edges of the diplexer bands. The effects are more obvious in continuum maps, which can be intertwined with uncorrected baseline drift, while line peak or integrated intensity maps (and thus velocity maps and P-V diagrams) are not obviously affected when the surrounding baseline along with what residual standing wave pattern is present are accurately fit and subtracted.

There are no compelling cases to warrant a recommendation by the ICC to obtain orthogonal maps in order to remove striping effects. This can be satisfactorily accomplished in interactive data processing as described above. Users can also combine the Level 2 HTPs of the separate H and V polarizations to crudely average out some artefacts, and then regrid to cubes. This works because it is noticed that the spectra from the two polarizations (separate mixer assemblies) do not generally drift together in time. It is also true that the baseline drift within any single polarization is somewhat random. This is illustrated below with an OTF map taken in the CO 5-4 line (Band 1b) of a compact source IRC+10216. In these data the standing waves have been well removed after standard pipeline calibration, and we can examine the remaining drift of baseline levels. Figure 28 shows the line-free median baseline levels for all Level 2 datasets in the map, which has 7 OTF legs and is repeated once (thus 14 scan lines in total). Each leg shows statistically significant baseline offsets from the expected zero level (little or no continuum emission is expected here). Within each scan leg the offsets do not vary smoothly with time, as shown in the zoomed plot of Figure 28. There is an obvious signal jump during the 9th leg and possibly trending through the 12th leg, but this cannot be directly correlated with the timing of the reference sky measurements since there is a reference taken at the end of every scan line in this observation, nor does it fit with the timing and usage of the internal load measurements, thus the jumps are created elsewhere in the instrument. This might show up in the data at some level as striping, but the readouts along each line from each of the two map cycles in this case get convolved so a striping effect in any scan lines does not become noticeable at the cube level.
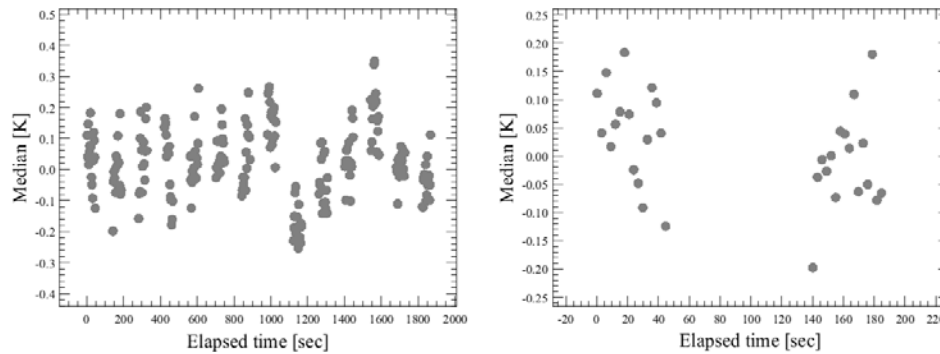
Figure 28: Median baseline levels of Level 2 spectra from a standard OTF map in Band 1b (1342210099). Spread about the zero level is quite noticeable, but the zoom on the right of the first two scan lines shows mostly random variation in time.

As stressed above, spectral line peak or intensity map, velocity maps, and other line-dependent measures should involve a compensation for the baseline drift. Figure 29 shows the integrated line fluxes from the same map as used in Figure 28, after the (more or less) randomly drifting baseline levels from the spectra have been removed (no standing waves have been present in the calibrated spectra). The behaviour of the line fluxes is highly consistent now between the two map cycles, where the flux in each leg shows the roughly Gaussian signal profile as the HIFI beam scans the compact emission source. The line signal history repeats very well in the 2nd map cycle.
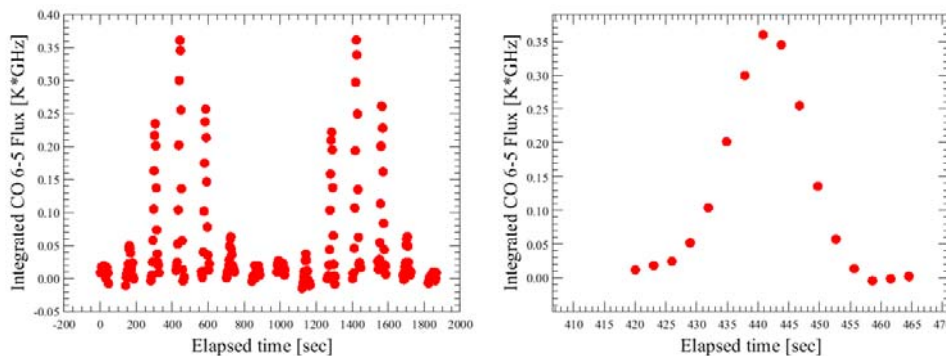

Figure 29: Integrated fluxes of the CO 5-4 line (plots are labelled incorrectly as CO 6-5) from the map used for Figure 28. The left shows the line fluxes for readouts of the 7 scan legs of 1st and 2nd map cycles (14 legs total) in time, the right shows a zoom on the 4th scan leg. The repeatability of the signal between the two map cycles as well as the source profile shapes in each leg is excellent, once the random baseline drift is removed.

5.3.2.4   OTF "Zig-Zag"

HIFI OTF maps are subject to a timing "jitter" in the chain between the mission planning system and the instrument data acquisition and telescope pointing commands, which may result in a shift of every other scan line by up to one beam size on the sky. Figure 30 illustrates how this can look in an OTF map using Frequency Switch and standard OTF mapping. The effect is not present in DBS Raster maps, and the source of the OTF problem in the uplink system has been elusive and efforts to repair the effect in data processing by manipulation of the attitude assignments to the data have not been

successful in a general way so far, but we can at least be reasonably sure that the problem is not originating from the contents of the Pointing Product nor how the attitude assignments are made to the individual datasets in the pipeline. In order to ensure that the sampling requested by the User in HSpot is not compromised by the zig-zag near the map edges, a modification to the OTF modes were made during PV-2, to add one readout along each scan line.
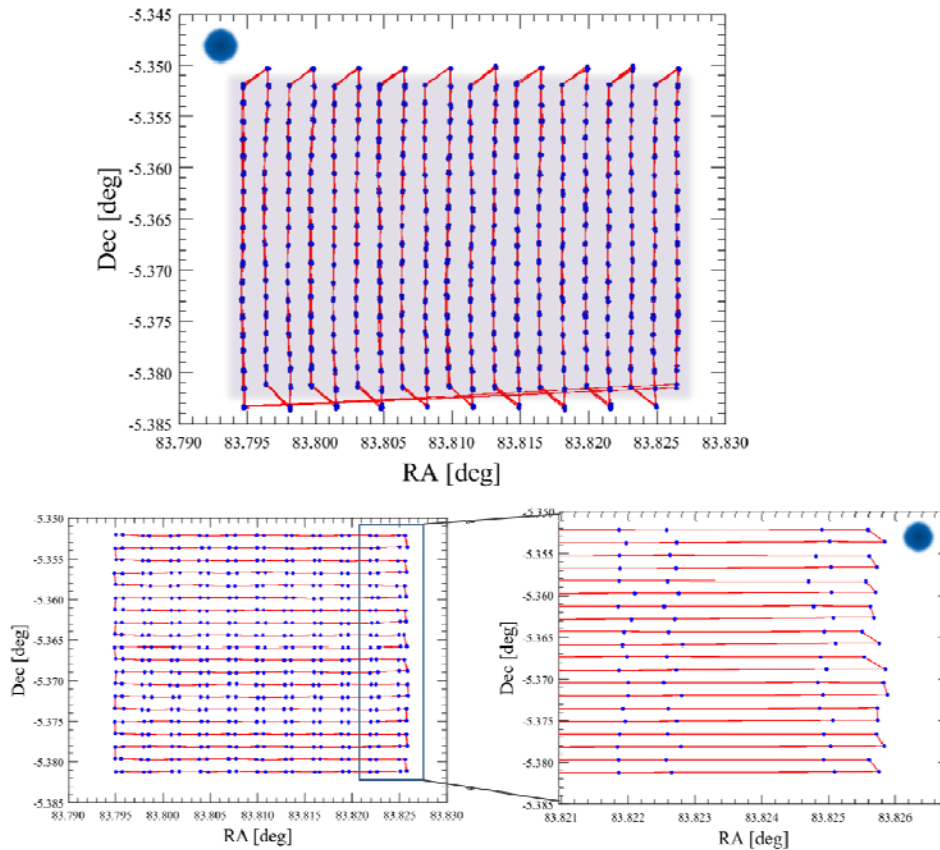

Figure 30: Sky positions of readouts (blue dots) from two example OTF maps using standard position switching (top) and Load Chop (bottom), with approximate beam sizes indicated (in both cases Band 7b). The zig-zag of up to a full readout between each leg can be seen in both maps. In the top map the shading indicates schematically where the User's requested sampling should be guaranteed over the dimensions specified in the HSpot time estimation. The bottom map, which was carried out with a 90° position angle, also shows the sky sampling expected with modes that also use internal switching (Load Chop and Frequency Switch).

At this time we simply alert the User to the existence of the effect, as it enters the data as a form of noise. The amplitude of the zig-zag depends on several factors including integration times or readout rates and telescope scan speed, while the effects (which are what the User is most interested in) depend also on the structure of the source at the sky frequencies being mapped. A rather extreme case is represented in a C+ map of the Orion Bar (Figure 31), which has very sharp signal gradients and structuring so that a checkerboard pattern along the Bar becomes obvious. The effect on measured line fluxes can be rather dramatic, as shown in the plot. While we expect some degree of digitization of signal depending on the gridding and pixel sizes, the normal curve of line fluxes across the Bar without zig-zag should be much smoother.
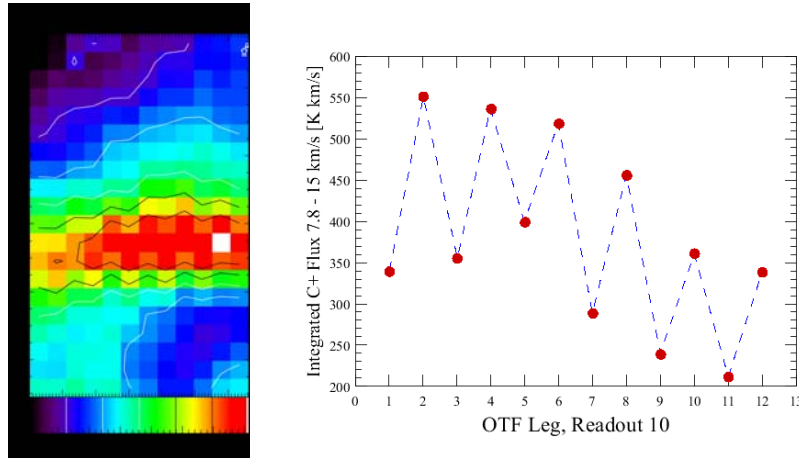
Figure 31: On the left is shown how the zig-zag appears in a standard OTF map of the Orion Bar in the C+ line at nominal Nyquist sampling. The observation was taken with a telescope position angle of 35°, and has been rotated. On the right are integrated C+ line fluxes measured from a single row of spectra along the Bar from left to right.

The effects of the zig-zag on measurement of lines in structured regions such as the Orion Bar shown above can also complicate the interpretation of the data from the separate H and V backend spectrometers, since the beams are not generally co-aligned (see Sections 8 and 11.1). The question of H and V imbalance in the presence of the zig-zag in maps is included in Section 11.

5.4 Spectral Scans

The noise in the Spectral Scans when measured before sideband deconvolution scales with [2 x redundancy] $^{-1/2}$, to the single sideband (SSB) noise when the gains are equal.

The noise values for the Spectral Scans shown in Figure 16 have been measured from the dual sideband (un-deconvolved) H+V averaged spectra at the reference frequency where noise is predicted in HSpot, and have thus been appropriately scaled by the factor [2 x redundancy] $^{-1/2}$. Note that this factor scales to the SSB noise when the gains in each sideband are equal. When the gains deviate from unity, the deconvolution algorithm should model these as well and the same scaling should apply. *There are some indications of a departure away from unity that can be distinguished in some bands, so far with sufficient certainty of sideband ratio study results in Band 2a to provide updated values in the HIFI calibration tree for range 634 – 654 GHz (see Sec. 12).*

Normally one would measure the noise at the reference frequency in the SSB, H+V averaged spectra. Numbers from the DSB single polarization data for the Spectral Scans are anyway plotted in Figure 16 to show the reasonably good agreement between predicted and measured noise before deconvolution, to stay clear of possible effects on the deconvolved output by manual pre-treatment of spurs, baseline drifts, standing waves, and other artefacts.

After running a sideband deconvolution application in HIPE (doDeconvolution), SSB RMS values are found to be in good agreement, but also sometimes 1.5 to 2 times higher than the HSpot predictions in Bands 1-5. A few examples are tabulated below for comparison to the points in Figure 16. (Note that the noise has not necessarily been measured at the reference frequency, but rather close to the middle of the covered range). Very early results indicated that the HEB Bands 6 & 7 may yield even higher SSB RMS noise values - between 2-3 times than predicted by HSpot. Each outlier case might be explained by how much or how well "pre-cleaning" of artefacts in the input Level 2 HTP is done before deconvolution (often tied to frequencies with potential stability or purity issues), however further tests with more recent software and data, follow-up study of the outlying cases, and more observations which use Frequency Switch and Load Chop modes, are needed to strengthen conclusions about the noise performances in Spectral Scans.

1342190187 1b DBS R = 8, H+V HSpot T_{mb} noise @ 1 MHz = 22mK

Freq	H+V avg (T_{mb})
558.35	25.48
568.56	20.26
578.00	21.45
584.83	27.87

Ratio: 0.9-1.3

1342190239 2a DBS R = 8, H+V HSpot T_{mb} noise @ 3 MHz = 9 mK

Freq	H+V avg (T_{mb})
683.75	9.67

Ratio: 1.07

1342190241 2a DBS R = 3, H+V HSpot T_{mb} noise @ 3 MHz = 9 mK

Freq	H+V avg (T_{mb})
683.75	10.53

Ratio: 1.17

1342190215 5a DBS R = 8, H+V HSpot T_{mb} noise @ 3 MHz = 43 mK

Freq	H+V avg (T_{mb})
1163.90	78.08

Ratio: 1.81

1342190904 5a FastDBS R = 8, HSpot H+V T_{mb} noise @ 3 MHz = 46 mK

Freq	H+V avg (T_{mb})
1163.90	74.60

Ratio: 1.61

It is clear that effective sensitivity is enhanced after sideband deconvolution. Lines that are undetectable in individual double sideband spectra may become visible in deconvolved spectral as shown in Figure 32.
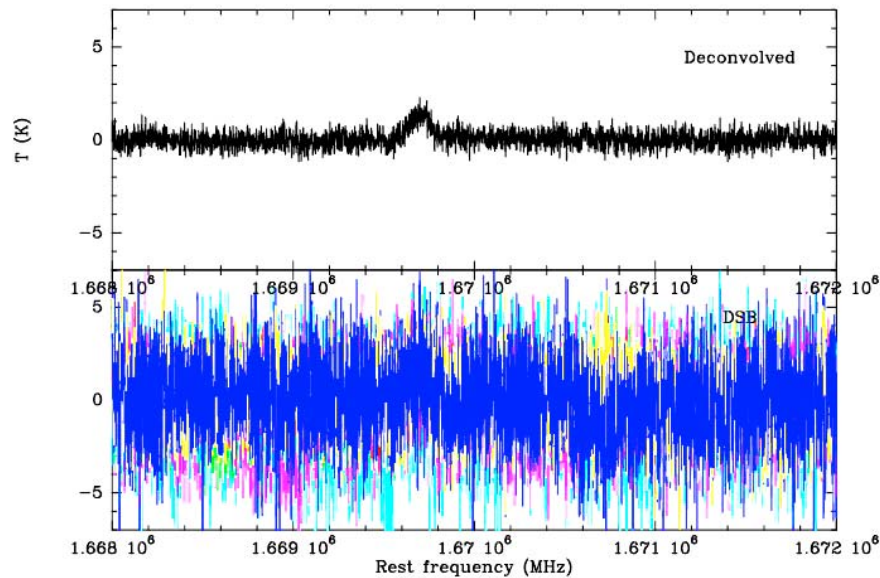
Figure 32: A survey of band 6b double sideband spectra taken at redundancy 8 with a fast-chop is overplotted in color in the lower panel, and the deconvolved single sideband spectra shown in top panel. The water line, invisible in the DSB dataset, is brought-out by the deconvolution.

There is not yet a clear distinction in noise performances between observations which use DBS and FastDBS modes (whereas it is reasonably clear that there is no distinction for fixed LO observations), meaning both modes appear to meet the noise performances as expected from the HSpot predictions. Where there might be some difference is in diplexed Bands 3, 4, 6 or 7 at some frequencies, where fast-chopping anyway will be more effective at removing standing waves and certain AOT commissioning tests using normal DBS in those bands exhibit poorer baseline quality.

Observers should keep in mind that the production of good SSB spectra is highly dependent on the removal all artefacts: standing waves, spurs, and the removal of all continuum baselines (linear or non-linear) prior to performing the deconvolution reduction step. An example of the value of "cleaning-up" spectra prior to deconvolution is shown in Figure 33.
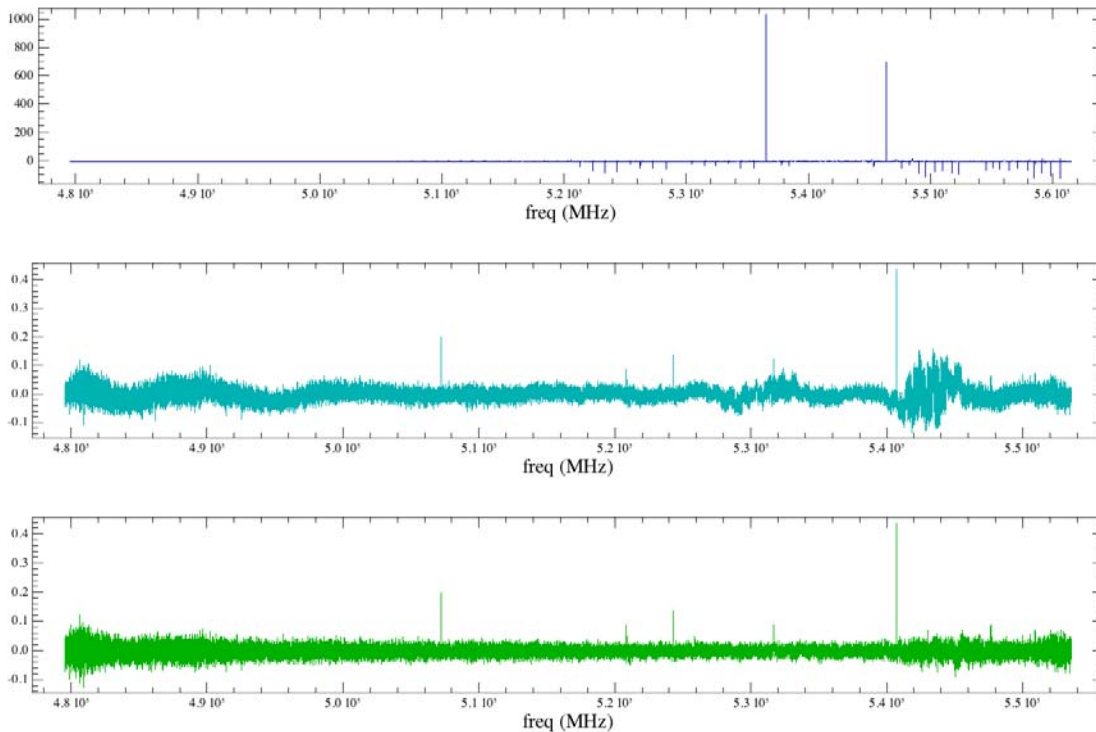
Figure 33: Band 1a spectral scan in various states of cleaning. The top plot shows the raw output from deconvolution. The effect of the spurs is obvious, as they echo throughout the solution. The centre plot has the spurs flagged-out, and the solution is much better, though issues with baselines are apparent. We applied a simple baseline removal routine, and the result is the spectrum on the bottom.

Summarizing the Spectral Scan observational results:
- The results have been generally very good, with nearly the expected noise levels in the spectral surveys regularly reached in most bands (within a factor of 1.5) with very comparable results obtained in both polarizations
- Both broad surveys (20-80 GHz in width) and narrow surveys (4-19 GHz in width) have been successfully observed and deconvolved. These include the so called "mini-surveys" which sample a narrow 4-6 GHz band without moving completely off of the target line while observing at high redundancy (R=12). These mini-surveys are useful in ruling out line blending and frequency ambiguities.
- No "ghost lines", symptoms of instabilities or insufficient sampling, have been found in any survey. When spectral artefacts and bad baselines are removed completely from the input prior to deconvolution, the deconvolution yields flat baselines with neither ringing, nor any added repetitive noise structures.

6. Performance/Sensitivities at IF Edges

In the diplexer bands 3, 4, 6 and 7, a substantial increase in system temperatures and thus decrease in sensitivity occurs towards the edges of the IF bandpass.

For Bands 3 and 4, the IF bandpass span is 4 GHz (4 – 8 GHz), and the last 500 MHz at either side, between 4.0-4.5 GHz and between 7.5-8.0 GHz, induces a significant increase of baseline noise since the diplexer mechanism introduces extra losses in those locations, and Tsys can increase up to 50-100% as compared to the central part of the IF (see Figure 34).
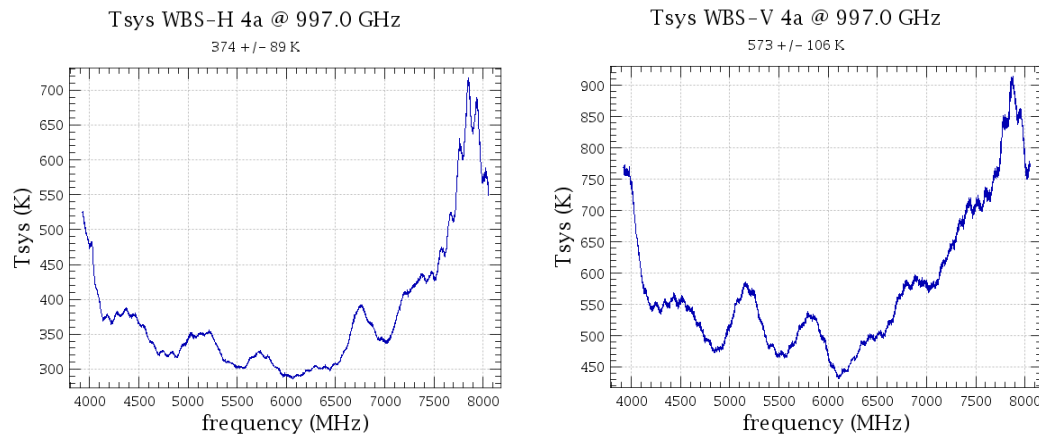
Figure 34: IF noise temperatures for the 4a LO chain tuned to 997.0 GHz.

Additional drawbacks include degraded stability performance (stronger standing waves and poorer baseline performance). Note that those stability issues can be mitigated by using Fast-DBS, but not the sensitivity degradation.

Thus it is not so much a lien or caveat on the Observing Modes, but rather a recommendation to avoid placing lines in the last ~500 MHz on either end of the IF in Bands 3 and 4, and in the last ~250 MHz in Bands 6 and 7, when using modes of the Point or Map AOTs. In cases where two lines are being targeted in the edges of the upper and lower sideband in a single AOR, it is better to devise separate AORs for each line despite the additional 180 sec slew tax, since time is not being saved in a single AOR when the noise and standing waves are impeding spectrum quality.   Figure 35 shows an example of the kind of setup which is not recommended.
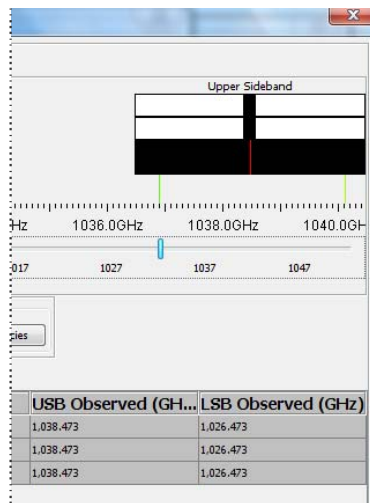

Figure 35: Example of a discouraged setup in Point or Map AORs, targeting lines at the edges of the IF in either or both of the USB or LSB in diplexer bands. Two separate AORs which place lines away from the edges of the IF should be devised when observing in Bands 3, 4, 6, or 7.

7. Standing Wave Residuals

The impact of optical standing waves in HIFI data on line and continuum calibrations is described in RD-6. The table which lists the various sources of optical standing waves is reproduced below.

Table 6: Summary of optical standing waves in HIFI (from RD-6).

Standing wave path	Distance (mm)	Frequency (MHz)
CBB - mixer	~ 1530	98
HBB - mixer	~ 1625	92
LO - mixer	~ 1490	100
RTM – mixer (only bands 3,4,6,7)	~ 240	620
Secondary - mixer	~4160	35

All of the periods listed in the table have been identified in HIFI data, except the last one which would be due to reflection between the telescope secondary mirror and mixers, common to radio telescopes. There is no clear evidence for this component, which may have been effectively suppressed by optical design modifications in HIFI for this purpose.

HIFI pipelines will arithmetically correct for standing waves using the sky reference measurements obtained during observing, and (so far) only on an individual observation basis. In the DBS modes available with all three AOTs, the sky references come automatically by definition of the switching scheme, at a rate depending on stability parameters and the User's AOR setup, employing telescope nodding plus chopping of the internal M3 mirror to fixed 3-arcminute throws on the sky. The sky measurements are otherwise referenced to a telescope position switch at User-selected coordinates within 2 degrees of the main target. If sky position switch measurements were skipped (they are optional but still recommended in the Frequency Switch and Load Chop modes), then no standing wave correction is applied. Otherwise, in the ideal case, standing waves are effectively removed by actuation of the doRefSubtract[1] step in the Level 1 pipeline. Real instrument behaviour in the telescope involves system drift which is not always well matched with adopted characteristic Allan times at all frequencies in all bands, and may result in standing wave residuals after standard pipeline processing.

Generally, the beam-switched modes tend to be less susceptible to drift and residual ripples since the ON and OFF positions have reversed optical paths when switched (thus standing waves with opposite sign) so that the ON and the OFF datasets are basically averaged on an individual scan basis. This also makes AORs using DBS, especially at the faster chop rates, more ideal to mitigate drift if the LOs are not completely thermalized after initial switch-on

---

[1] The reader is referred to either the HIFI Pipeline Specification or HIFI User Reference Manual (RD-4) for a description of the doOffSubract and doRefSubtract pipeline tasks which apply the algorithms appropriate for each Observing Mode.

and warm-up. This is most strongly relevant Bands 6 and 7 where the LOs have very long times to reach thermal stability.

Conversely, total power mode observations employing a telescope Position Switch can be expected to exhibit residual standing waves, since telescope slews are generally long compared to applicable Allan times. The pipeline must perform some appropriate temporal interpolations on a baseline of sky reference measurements for multiple scans. LO bands 6 and 7 with the shortest Allan times are thus where residual baseline drift and standing waves are not unusual in some fraction of the calibrated Level 2 spectral datasets. The Spectral Scan AOT and OTF mapping modes may be most susceptible. For both chopped and total power modes, astronomical sources with continuum emission may be expected to show ripples in the Level 2 spectra that multiply between the source and whatever internal residuals exist. The impact of the standing waves on science is obviously less and may even be ignored in some cases of sources with very narrow lines and where surrounding baseline or continuum levels are unimportant to the User's science goals.

Baseline drift and standing waves or their residuals after calibration can be mitigated in interactive analysis, using certain tools in HIPE.

1. The most common approach at Level 2 involves applications of fitHifiFringe and fitBaseline, and is discussed further below in particular with respect to OTF mapping mode performance. The fitHifiFringe tool works on the basis of sine waves, which are suited to the optical fringe patterns in the SIS beam-splitter bands (1, 2, 5) but less ideal for the diplexer bands (3, 4, 6, 7). HEB bands 6 and 7 in particular exhibit electrical non-sinusoidal standing waves that may drift in amplitude and phase, but a sine-wave approximation of the residual ripples in any of these bands can yield quite significant improvements to the S/N qualities of many if not most datasets in an observation.

   Meanwhile there are two other approaches in development for HIPE 8.0/9.0 to work more precisely with the characteristics of the data as User scripts in the Level 1 pipeline (the reader is referred to the HIFI Calibration Web, see RD-4, for links to documentation about these developing methods):

2. A baseline pattern-matching technique emphasizing the HEB bands, to find best fits to the residual baseline pattern from a databased collection of binned patterns, exploiting the fact that the standing wave amplitude is chiefly a function of the difference in mixer currents between the observation phases while the profile is independent of frequency. This method should (eventually) be applicable to all observing modes. More discussion on this scheme may be found in RD-5. Users who have been interested in experimenting with this technique have been encouraged to be in contact with the HIFI ICC (via the helpdesks) but it is also planned to incorporate scripts in HIPE starting in UR 8.0 (TBC).

3. For many observations and especially those which have targeted continuum sources, baseline quality (at any arbitrary frequency) might benefit from smoothing the calibration loads before they are applied in the pipeline for bandpass calibration. This is a so-called "modified calibration scheme" which can reduce the standing wave-induced calibration errors in Bands 1 and 2 from 3-4% to ~1%, and reduce the residuals in the central IF part at frequencies in Bands 3 and 4. The method requires that a sky reference measurement is also taken at the same frequency, thus this would not apply to the "NoRef" modes of Frequency Switch and Load Chop (in which

the User has opted out of the sky measurement in HSpot). More discussion of this scheme may be found in RD-6.

Generally speaking for the sake of optimal scientific returns from HIFI observations, individual spectra should always be carefully examined to determine if interactive corrections are needed before further processing, e.g., into averages in Point AOT observations, or before sideband deconvolution of Spectral Scans, or convolving datasets from mapped observations into spectral cubes.

A summary is given next on the presence of residual standing waves in Level 2 data that have all been reference-corrected in the standard fashion.

7.1 Bands 1-5 (SIS Mixers)

7.1.1   DBS Modes

Bands 1-5 data taken in DBS mode generally do not show standing waves at Level 2. Exceptions are sometimes observed, however, and in these cases the User can remove the waves with the sine wave fitting task 'FitHifiFringe' in HIPE.

Two cases are shown below.

- In Band 4b the diplexer causes a 650 MHz ripple. Figure 36 shows a sine wave fit (red) relative to a baseline (green), automatically determined with FitHifiFringe.
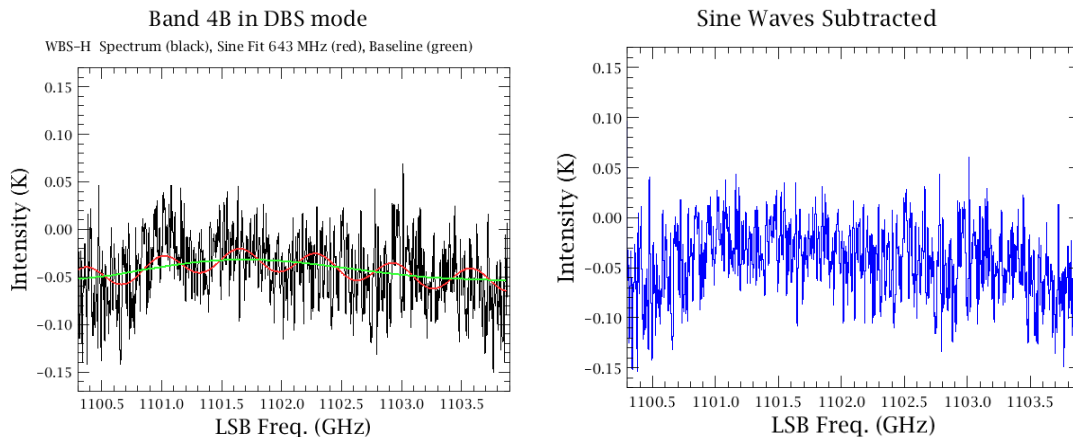

Figure 36: Standing wave residual at Level 2 in a DBS observation on the left, with the fitted sine wave (red) relative to a smoothed baseline (green), and corrected spectrum on the right.

Strong continuum sources show the effect of ripples in the passband calibration. The periods are typically in the 90-100 MHz range, and the amplitudes are at most 2% relative to the continuum. See Figure 37 for a case where 92 and 98 MHz since waves are present.
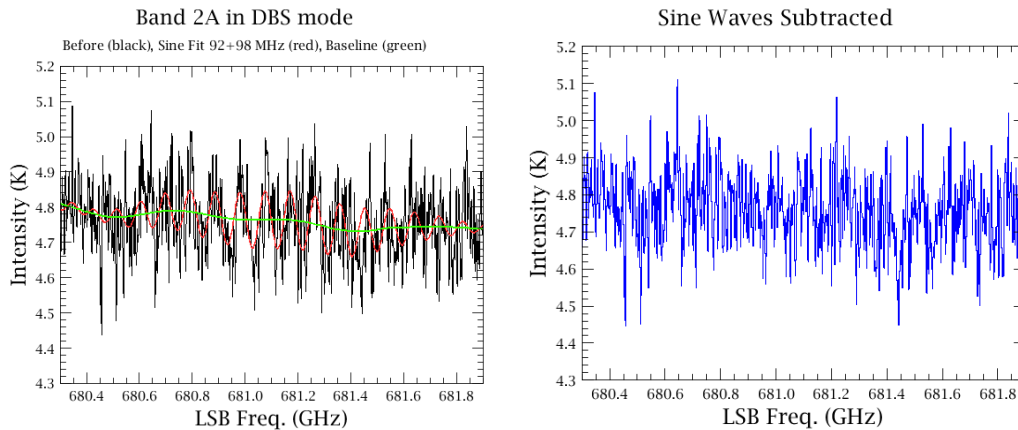
Figure 37: Strong continuum source with two standing wave components (red) relative to the baseline (green) on the left, and corrected spectrum on the right.

7.1.2   Position Switch, Frequency Switch, Load Chop Modes (Point and Spectral Scan AOTs)

Like calibrated observations taken with the Point or Spectral Scan AOTs using the DBS modes, the Position Switch, Frequency Switch (with sky reference measurement), or Load Chop (with sky reference measurement) modes in beamsplitter Bands 1, 2, and 5 also show the cleanest calibrated spectra. If any residual waves are present in the Level 2 products, they have the shape of pure sine waves and can be subtracted using the fitHifiFringe task in HIPE.

Observations in diplexer Bands 3 and 4 often show residual waves with larger amplitudes compared to the DBS modes. Waves generated in the diplexer rooftop are not pure sine waves. Amplitudes increase strongly toward the IF band edges. It is thus always advised to place the line of interest near the middle of the IF band when possible, in WBS sub-bands 2 or 3. Although fitHifiFringe only fits sine waves, fits to the diplexer waves can be approximated using multiple sine waves, typically around 600 MHz. The approximation is not as good at the IF band edges. Examples are shown for Bands 3 and 4 below. Note that the baseline is strongly curved in both observations, and the User can treat those separately in HIPE, using polynomials with fitBaseline.
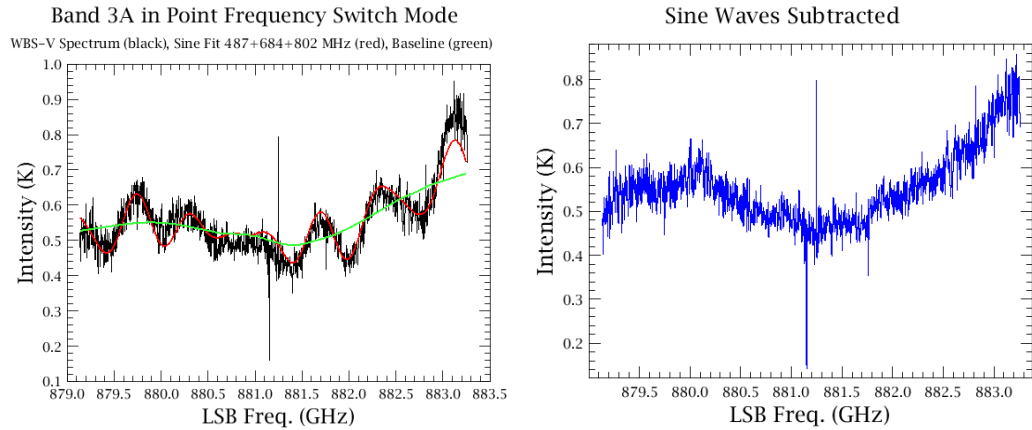
Figure 38: Band 3b observation using Point Frequency Switch at Level 2 after sky subtraction (left) and after interactive fringe fitting and removal (right). Note the poor edges in the spectrum on the right.
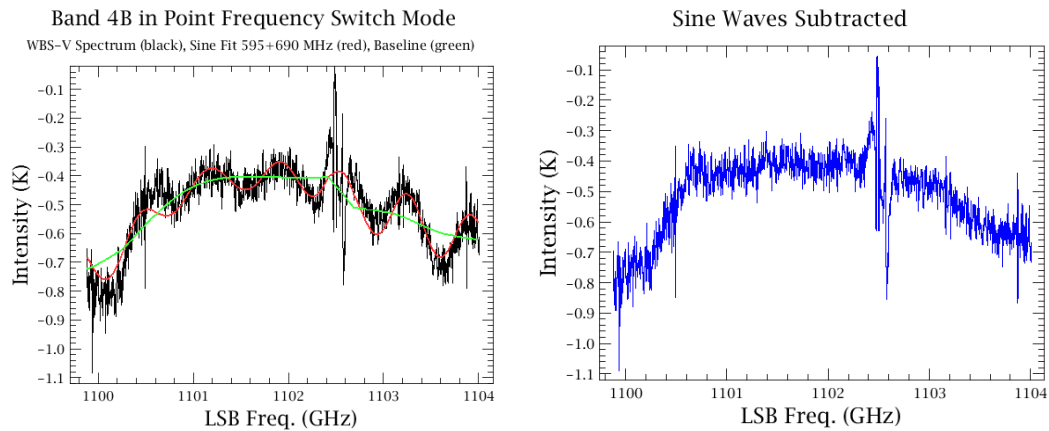

Figure 39: Band 4b observation using PointFrequencySwitch, showing a strong residual standing wave (black). Its period (~600 MHz) and increasing amplitude toward the band edges are those expected for diplexer bands. It was fitted with a combination of sine waves using FitHifiFringe (green). The corrected spectrum (blue) still shows a strongly curved baseline that can be subtracted with a polynomial fit in HIPE.

7.1.3   OTF Mapping Modes

Refer to Section 5.3.2.2 on baseline drift and standing waves in OTF maps.

7.2 Bands 6-7 (HEB Mixers)

The HEB mixers generate waves with characteristics that depend on the mixer current level, but since there is a dependence on LO power which may not be stabilized (between ON and OFF spectra), both electrical and optical standing wave residuals can

be mixed together. Data taken with all observing modes analyzed so far show residuals at Level 2, where the non-DBS modes tend to show larger and more complex residuals.

7.2.1 DBS Modes

Bands 6-7 are less stable than bands 1-5, and Level 2 data occasionally show residual waves. Examples are shown in Figure 40 for portions of Bands 6a and 7b. The latter was box-car smoothed by 5 channels.
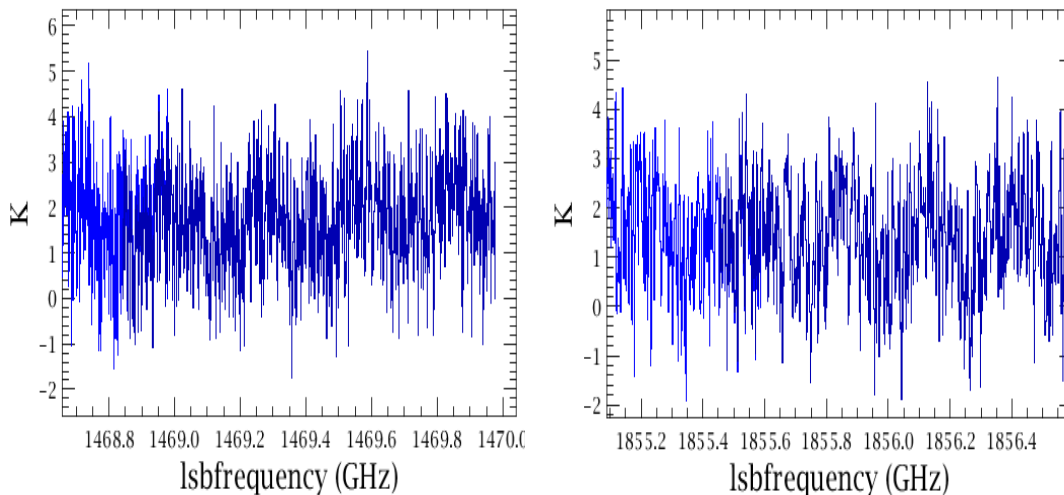

Figure 40: Standing wave residuals in Band 6a (left) and 7b (right).

These 'electrical' standing waves have periods of ~300 MHz, but they are not sine waves and 'FitHifiFringe' can only approximately remove them.

As for the presence of these waves the following general guidelines can be given:

- Band 6b is most stable and is least affected.
- FastDBS mode spectra tend to show weaker standing waves than 'slow chop' DBS mode spectra
- In Band 7, spectra taken with the vertical polarization spectrometers tend to show stronger waves than from the horizontal polarization. Sometimes this effect is very strong, as shown in the Band 7a observations below (Figure 41 and Figure 42).
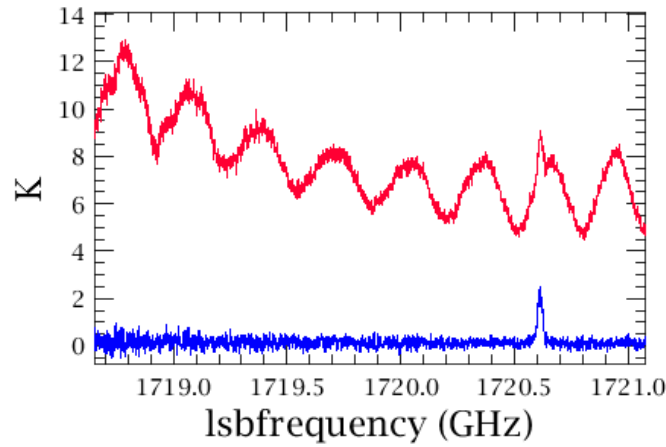
![HiFi ICC SRON logo]

HIFI Observing Modes
Performance Notes

Doc.: ICC/2010-009
Date: 24/09/2011
Issue: Version 3.0

Figure 41: Standing wave pattern in the Level 2 in Band 7a for WBS-V (red) and WBS-H (blue).

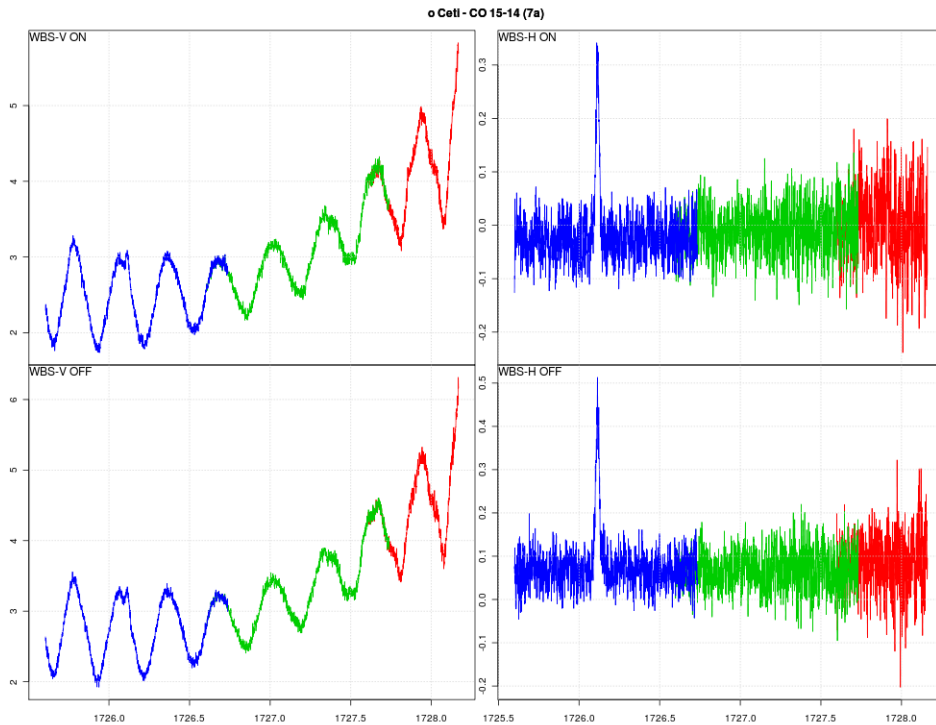*Figure 42: During the analysis of the FPG-3 raster map done on OD 278 (obsid 1342190805:Fpg3_M_FastDBSNoC_7a_CO_15-14_oCeti_3x3) it was found that the quality of the WBS-V has much poorer data quality, due to a large ripple, than WBS-H. The latter shows hardly any ripple at all. These data were processed using a "level1WithoutOffSubtr" algorithm and the plot shows both the ON and OFF phase for both polarizations. As can be seen the ripple in V in the ON and OFF phase will not cancel when averaged. When subtracted, most of the ripple is gone, but so is the line.*

7.2.2 PosSwitch, Frequency Switch, Load Chop modes

Non-DBS observations can show rather strong residuals in Level 2 spectra, with no specific tendency for the strengths or number of affected observations to be any better or worse by mode. However, since the problems occur primarily at frequencies where LO power has long stabilization times, we might expect Frequency Switch observations to have the poorest quality baselines with the artefacts of drifting instrumental response between measurements at f_1 and f_2. That there are ugly Frequency Switch data is true but there are no significantly fewer affected observations using standard Position Switch or Load Chop. Nonetheless, in releasing these observing modes at most frequencies, and through efforts to stabilize the instrument at important but problematic frequencies, the residual ripples in data which employ taking a sky reference as recommended are deemed treatable in software.

The best method to deal with ripples in the HEB bands is with the alternative calibration scheme mentioned in the introduction to this section (Sec. 7 point 2), using a database of OFF spectra which may be selected on the basis of ripple period, amplitude, and phase and possibly other housekeeping measures such as mixer current level. This approach should reduce the amplitudes of the residual standing waves considerably. The method requires a large database of ripple spectra and extensive testing with data from each observing mode at a time.

Presently in HIPE, the User may apply fitHifiFringe to remove the waves in Level 2 spectra. This method has limitations, because the HEB waves are not pure sine waves: they disperse over the IF band (i.e. their 'phase' changes). Examples are shown below for PointLoad Chop and PointPSwitch observations. As can be seen, the line shape in the WBS-V and WBS-H spectra differ somewhat after subtracting the sine-wave fit. This highlights another limitation of FitHifiFringe: *for broad lines covering much of the IF, insufficient surrounding baseline may be left to obtain accurate sine wave fits. In addition, as for the diplexer bands, solutions are less accurate for lines close to the IF band edge.*
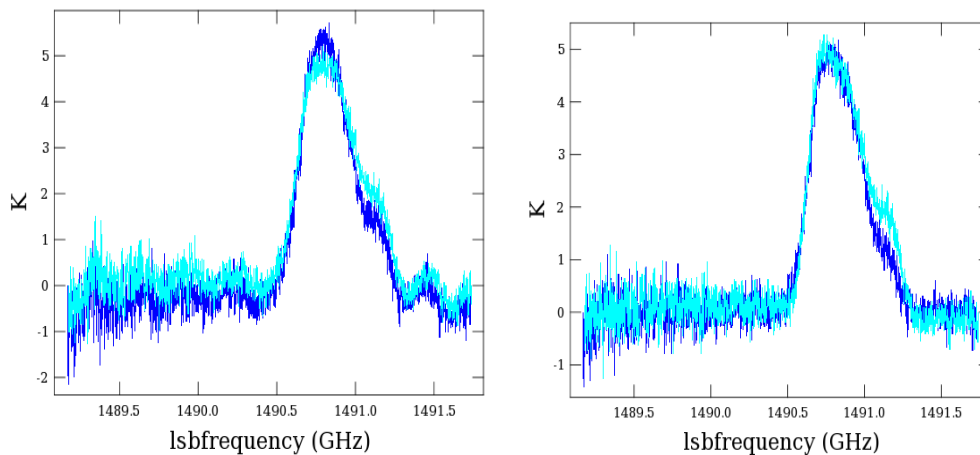

Figure 43: Band 6a PointLoad Chop observation showing residual waves in each of the H (dark blue) and V (light blue) after standard level 2 pipeline processing (left), and after standing wave removal using FitHifiFringe (right). The fringe-corrected spectrum has been shifted and a small scaling applied along the intensity axis so that the H and V peaks agree.
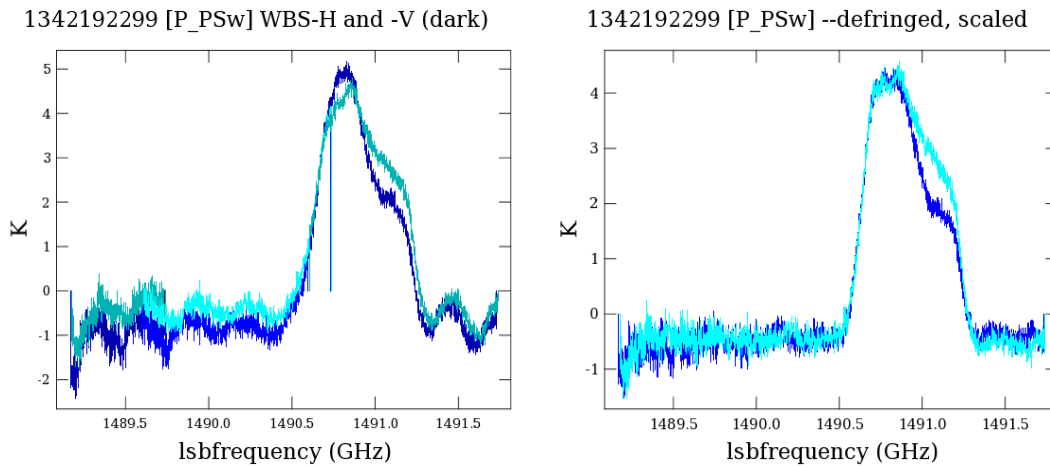
Figure 44: Same as Figure 43, using PointPSwitch.

8. Pointing

8.1 Focal Plane Geometry Calibrations "Part 3"

In PV-2 a first set of so called "FPG-3" observations were carried out, dedicated to refining the focal plane geometry parameters and beam properties, using CO and H_2O emission lines from AGB stars to check the pointing in a number of HIFI bands. They served the following purposes:

- Check the performance of the (Fast) DBS raster and DBS cross mode.
- Establish the S/N of the observed spectral lines and their usefulness for pointing verifications.
- Build up a database of pointing results on which eventually a SIAM update for the HIFI aperture entries may be based.
- Provide a set of raster maps to cross-compare with OTF mapping modes.

8.2 Observations

Table 7: List of FPG-3 observations carried out in PV-2, Blocks 1 and 2.

OD	ObsId	Source	Size	Line	Band	Mode	Comment
264	1342190237	o Ceti	5 x 5	CO 6-5	2a	DBS	
264	1342190238	o Ceti	3 x 3	CO 6-5	2a	DBS	
264	1342190243	o Ceti	3 x 3	CO 6-5	2a	DBS	
265	1342190156	NML Tau	3 x 3	CO 11-10	5b	DBS	no detection
265	1342190161	o Ceti	3 x 3	CO 9-8	4a	DBS	
266	1342190179	o Ceti	3 x 3	CO 5-4	1b	DBS	Failed due to SEU
266	1342190199	o Ceti	3 x 3	CO 6-5	2a	DBS	
266	1342190200	NML Tau	3 x 3	CO 6-5	2a	DBS	
267	1342190212	o Ceti	3 x 3	CO 7-6	3a	FastDBS	

267	1342190214	o Ceti	3 x 3	CO 10-9	5a	DBS
278	1342190805	o Ceti	3 x 3	CO 15-14	7a	FastBS
278	1342190806	NML Tau	3 x 3	H_2O 303-212	7a	FastDBS
279	1342190762	o Ceti	3 x 3	CO 14-13	6b	FastDBS
279	1342190765	NML Tau	3 x 3	H_2O 212-101	6b	FastDBS
281	1342190844	o Ceti	3 x 3	CO 5-4	1b	DBS
283	1342190902	R Dor	cross	CO 10-9	5a	FastDBSX
283	1342190903	R Dor	cross	CO 10-9	5a	FastDBSX
283	1342190908	R Dor	3 x 3	CO 7-6	3a	FastDBS

Table 8: CO transitions targeted as part of FPG-3.

Frequency	El	transition	band
MHz	*cm-1*		
576267.931	38.4481	5-4	1b
691473.076	57.6704	6-5	2a
806651.806	80.7354	7-6	3a
1036912.393	138.3904	9-8	4a
1151985.452	172.9780	10-9	5a
1267014.486	211.4041	11-10	5b
1611793.518	349.6975	14-13	6b
1726602.507	403.4612	15-14	7a

8.3 Results

In the following we show individual spectra and integrated intensity maps for all ObsIds. Note, that the data were pipelined using a Level 1 *without OFF subtraction* algorithm, this in order to assess the pointing of the ON and OFF phase of the DBS raster scheme separately.

The individual spectra show baseline ripples with opposite phase as expected, the final DBS spectra (not shown here) therefore will have flat baselines. Because the spectral lines sit on top of the ripple at different phase, they do not match up perfectly in the spectrum maps.

Noteworthy is the non-detection of the CO 11-10 line and very weak detection of CO 6-5 in NML Tau. This latter observation was carried out immediately after the same line in o Ceti, which looks fine, so it is not expected that this observation suffers in any way from the aftermath of the SEU. In fact, the lines in NML Tau are expected to be considerably weaker and broader than in o Ceti, according to APEX results. The purity issues in Band 5b (Sec. 4.3.1.3) at the time of the measurements may have complicated the detection as well. Note however, that NML Tau could be used to check pointing alignment in Band 7a, where the H_2O 3_{03} - 2_{12} 1721.3 GHz emission line is well detected in the same map (i.e. set up in the AOR to observe both possible lines).
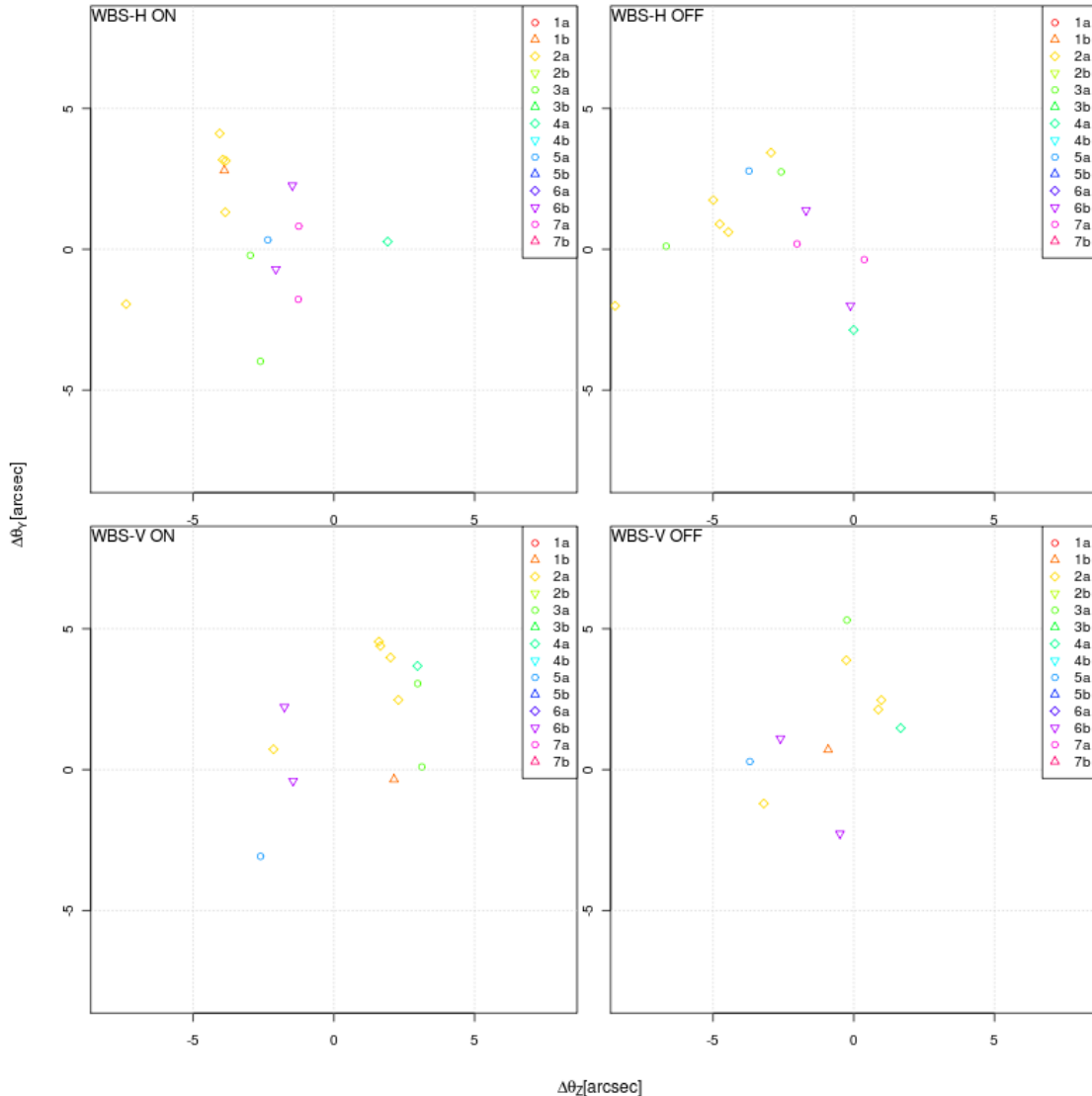
Figure 45: Observed and fitted focal plane offsets.

Figure 45 shows the fitted focal plane offsets colour coded by band. Note, that the measurements were all carried out using the SIAM entry for the synthesized HIFI beam in each band, which is an average of the beam positions of the H and V mixers (discussed further below in this section).

In all pointing maps observed during PV-2, the central grid position always showed the strongest signal, i.e. all of these observations would have succeeded as single point observations. Based on these results there is at present no need to update the HIFI SIAM entries.

The SIAM provides entries for the angular rotations from the telescope boresight (optical Attitude Control Axis) to the set of HIFI beams in the focal plane. The SIAM contains offsets for each of the seven H polarization mixer beams, one per band, and corresponding so-called synthetic beams which are effectively the average of the H and V mixer beams in focal

plane coordinates. The commanded pointing is always referenced to a synthetic beam as the prime instrument frame. Figure 46 schematically illustrates the offsets of the HIFI beams in the focal plane. These offsets should be kept in mind when comparing spectra from the two separate polarizations (taken simultaneously at slightly separated positions on the sky, and processed separately in the pipeline), especially on extended sources which may be intrinsically polarized at frequencies of interest.
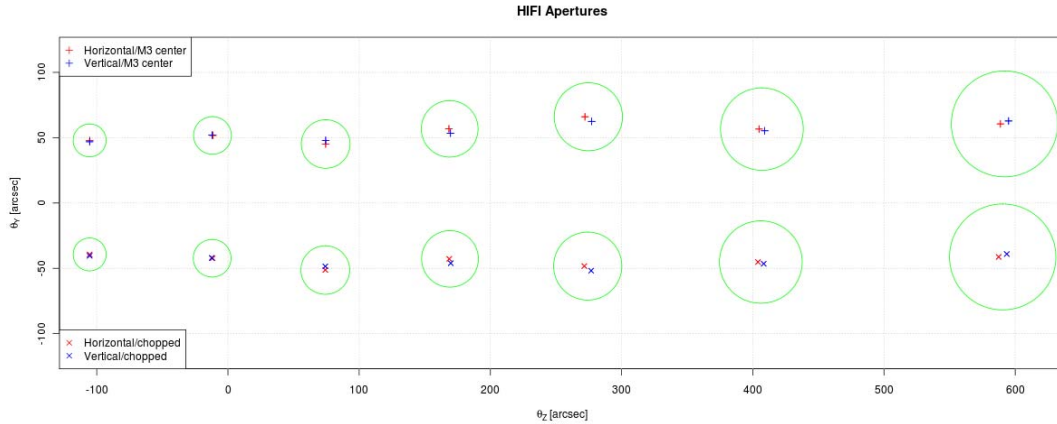

Figure 46: Locations of the HIFI apertures, highlighting the difference between H and V. Only H apertures are represented directly in the SIAM, the V entries are calculated from these and the locations of the synthesized beams, assuming a symmetric location of H and V with respect to the synthesized ones. The green circles represent HIFI FWHM beams centered on the synthesized beam locations.

Since the angular separation between the H and V beams may be important when interpreting observations on extended sources, the User may deduce the relative offsets directly from the SIAM with a script which is provided in the Appendix.

9. Intensity Calibrations

The 12 m APEX telescope uses a number of AGB stars as standard sources for line calibration. In particular the results obtained by Risacher and van der Tak [1] for the CO 6-5 line at 691.4730763 GHz offer the opportunity to compare with HIFI results during PV-2.

9.1 Observations

Table 9 lists operational day and ObsId for those observations which were analysed for this report.

Table 9: List of observations

OD	ObsId	Source	Observation
264	1342190237	o Ceti	DBSRaster
264	1342190238	o Ceti	DBSRaster
264	1342190243	o Ceti	DBSRaster
266	1342190199	o Ceti	DBSRaster
264	1342190242	R Dor	DBSPoint
264	1342190240	IK Tau	DBSPoint
266	1342190200	IK Tau	DBSRaster

266	1342190196	W Hya	DBSPoint

9.2 Results

Table 10 lists observed peak intensities and line widths, obtained by fitting Gaussian profiles to the observed lines. Note, that the assumption of this type of profile is not necessarily justified, e.g. o Ceti shows signs of self-absorbed CO lines. However, it allows a standard procedure to be used for the derivation of quantitative values for the purpose of this report.

Table 10: Observed line intensities and widths.

| | | HIFI | | | | | APEX | |
| | | **H** | | **V** | | | | |
Obsid	**Source**	**peak** [K]	**width** [km/s]	**peak** [K]	**width** [km/s]	**H/V**	**peak** [K]	**width** [km/s]
1342190237	o Ceti	3.29	5.4	3.51	5.4	0.94	34.5	4.8
1342190238	o Ceti	3.28	5.4	3.51	5.4	0.93		
1342190243	o Ceti	3.23	5.6	3.51	5.6	0.92		
1342190199	o Ceti	3.32	5.5	3.52	5.5	0.94		
1342190242	R Dor	1.52	9.1	1.66	9.1	0.92	17.1	9.1
1342190240	IK Tau	0.36	24.8	0.49	24.8	0.73	6.6	24.2
1342190200	IK Tau	0.39	25.9	0.49	25.9	0.80		
1342190196	W Hya	0.88	11.4	0.91	11.4	0.97	?	?

The beam width of the Herschel telescope at the frequency of the CO 6-5 transition is Θ_H = 32.7", whereas the APEX telescope has a HPBW of Θ_A = 9.5" at this frequency.

Given a source size Θ_S, also in arcsecs, the expected intensity scaling between main beam brightness temperatures observed by APEX (I_A) and HIFI (I_H) can be expressed as

$$I_H = I_A * (\Theta_S^2 + \Theta_A^2)/(\Theta_S^2 + \Theta_H^2)$$

Solving for the source size we get

$$\Theta_S^2 = (\Theta_A^2 I_A - \Theta_H^2 I_H)/(I_H - I_A) \qquad \text{(Eq. 1)}$$

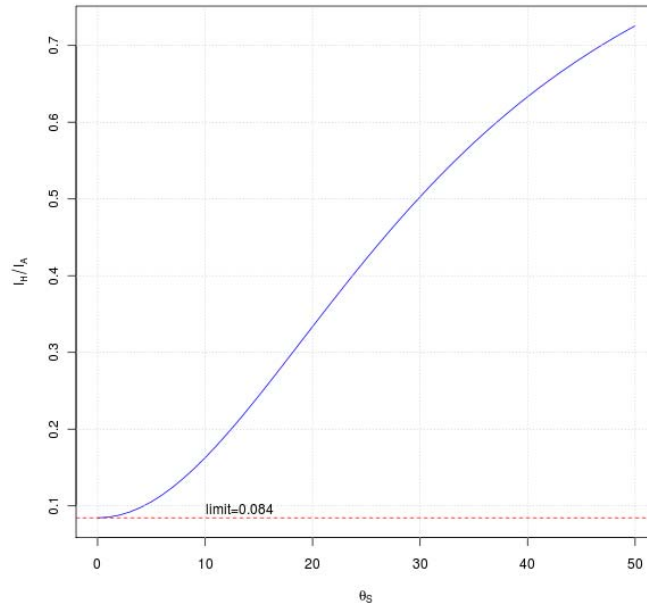Figure 47 shows the expected intensity ratio as a function of source size.

Figure 47: Expected ratio of HIFI to APEX main beam brightness as function of source size.

We use a main beam efficiency of η_{mb} = 0.74 to convert observed antenna temperatures for HIFI to a main beam brightness scale.

For o Ceti we get a source size of 4.1", corresponding to $7.8*10^{15}$ cm at an assumed distance of 128 pc. For R Dor the size calculated according to Eq. 1 is 3.2", or $2.9*10^{15}$ cm at a distance of 61 pc. Finally, for IK Tau Eq. 1 does not produce a real-valued solution for Θ_S, because the ratio I_H/I_A is lower than the value of 0.084 predicted by Eq. 1 in the limit of vanishing source size (see Figure 47). Note, that there is also a very deviating H/V ratio for this source in Table 10. However, comparison with the overall predicted spectrum shows no obvious problem with the observed intensities.

10.   Frequencies and Velocities

Summarizing, there are no systematic errors seen in the HIFI frequency calibration, either instrumentally or in the pipeline. The user can expect that frequencies as presented in any of the three defined frames (LSRk by default; SSBC, Geocentric, and spacecraft("HSO") available) are absolutely correct to 100kHz or better in WBS spectra, and ~50 kHz for HRS spectra.

10.1 Outstanding Issues

Presently there are no issues which affect the quoted frequency calibration accuracies, following several minor changes or clarifications since launch in how velocities of the spacecraft are computed in the fiducial reference frames, and used in the pipeline.

Users may be aware, however, of a hardware issue with the comb generator in the V section of the WBS, that the signal has been noticed to weaken over time. This was first

noticed in ground-based testing but already when the instrument was fully integrated into the telescope, and has weakened in steps over the mission. At the moment the signal is strong enough that fits to the individual comb lines still provide required accuracies of the WBS frequency calibration (100 kHz). In the event that the comb signal begins to compromise accuracies (and this is routinely monitored), an alternative cross-calibration scheme using the HRS has been tested and is ready, offering somewhat degraded performance (~500 kHz). The ICC continues to improve the method and expects to close in on the comb accuracy by the time the scheme is in actual use in science observations.

10.2   Absolute Frequency Consistency

Literature velocities have been compared with a set of HIFI line measurements, and in all cases good agreement was found given the uncertainties (e.g. different species, data S/N ratios). An example shown below is CO 6-5 in IK Tau, in which the measured velocity shift is in excellent agreement with the intrinsic source velocity.
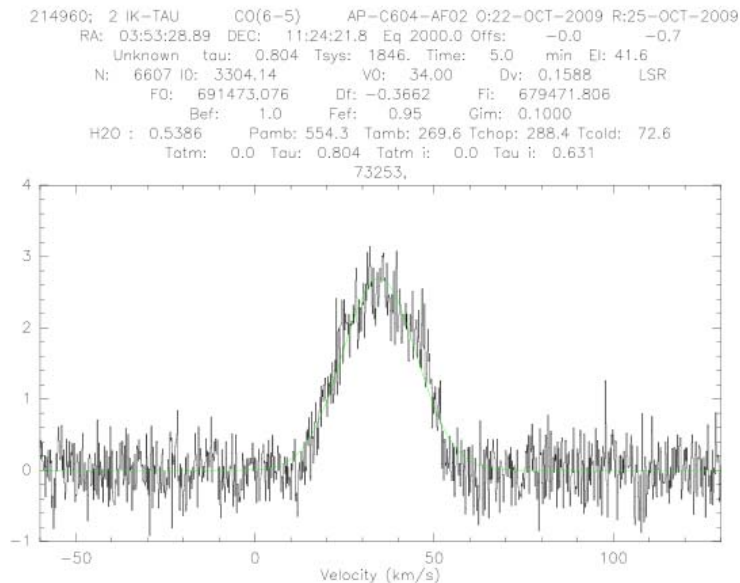

Figure 48: CO 6-5 in NML Tau (IK Tau), with a measured velocity shift of 34.0 km/s that agrees with the intrinsic velocity of the source, and with APEX measurements.

When possible, a cross-comparison between modes and a check of the spectral line repeatability has been made, e.g. using the CO 5-4 line towards o Ceti, also observed from the ground by APEX. Agreement between H and V and both spectrometers HRS and WBS has been verified, in terms of line center frequency and width. Agreement is nominal, except for a (now fixed) misplacement of the HRS band center due to a difference in the treatment of reference frames in the proposal and mission planning software. The effect was significant only for the HRS when used in high resolution mode in the high frequency bands.

10.3 Multi-epoch Frequency Consistency

Observations of the same line and source at multiple epochs have also been compared, and the detected line frequencies match. The longest check was for source LDN1157- B1, taken 186 days apart, and the motion of the spacecraft is correctly removed to an accuracy of better than 0.5 MHz (0.3km/s).   A detailed summary of H and V profile agreement is given in Sec. 11.
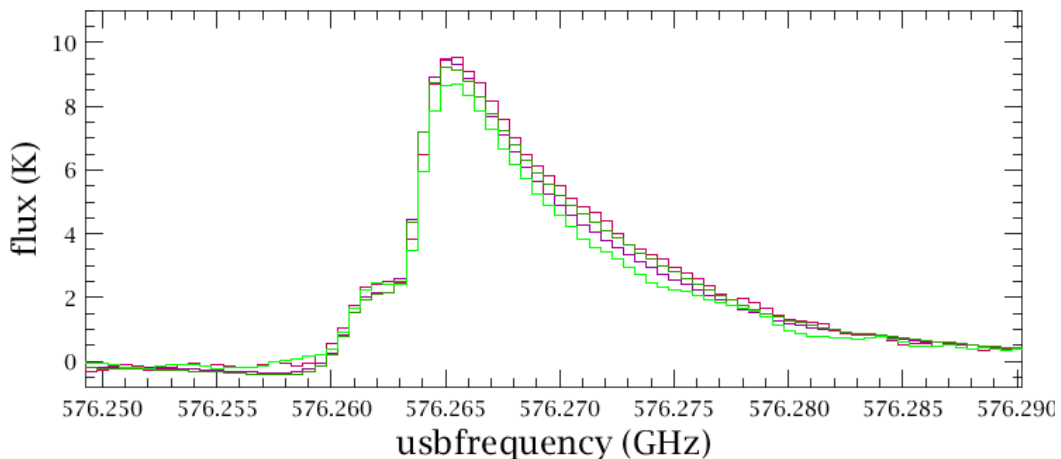
10.4 Solar System Objects

In the case of SSOs, the default HIFI pipeline produces spectra with frequencies in the rest frame of the target. The target motion is defined in an ephemeris, produced by the JPL Horizons project, and may be accessed in HIPE as an auxiliary data product in the observation context, namely obs.refs["auxiliary"].product.refs["HorizonsProduct"].product. As noted above, the SSO orbit prediction might improve some time after processing in earlier versions of the pipeline, in which case you should reprocess in HIPE or request reprocessing with the new Horizons ephemeris.

Tests with comet Wild-2 on 01 and 04 February 2010 (see examples in Figure 49) showed line velocities constant with ~50 m/s uncertainty (in the SSO frame) while the apparent radial velocity over the same period changed by 420 m/s.

1342190231.WBS–H lev 10

LO=1107.378

1342190231.HRS–H lev 10

LO=1107.378
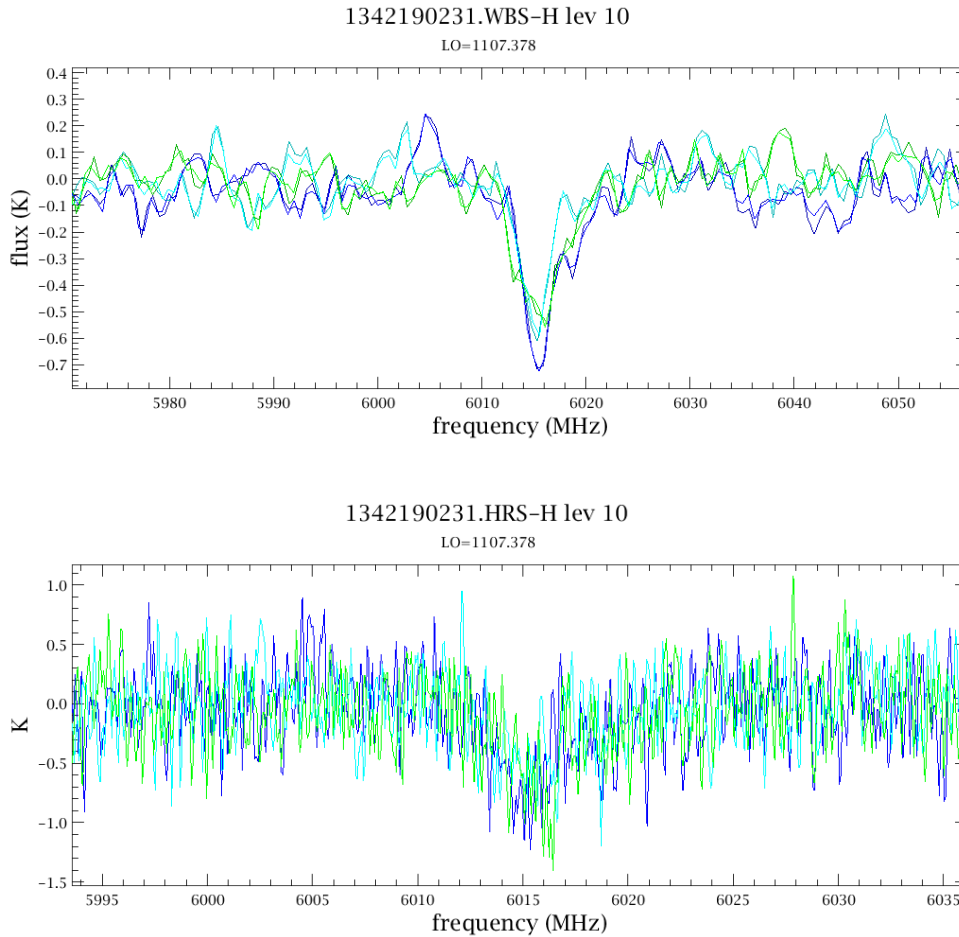
Figure 49: Example Wild-2 spectra from the WBS (top) and HRS (bottom) at Level 1. Note that these data were taken with the FastDBSCross mapping mode (no longer offered in HSpot), and negative amplitudes are a result of the ON an OFF phases being out of synchronization. The Level 2 frequency scale below is in the LSR frame.

10.5 Velocities in the HIFI Observation Context

There are a various velocities and LO frequencies to be found in a HIFI observation context. Here is some explanation for the interested User (as of HIPE 6.1):

a. ObservationContext.meta['radialVelocity'] :

This is the velocity of the spacecraft, as seen by an observer at rest in the LSR, in the direction of the target. It is <u>not</u> used in the HIFI pipeline. Note that the sign convention is opposite to the astronomical "radial velocity." This has caused confusion and there are plans to change the sign and the explanatory text in the metadata.

Our advice is not to use this datum in any calculation where precision matters.

b. htp.meta['vlsr'] :

This is the user-entered target redshift from HSPOT, used in setting the LO in uplink so that the desired line is in the IF band, but has no role in the default pipeline.

It is used if the user transforms frequencies to the frame of the (nonSSO) target with the task doVelocityCorrection, in which case correct interpretation of the 'vlsr' value requires the metadata 'redshiftType' and 'redshiftFrame' to be defined -- see the doVelocityCorrection documentation (HIFI Pipeline Specification or HIFI URM, see RD-4).

c. columns at dataset level:

i. 'velocity_hso_1', _2, and _3 are the three components of spacecraft velocity in the SSBC frame at the midpoint of the integration. This velocity is used to transform from spacecraft to other frames. The coordinate axes are the DE405 system, ie J2000.

We recommend using these values in calculations, as they are appropriately time-tagged.

ii. 'LoFrequency_measured' is the real insrumental LO setting.

iii. 'LoFrequency' is LO adjusted for radial spacecraft motion in the LSR. This is inserted at Level1 for bookkeeping purposes and the use of the deconvolution task.

11. H and V Profiles

11.1 Contributing sources of H and V profile disagreements

The agreement between H and V profiles of lines observed during PV has been investigated, with particular attention paid to an outflow source, L1157-B1, which was originally observed during PV-1 in August 2009 and exhibited a deviation between the H and V line intensities of up to 20% and re-observed twice during PV-2. The levels of agreement (or disagreement) are important to characterize, since contributing factors may include any of telescope pointing, angular separation of the H and V beams on the sky (cf. Sec. 8.3 and the table below), possible intrinsic polarization of the source at the line frequencies of interest, and instrument calibrations (different beam efficiencies or sideband gains) or power level output from the spectrometer back-ends. The internal calibrations could account for up to 6-8% disagreement between H and V profiles, measured as integrated fluxes.

IF spectral repeatability of point sources (see Sec. 12.2) show that H and V profiles are in good agreement across bands 1, 2, 4 and 5 to within 3%. The beam efficiencies have been more fully characterised using observations of Mars in April 2010 (see e.g. RD-1) and will be further refined as part of the Routine Phase calibration plan when Mars, Uranus, and/or Neptune are available in the Fall of 2011.

The effect of pointing offsets between the two polarisations on line profiles in the case that the emission is extended or has a strongly varying velocity structure is harder to quantify.

![HiFi ICC SRON logo]

**HIFI Observing Modes
Performance Notes**

Doc.: ICC/2010-009
Date: 24/09/2011
Issue: Version 3.0

The difference in H and V co-alignment was measured during the Check-Out Phase and the findings are given in the Table below.

Table 11: Co-alignment of H and V beams as measured during CoP.

Band	ΔHV in Y (")	ΔHV in Z (")
1	-6.2	+2.2
2	-4.4	-1.3
3	-5.2	-3.5
4	-1.2	-3.3
5	0.0	+2.8
6	+0.7	+0.3
7	0.0	-1.0

11.2 Compact Sources

Line centres and line shapes are in excellent agreement between H and V profile among the AGB stars observed during PV-2. In many cases, the V polarisation shows the stronger line but typically the peak values of the H profiles fall within 7% of the peak in V.

One exception to this is NML Tau, which showed differences in the peaks of profiles of over 30%, in some cases. Some of the profile discrepancies (e.g., obsid 1342190160 where the peak of the V profile was 1.275 times that of the H) can be attributed to data quality that suffers from when the line is located at the band edge in a region of high Tsys (see Sec. 6). In two other cases it was found that there was a greater scatter of individual datasets at Level 1 about the mean in one polarisation (V) than the other (see Figure 50 below), possibly reflecting different power output levels between H and V.
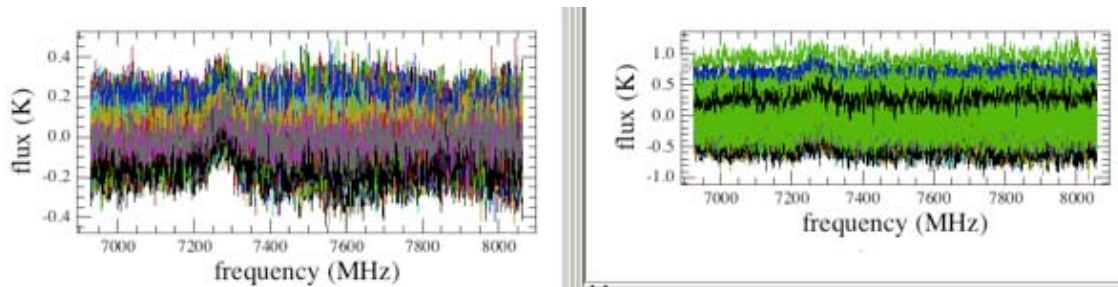

Figure 50: The spread in datasets at Level 1 in V (right) is three times that of H (left), this contributed to a 22% difference in the peaks of the H and V Level 2 profiles in obsid 1342190160.

In certain cases this effect at Level 1 leads to an apparent shift in line centre in the V polarisation at Level 2, but this could be remedied by removing outlier scans from the Level 1 data before averaging.

Beyond these cases, there remains a larger difference in H and V profiles than is expected from uncertainties in sideband gain or beam efficiency correction. In the spectrum below of NML Tau the peak in H is 74% of that in the V polarisation. After simply scaling the H polarisation up it is seen that there is no mismatch in profile shape.
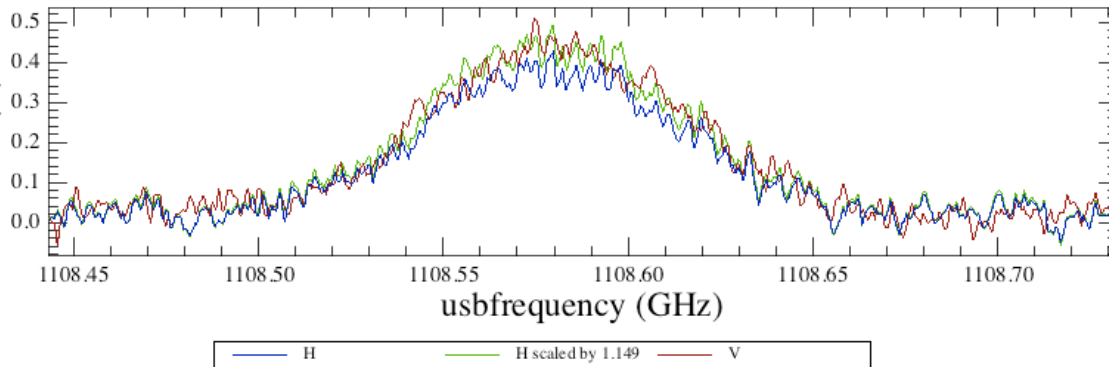
Figure 51: H and V profiles in this observation differ by 26% at the peak, rescaling so the peaks match show no difference in line shape

11.3 Extended Sources

- **Example 1: LDN1157-B1**

L1157 is a well-known Class 0 proto-star associated with an energetic outflow that displays shocked structures along its length including a bow shock in the blue lobe. The velocity structure around the source is also complicated by in falling and accreting material.

Observations in the blue lobe of L1157 were made in Band 1b in Spectral Scan DBS mode with (1342181161) and without (13421811160) continuum optimization during PV-1 in August 2009. The two observations were well matched with each other but displayed a pronounced discrepancy in CO 5-4 H and V profiles reaching up to 20% in the line wings. The profile discrepancy was still seen even after the peak in the H polarisation was scaled up to align with that in V profile, with the V remaining stronger in the wing.

L1157-B1 was observed again in Band 1b 186 days later in PV-2, using the PointFastDBS mode with continuum optimization (1342190183) and in PointDBS without continuum optimisation (1342190184), and the latter observation repeated again in the same 40 days later (1342192229). The roll angle of the telescope is ~180° with respect to the PV-1 observations. In all cases the V polarisation displays a higher intensity line than the H. Figure 52 shows the H and V line profiles for observations 1342181160 (160), 1342190184 (184), and 1342192229 (229), scaled so that all the peaks (per observation and polarisation) align.
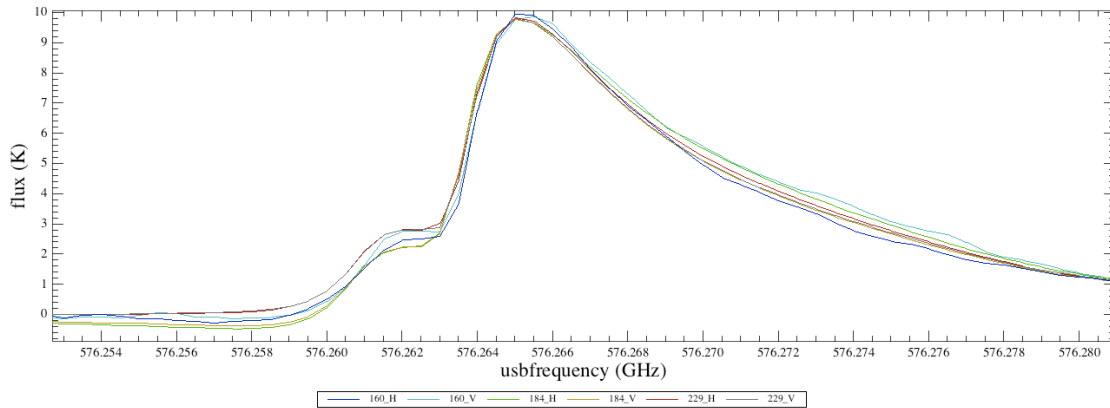
Figure 52: H and V profiles for obsids1342181160, 1342190184, and 1342192229, scaled so line peaks match.

There are several things to note from this figure:

- The polarisation discrepancy in the wing is in the opposite sense for 160 and 184.
  - As the observations were performed 6 months apart, this could imply that there is some bright region of the outflow contributing to the profile mismatch rather than an intrinsic polarisation effect.
- It can be seen that the profile discrepancy has reduced with successive observations from approaching 30% in 160, to 10% in 184, until in 229 there is a difference in profile in the wing of only 4% (Figure 53).
  - 184 has a lower noise goal resolution than 160, while 229 is free from emission in chop positions.

The discrepancy at the peak of the line is very similar for 160 and 229, and is approximately 8% but is only ~4% for 184. This could be an effect of the emission in the chop position (see next bullet).
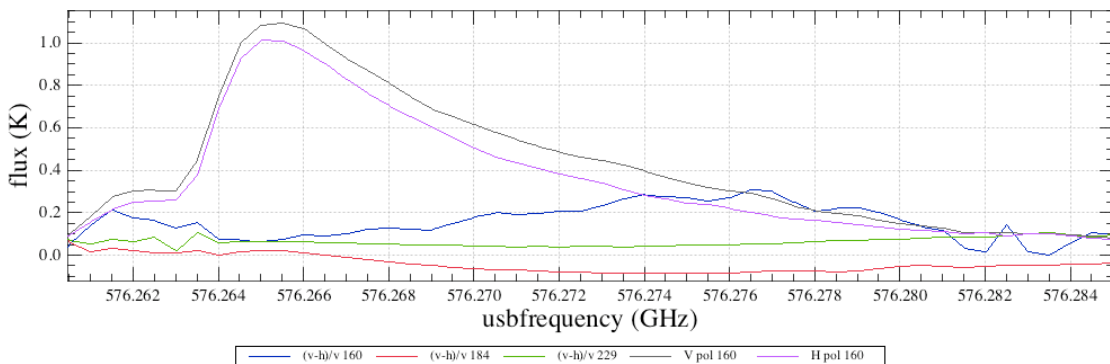

Figure 53: Fractional differences in H and V profiles approach 30% (160), 10% (184) and 4% (229). The H and V profiles of 160 are plotted to illustrate the variation across the line.

- There is a clear dip before the line peak in 184 (also seen in 183) and a hint of the same in 160.
  - Investigation of the reference positions at Level 1 show that there is emission in the reference position when chopping off the source for 184 (Figure 54).

- o There is no emission is the reference positions for 229.
- o The H and V profiles in 184 and 160 show some discrepancy at frequencies below the line shift, while 229 does not, this effect is due to the emission in the chop position.
- o The contaminating emission does not affect the line profiles in the wing. There is no evidence of differing levels of emission in the two reference positions, but this does not preclude the possibility that both reference positions contain an equal level of emission. However, this shows that the differences in profile in the wing are not a product of chopping into source.
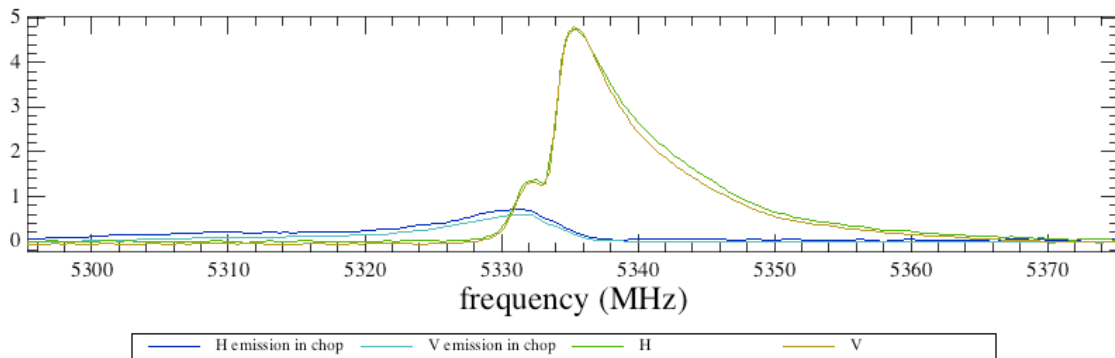
Figure 54: 1342190184. Emission in chop position from On source. The contaminating emission affects the line profile until just beyond the peak, and so has no influence on the discrepant H and V profiles in the wing.

From the above, an investigation of the separate emission in the reference positions and ON source is warranted. To do so, the observations were reprocessed, skipping the doRefSubtract and doOffSubtract steps of the Level 1 pipeline (using HIPE 2.6). The reference and source measurements could then be investigated in the ON and OFF positions. Figures Figure *55* and Figure *56* show the H and V profiles derived from the ON and OFF positions separately for 184 and 229, respectively. A profile difference can be seen even in one polarisation between the two positions.
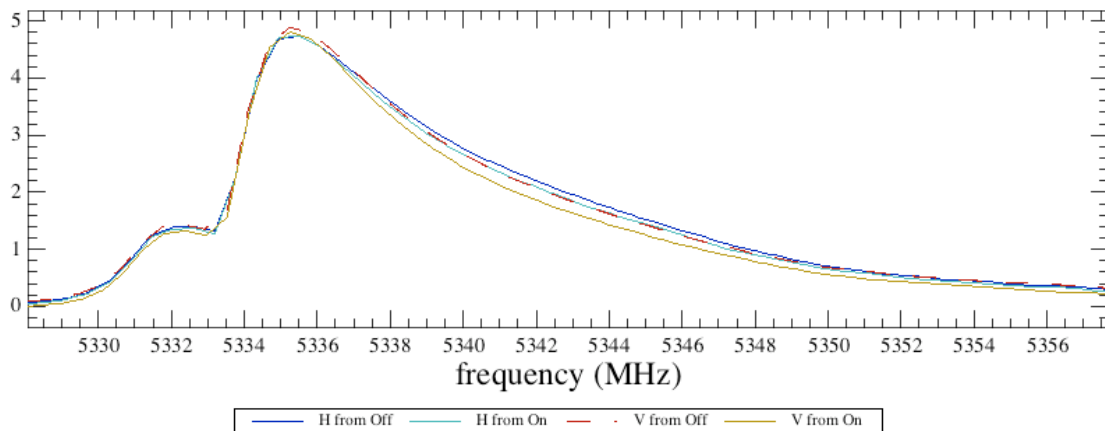
Figure 55: H and V profiles derived from ON and OFF positions separately for 1342190184. It is interesting to note that the V profile from the OFF position corresponds exactly with the H profile from the ON position.
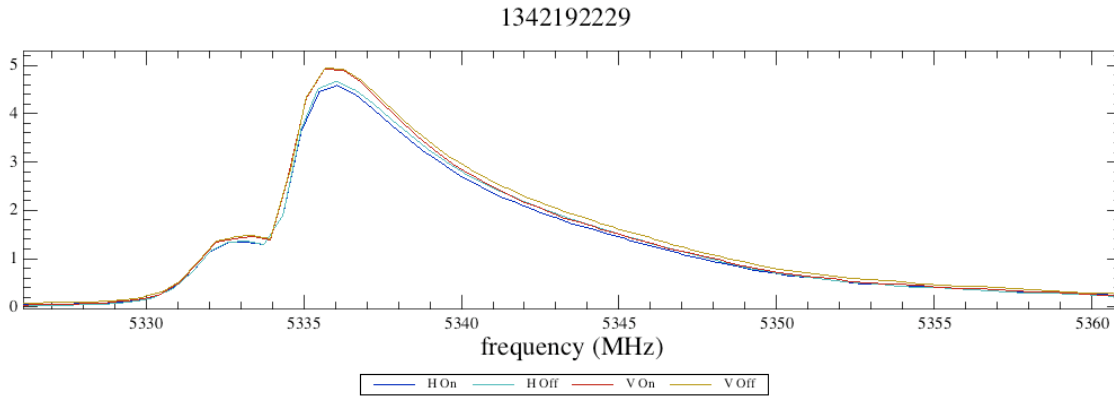

Figure 56: As for HV-6 but for 1342192229. The same behaviour is seen but the overall spread in profiles is smaller than for 184.

One possible reason for this behaviour could be that there is some scatter in where HIFI points for each integration due to shifts after telescope slews between the ON and OFF positions and as HIFI chops between source and reference. Figure 57 shows the pointings for each integration on source for 184, the spread is approx 2" (and is very similar for 229).
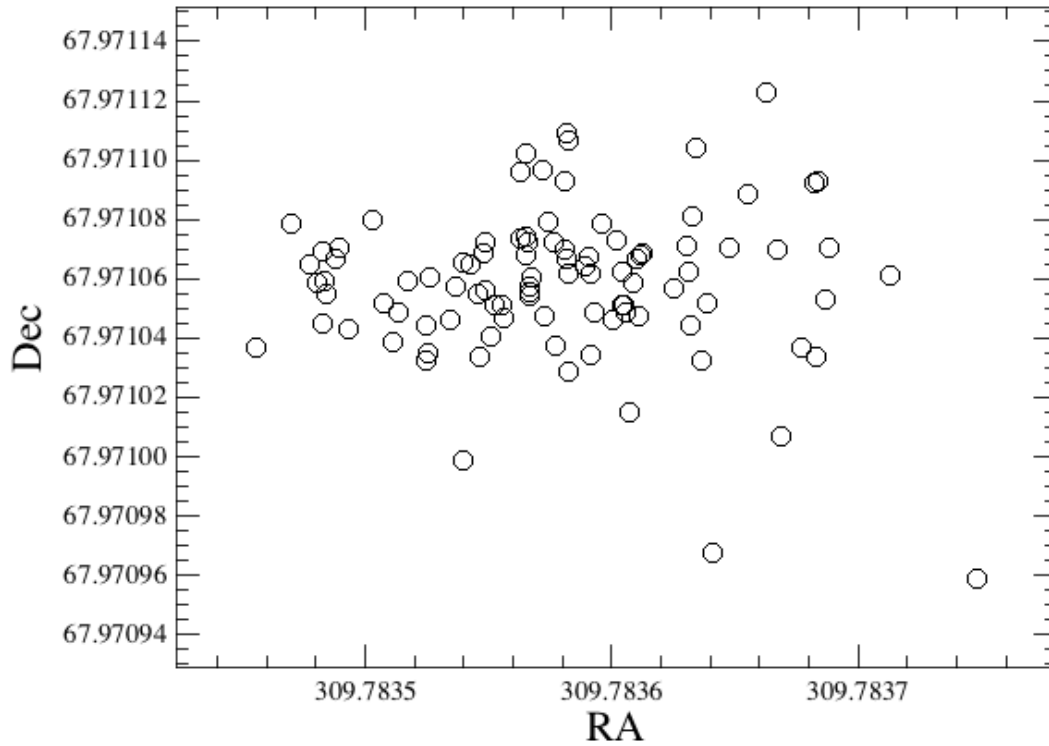
Figure 57: Pointings of each integration on source for 184.

This scatter in pointing (and perhaps in combination with velocity structures arising in shocked regions in outflows) could give rise to the difference in profiles seen between the ON and OFF positions. In support of this theory, the fractional difference in intensity relative to the mean intensity of each integration for each polarisation are plotted in Figures Figure *58*, Figure *59*, and Figure *60* for the ON and OFF positions. A line profile is plotted in each case to show variation with position in the line. If variations between individual integrations are affecting the profile in the wing then the fractional difference should increase there.
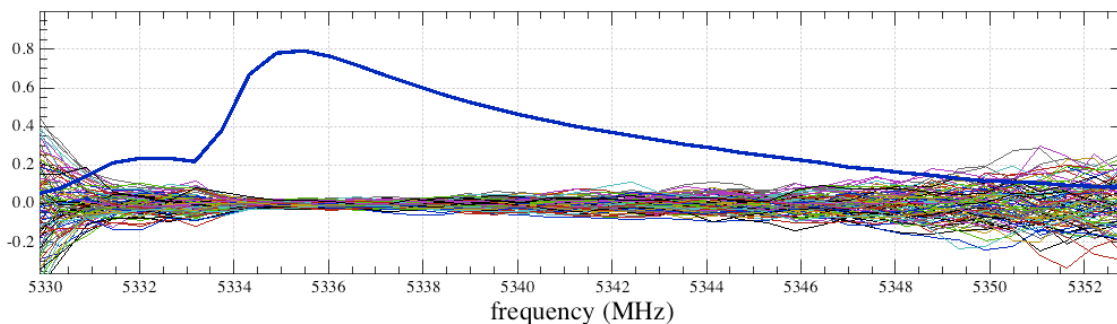

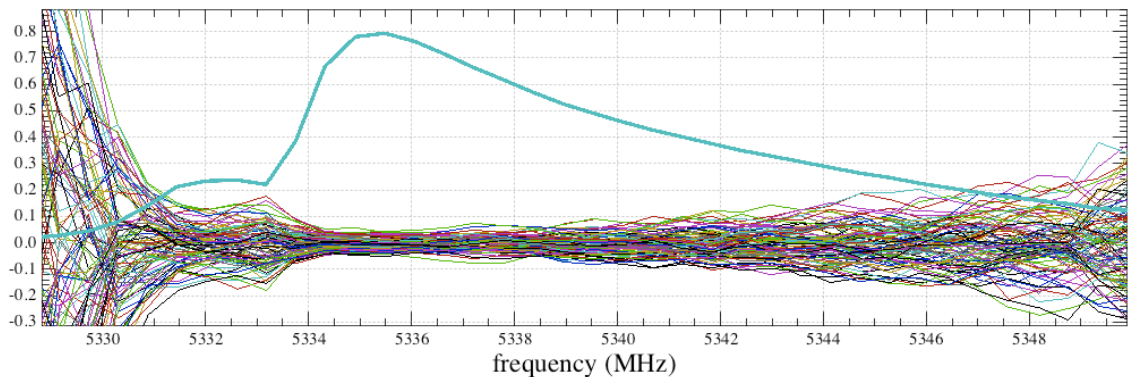
Figure 58: (H-Hav)/Hav for the Off position for 1342190184.

Figure 59: (H-Hav)/Hav for the On position for 1342190184. The spread is greater at the low frequency end of the line than for the Off position, this may be due to the emission in the chop position.
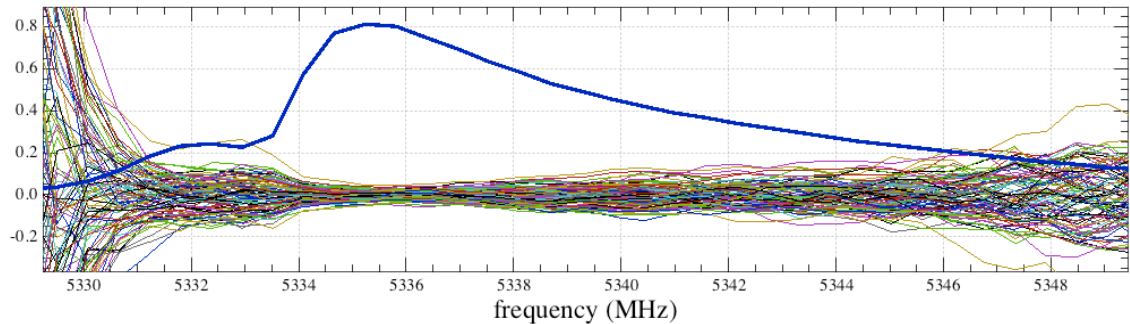

Figure 60: (V-Vav)/Vav for the ON position for 1342190184.

The fractional difference reaches (and even exceeds) 0.1 in the wing of the profile, compared with <0.05 near the line peak. In band 1 the offset between the H and V beams is (-6.2", 2.2"). It seems reasonable that if a scatter in pointings can give rise to a difference in one polarisation between ON and OFF positions then this further difference in pointing in H and V could cause differences in H and V profiles. Furthermore, if the chop direction was along the outflow, as was the case for 160 and 184 this could generate a significant difference in H and V in the wing of the profile.

- Example 2: Orion Bar (OTF Map)

It was shown in Section 5.3.2.4 how the presence of the OTF "zig-zag" can affect line flux measurements, especially where source signal gradients are strong. A related question is the agreement between H and V spectra taken at the same time but slightly offset due to imperfect beam alignment. For obsid 1342217720 (a Spectral Scan observation of a selected position in the Bar in Band 4b), a large difference is seen for the ^{13}CO (10-9) line (1101.35 GHz). The difference between H and V is close to 30% (see *Figure 61*). We can examine the standard OTF Position Switch map 13422215970 on a water line in Band 4b in the same region in order to verify if there is an H/V imbalance in the Orion Bar due to pointing differences of the two beams on the sky, or if instead this is due to some internal stability issue.
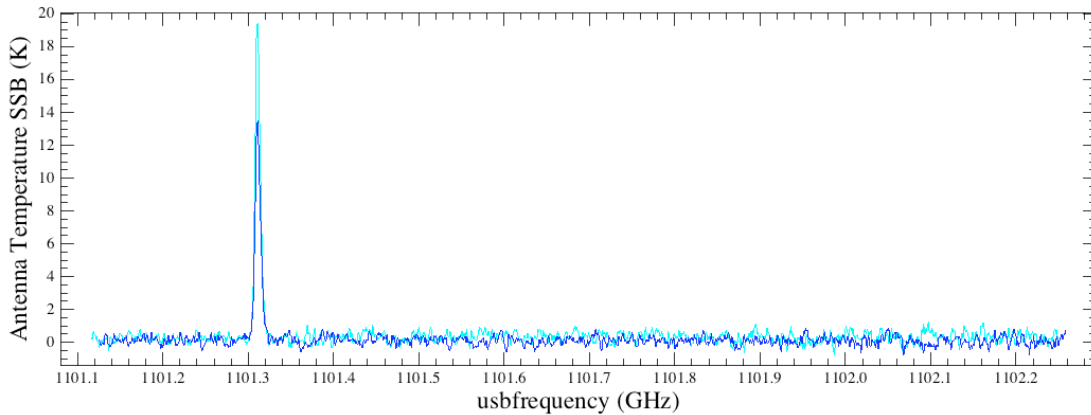
![HiFi ICC SRON logo]

**HIFI Observing Modes
Performance Notes**

Doc.: ICC/2010-009
Date: 24/09/2011
Issue: Version 3.0

Figure 61: ^{13}CO (10-9) in 1342217720, H (light blue) and V (dark blue).

Figure 62 shows the data from WBS-H before any corrections for baseline levels or fringes.
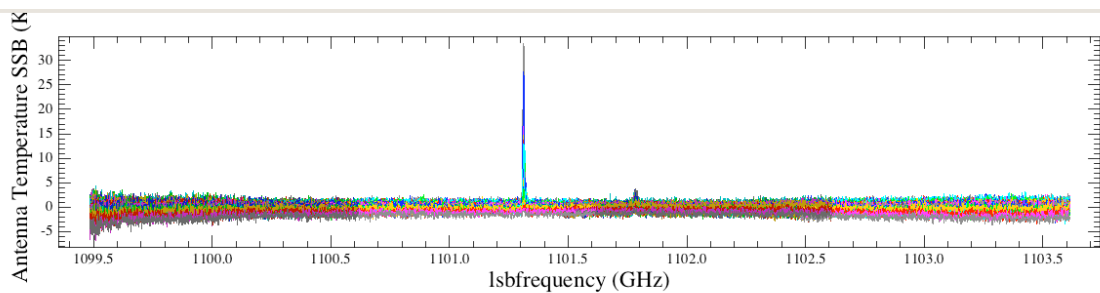

Figure 62: Spectra of 1342215970 in WBS-H-LSB before any correction of the fringes and baseline levels.

Figure 63 shows the mapping grid for this observation, consisting of 13 points (spacing of 8″.7) and 7 OTF lines (spacing of 9″.0). The cubes were built using a beam size of 21″ (suited to Band 4b) and a pixelSize of 9″ x 9″, and taking into account the rotation of the OTF mapping (**NB:** for users of the HIFI doGridding task, the WCS parameter "crota2=35" i.e. (180° - flyAngle) where flyAngle was set in the AOR to 145°. This produces a map of 13 x 7 pixels (see Fig. 5, right image).
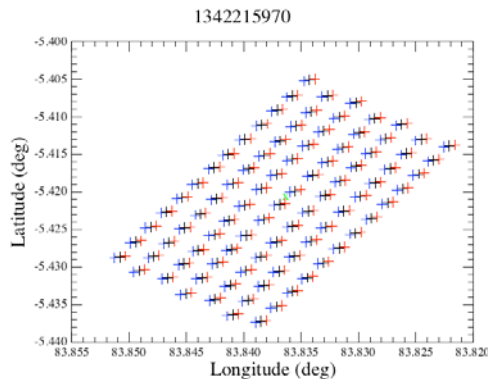

Figure 63: Mapping grid of the scanning direction for 1342215970 (Band 4b) with Red=H, Blue=V, and Black=Synthetic pointing. This grid matches the orientation of the cube before a rotation is applied (see Figure 64).
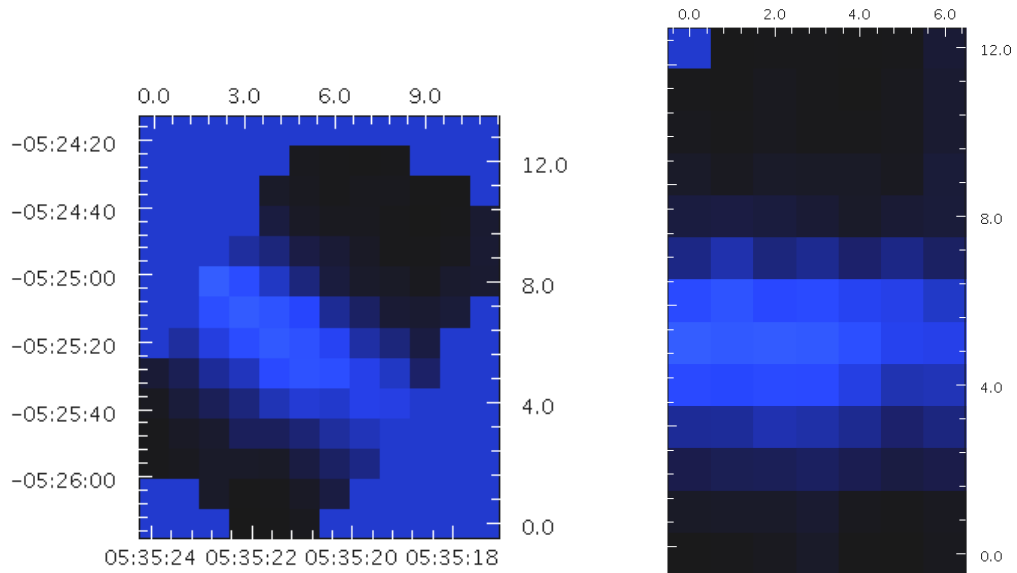
Figure 64: Cube channel image at 1101.31 GHz, before applying the rotation (left), and after applying a rotation of 35° (right) of WBS-H-LSB created with pixelSize 9" x 9" and a beam of 21".

The averaged cube spectrum for both H and V of WBS sub-band 3, where the water line is detected, yields practically no difference (see Figure 65).
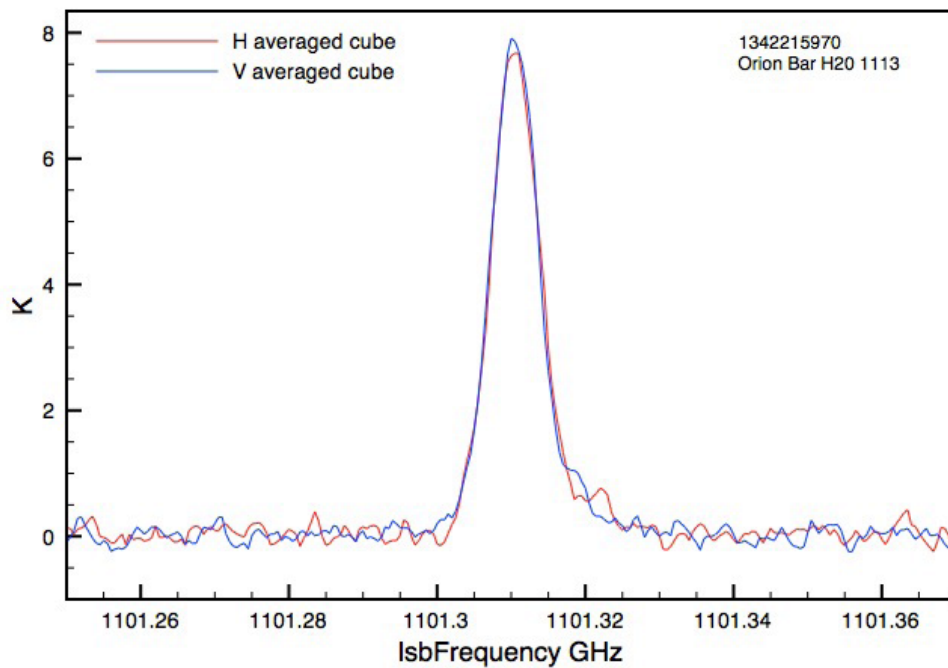

Figure 65: Cube averages of the H_2O line in H (red) and V (blue).

We compared the spectra extracted from a few individual pixels of both cubes. Table 12 gives values for the two brightest pixels ([H_1,V_1] and [H_2,V_2]). The offset of the RA and Dec between H and V for each pixels is small enough (between 0″.2 and 1″.5, over a beam of 21″) to allow for a direct measurement pixel by pixel between H and V.   An exact match of the RA and Dec between H and V is actually found near the junction of two pixels. From the flux profile of pixel [0.0,5.0] the brightest pixel, and of pixel [2.0,5.0], the second brightest pixel, we see that there is a ~6% difference between the H and the V flux values. But, when we look at the third pixel [5.0,7.0], which is fainter, we see a difference of almost 32% between H and V at peak value. See Figure 66.
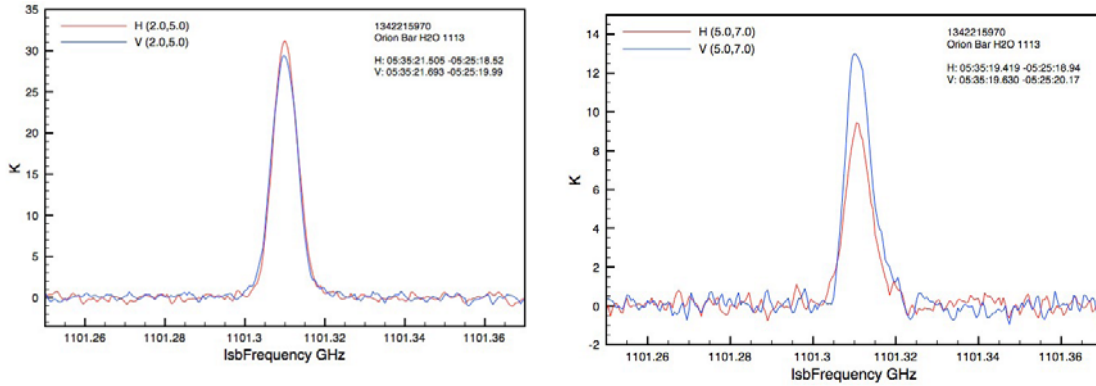

Figure 66: Flux profile for pixel [2.0,5.0] on the left, which is the second brightest pixel, showing an difference of flux levels between H and V of ~5% (same for the brightest pixel. On the right, the profiles of the fainter pixel at [5.0,7.0], showing a difference of ~32%.

Table 12: Values for the two brightest pixels, and a third fainter pixel in each of H and V for the bright line at 1101.31 GHz. Notice a large difference (31.6%) in the peak values between H and V for the fainter pixel (5.0,7.0) than for the two brightest pixels which are of the order of 5-6%.

H	Flux value (K) at peak	Pixel position	RA/Dec	RA/Dec offset H-V	Flux difference H-V
Pixel H_1	32.396	0.0,5.0	05:35:22.412 -05:25:08.77		
Pixel_H_2	31.239	2.0,5.0	05:35:21.505 -05:25:18.52		
Pixel_H_3	8.9112	5.0,7.0	05:35:19.419 -05:25:18.94		
V					
Pixel V_1	30.609	0.0,5.0	05:35:22.618 -05:25:09.54	-0″.206 -0″.77	1.787 (5.5 %)
Pixel V_2	29.351	2.0,5.0	05:35:21.693 -05:25:19.99	-0″.188 -1″.47	1.888 (6.0%)
Pixel V_3	13.024	5.0,7.0	05:35:19.630 -05:25:20.17	-0″.211 -1″.23	-4.1128 (31.6%)

![HiFi ICC SRON logo]

**HIFI Observing Modes
Performance Notes**

Doc.: ICC/2010-009
Date: 24/09/2011
Issue: Version 3.0

We can explain this difference in connection with the original Spectral Scan which also exhibited a ~30% difference between the ^{13}CO fluxes in H and V spectra. In the Spectral Scan data, the region where we find a large difference between H and V is near a region where there is an abrupt drop in source flux. The coordinates of this region (which is at the synthetic pointing position for the Spectral Scan) sits near the edge of a pixel in the OTF map, and if we examine more closely the 5 pixels surrounding that position (Figure 67), we see that apart from one pixel where the H/V difference is about 5%, the other pixels show a large variation of 15-29% in the H/V line fluxes.
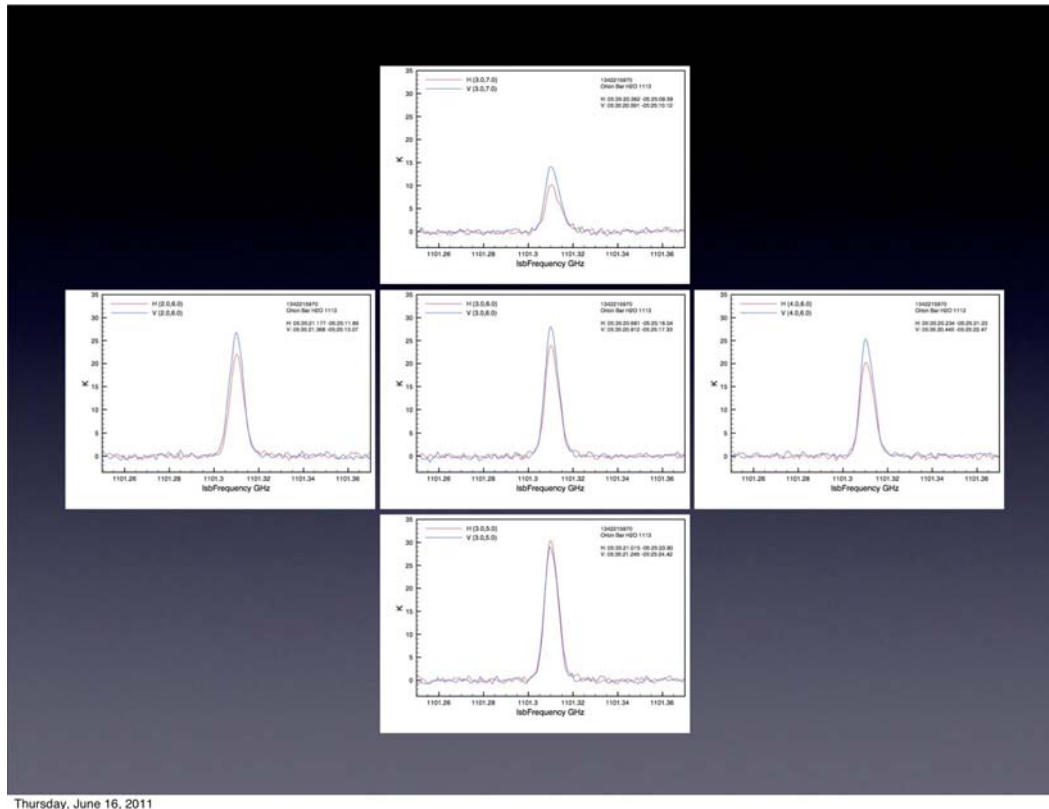

Figure 67: Mosaic of the 5 pixels surrounding the region 05:35:20.61 -05:25:14.0 (frequency 1101.31 GHz).

Although the optical misalignment of the two beams is relatively small, it could be that the variation in the fluxes seen near the region where there is an abrupt drop in the source flux is an indication that the H beam, being the first to lead in the scan direction, will be the first to register the drop in the sky intensity. Figure 67, helped by Figure 63, seems to support this scenario. Note that this also explains the large variation seen at pixel [5.0,7.0] (see Figure 66). If this scenario is the correct one, it would explain the large variation seen in the Spectral Scan caused by the two polarization beams not seeing the same part of the sky while the observation is carried out.

11.4 Summary and Conclusions

- Comparison of H and V profiles in compact sources show that the line profiles agree to within 7%, which is within current calibration uncertainties.

- An exception to this is NML Tau, which shows deviations of up to 30%
- Some of these discrepancies were found to be due to issues with the data such as poor line placement or scatter in data at Level 1.

- It is harder to disentangle the effects of extended emission and pointing offsets between the H and V beams, particularly in OTF maps where some zig-zag may be present. However, maps of highly structured sources (such as the Orion Bar) can aid in the analysis of fixed position observations where differences between H and V spectra have been observed. So far these investigations do not reveal any intrinsic calibration or stability problems between H and V sections of the instrument, but that the imbalances in cases examined so far, even as high as 30% or more, can be explained by source structure and the slight misalignment of the HIFI beams on the sky. As a consequence,
  - Artificial polarisation effects can be created due to the H and V beam offset in structured sources.
  - The User may wish to avoid averaging H and V spectra from separate cubes together, which will smear the spatial information that is provided in structured regions.

12. Mixer side-band gain response

12.1 Side-band gain ratio and line/continuum calibration

The current calibration of HIFI assumes that the mixer Side-Band gain Ratio (SBR) is equal to unity everywhere except in the lower end of band 2a (see Figure 68 – note that in terms of calibration parameter, a SBR of 1 translates into a value of 0.5, because the side-band gain ratio used in the HIFI calibration equation is normalized by the sum of the gains in the respective side-bands). The error on this approximation is of order 3-4% in Bands 1-2, 4-6% in bands 3-4, 11% in band 5, and 5-8% in bands 6-7 (see also Roelfsema et al. 2011 RD-1). Future refinements of the detailed gain response over the HIFI operational range are currently being worked on.
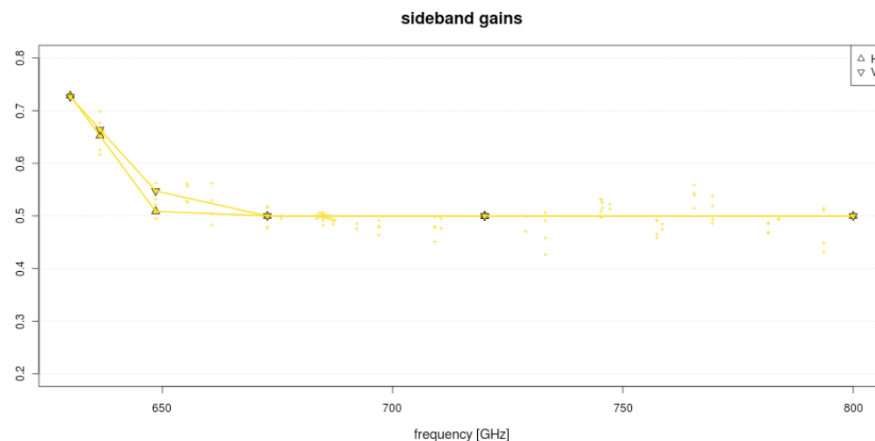

Figure 68: Overview of the SBR assumption in HIFI band 2a – it is assumed to be 0.5 (i.e. perfect side-band gain balance) in all other bands. The points corresponds to direct measurements of the SBR during the ground calibration campaign.

One important aspect about the SBR correction is that it applies to line intensity calibration, but not to the continuum. This means that when a non-unity SBR is applied, an offset in the continuum is introduced in the Level 2 products. Figure 69 illustrates this effect in the lower end of band 2a, where a sample of spectra from the respective Upper Side-Band and Lower Side-Band are over-plotted. When a unity SBR is applied, continuum levels from the USB and LSB match well, while the line intensities show large discrepancies - a direct indication of the non-balance respective side-band gains. When the non-unity SBR is applied, the continua no longer match, while the line intensities are in much better agreement, as is illustrated when bringing all baselines to a zero-level.

Users should therefore pay particular attention to the calibration of the continuum level of their observations. In single LO frequency AORs, the continuum can be recovered as the average of that in the respective LSB and USB spectra. For Spectral Scan, changes are being made in the HIPE Software (expected in HIPE 8) in order to force a unity SBR everywhere at the Level 2, and apply the known variation of the SBR in the deconvolution process to find the best Single-Side-Band solution.
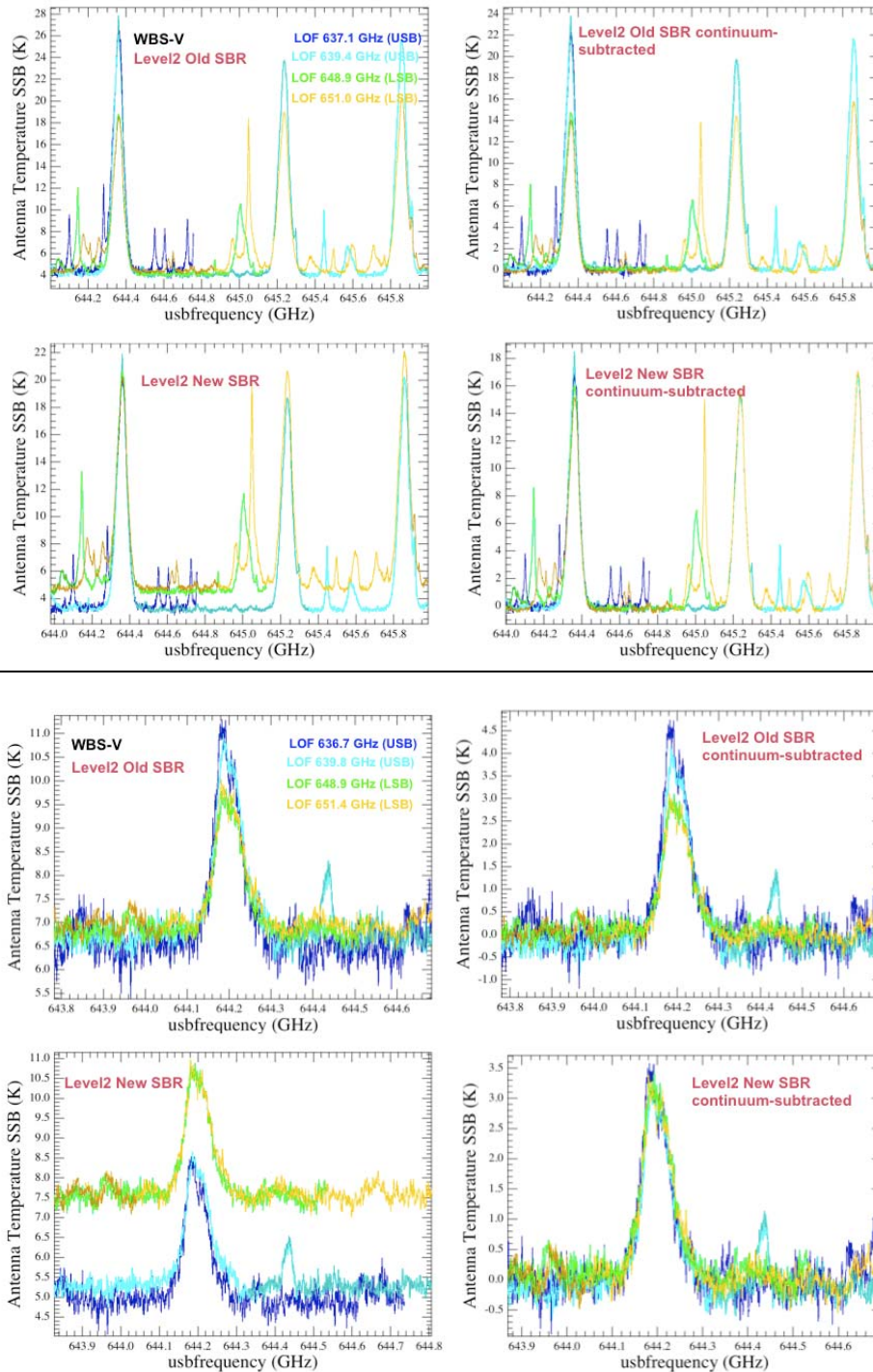
Figure 69: Illustration of the effect of the side-band gain ratio correction on line intensities and continuum at the lower end of band 2a. Examples are given for two different sources.

12.2 IF Spectrum Repeatability (Sideband Line Ratios)

Specific tests have been carried out in the laboratory and on-orbit since the first checkout phase and again during CoP-II and PV-2, to assess the repeatability of spectral lines occurring at different IF frequencies in both upper and lower sidebands.   On orbit these tests have been done so far in beam splitter Bands 1b, 2a, and 5a, and diplexer Band 4a, towards NGC7538 IRS 1 using the strong CO lines. The frequency was gradually changed so the line was stepped across the band to look for changes in intensity. Figure 70 shows how this looks in the Band 1b engineering test, with all 15 spectra of the same CO 5-4 line over-plotted in IF frequency in the upper sideband of the WBS-V. Figure 71 shows a similar example, taken from a different source using a standard Spectral Scan in 1b on the H_2O $1_{10} - 1_{01}$ 557 GHz line.

All of the tests were done in DBS mode. The line signal is typically 10-20K and noise less than 0.2K, resulting in a S/N ratio of over 100.
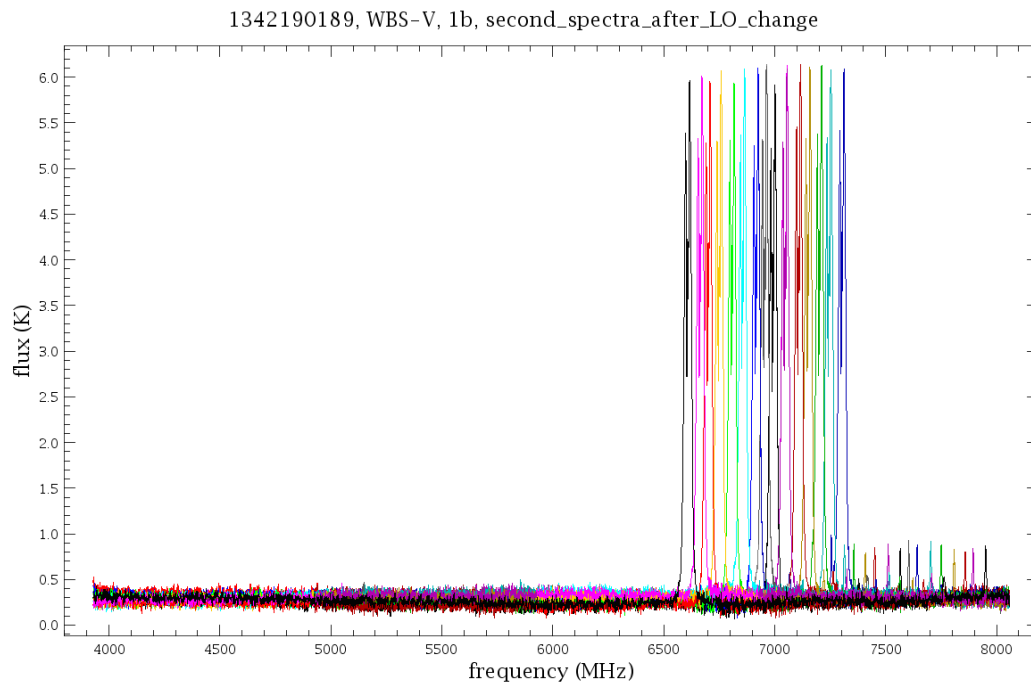
Figure 70: CO 5-4 with WBS-V, spaced across the upper sideband from an engineering Spectral Scan.
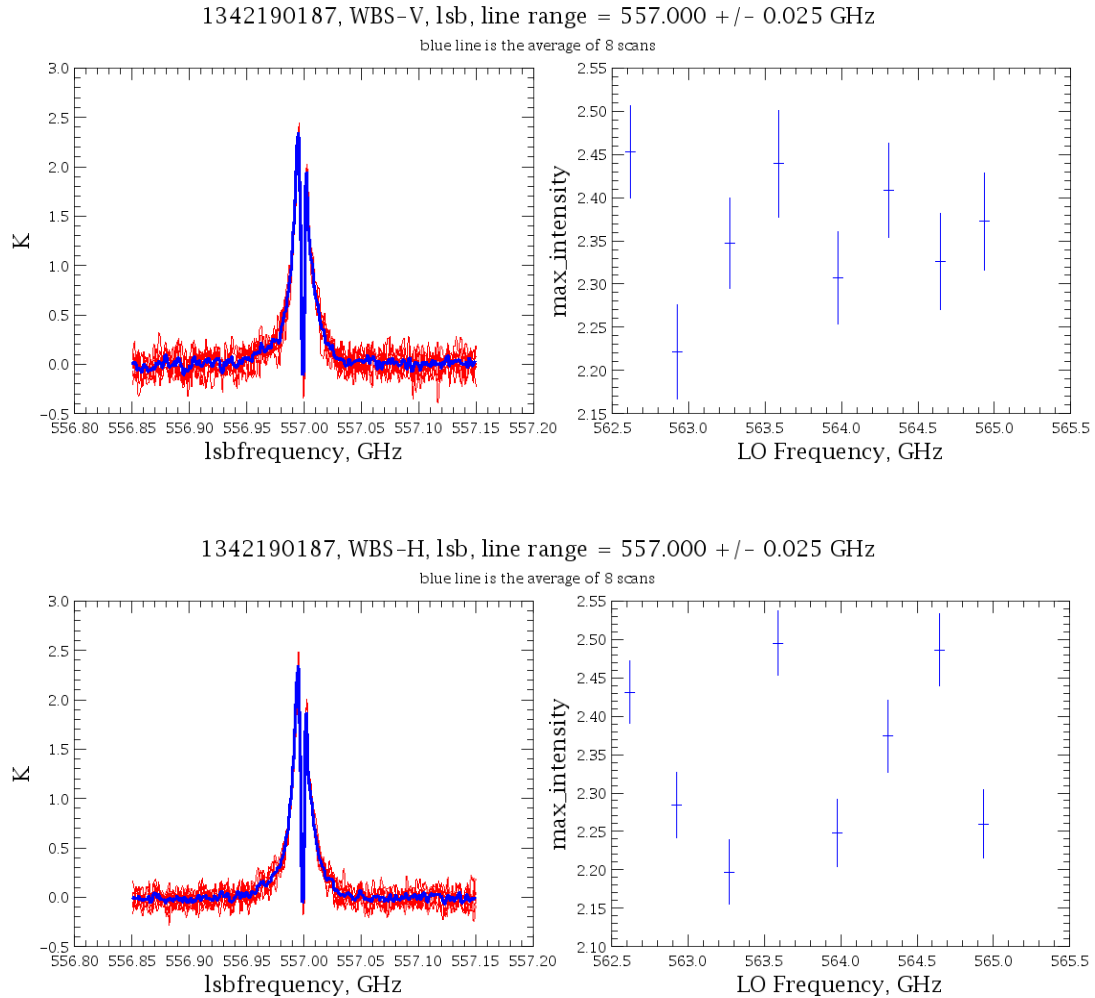
1342190187, WBS-V, lsb, line range = 557.000 +/- 0.025 GHz
blue line is the average of 8 scans

1342190187, WBS-H, lsb, line range = 557.000 +/- 0.025 GHz
blue line is the average of 8 scans

Figure 71: Measurements of the 557 GHz water line at 8 positions in the LSB in WBS-V (upper) and WBS-H (lower).

While the comparison between flight data and ground-based gas cell measurements is ongoing, the following conclusions are reached for the bands without diplexers:

- **Band 2a**: the integrated line intensities vary by less than 1% around the average value.

- **Band 5a**: there is a slight USB/LSB line strength difference (3%). This is true for both polarizations. The (H-V)/H intensity difference is also 3% on average; true for both sidebands. This could be due to pointing offsets between the polarizations.

- **Band 1b**: similar to Band 2a.

For **Band 4a**, the only diplexer band tested so far, the SBR test was carried out without retuning the diplexer, and then the same test was redone but with retuning. The conclusions are reached:

1. The observations *without* diplexer retuning show that in the unlikely event of a diplexer mistune, the diplexer window significantly affects calibration. At least some of this variation can be eliminated by recalibrating with the ratio of the noise levels at the frequency for which the diplexer is correctly tuned. This should not happen for normal observing.

2. The Standing Wave test showed no convincing effect -- the variation is less than \pm 2% and this slight variation does not show a 650MHz period like the diplexer standing wave.

3. With the diplexer retune, and only taking into account the scans preceding the sharp increase in noise level, the CO 9-8 line seen in the LSB is a few percent weaker than in the USB. It remains to be seen if this is a real SBR effect or rather due to the diplexer. All of the variations seen are greater than identical spectra affected only by random noise at the RMS noise level.

4. The V polarization is systematically stronger than the H but the line profiles are different (see Figure 72), suggesting that at least part of the difference is due to a pointing offset.

5. The RMS noise was much greater when the CO line was in the LSB (high LO frequency) and this was true for both polarizations.

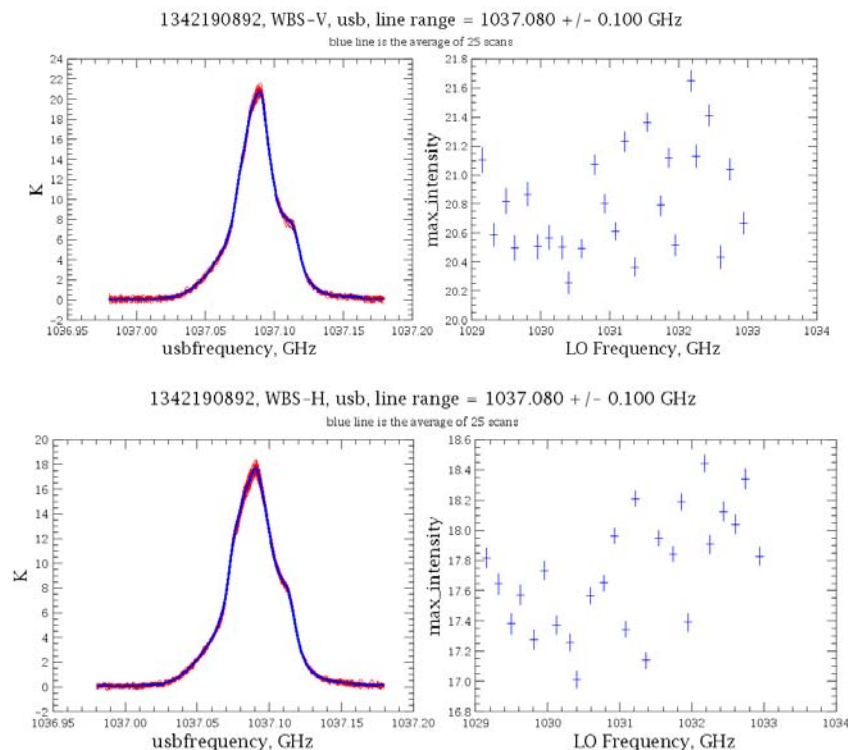A summary of these results is represented in Figure 73.

Figure 72: Measurements of the 1037 GHz CO 9-8 line at 25 positions in the USB in WBS-V (upper) and WBS-H (lower).
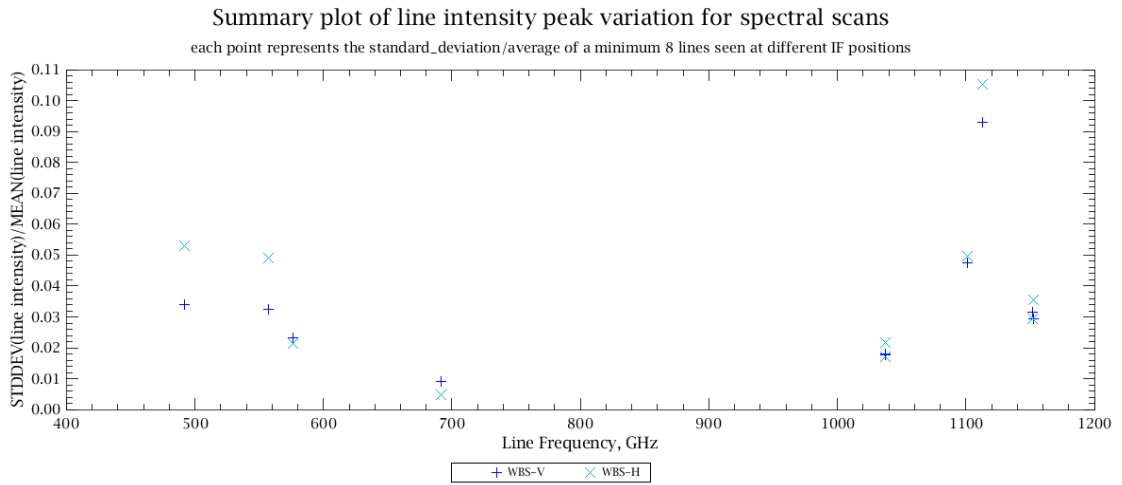
Figure 73: Peak intensity variation of spectral lines as measured at 8 or more positions in the IF, from PV-2 Spectral Scans.

13.   HIFI intensity calibration budget

This section is relegated to the HIFI Instrument and Calibration Web for the current status of calibration work and the error budget. As of the OT2 proposal submission deadline (September 2011), the following table summarizes the main sources of error to the HIFI intensity calibrations, adapted from the Instrument performance paper in A&A (RD-1).   Users are encouraged to check the HIFI Calibration page when new observations are obtained, http://herschel.esac.esa.int/twiki/bin/view/Public/HifiCalibrationWeb#HIFI_instrument_and_calibration for up to date knowledge on the calibration error budget and for related documentation.

Table 13: Relative calibration errors (percent) of the HIFI instrument (as of October 1, 2011).

Error source	HIFI mixer band			
	1 & 2	3 & 4	5	6& 7
Sideband ratio	3-4	4-6	4	5-8
Hot load coupling[1]	<1	<1	<2	<3
Cold load coupling[1]	<1	<1	<2	<3
Hot load temp.	<1	<1	<1	<1
Cold load temp.	<1	<1	<1	<1
Planetary model	<5	<5	<5	<5
Beam efficiency	<5	<5	<10	<5
Pointing[2]	<1	<3	<4	<8
Opt. standing waves	4	4	3	3

1. The coupling error in bands 6 & 7 is likely an overestimate and may include standing wave effects.

2. This relative intensity error is given for an Absolute Pointing Error (APE) of 2 arcsec for a single point observation of a point source. Uncertainties in the focal plane alignment of HIFI in the telescope are included in the beam efficiency error.

14. Acknowledgements

The special circumstances of HIFI's switch to redundant side operations and resuming with a compressed Performance Verification phase and accelerated Observing Mode release has been supported by not only the core group of HIFI Calibration Scientists and Instrument Engineers over the "long haul", but also the KP team apprentices who have been variously present at the HIFI ICC in the Fall of 2009 and during PV-2 starting end-January 2010, and also the HIFI software development team who have been available at all times.   AOT test planning has been done in consultation with the KP PIs coordinated by X. Tielens, Instrument P.I. F. Helmich, Project Manager P. Roelfsema, and with the Mission Scientist J. Cernicharo.   These persons should be acknowledged, as having directly supported the flight qualification of HIFI as a science instrument.

AOT/Uplink Engineering Team:
P. Morris (NHSC/Caltech), M. Olberg (SRON/Chalmers), V. Ossenkopf (U. Köln), C. Risacher (SRON), D. Teyssier (HSC/ESA).

Instrument Engineers and System Architects:
P. Dieleman (SRON), K. Edwards (SRON), W. Jellema (SRON), A. de Jonge (SRON), W. Laauwen (SRON), J. Pearson (JPL).

HIFI Calibration Scientists:
I. Avruch (Kapteyn/SRON), A. Boogert (NHSC/Caltech), C. Borys (NHSC/Caltech), J. Braine (U. Bordeaux), F. Herpin (U. Bordeaux), R. Higgins (U. Maynooth), S. Lord (NHSC/Caltech), T. Marston (HSC/ESA) C. McCoey (U. Waterloo), R. Moreno (Obs. Paris), M. Rengel (MPS), S. Beaulieu (U. Waterloo), M. Mueller (SRON).

HIFI Software Development Team:
R. Assendorp (SRON), B. Delforge (SRON), A. Hoac (NHSC/Caltech), D. Kester (SRON), A. Lorenzani (Obs. Acetri), M. Melchior (U. Appl. Sci. NW Switzerland),W. Salomons (SRON), B. Thomas (SRON), E. Sanchez (CSIC), R. Shipman (SRON), Y. Poelman (SRON), J. Xie (NHSC/Caltech), P. Zaal (SRON)

HIFI KP student/postdoc visitors:
E. DeBeck (U. Leuven), T. Bell (Caltech), N. Crockett (U. Michigan), P. Bjerkeli (Chalmers), P. Hily-Blant (Obs. Grenoble), M. Kama (U. Amsterdam), T. Kaminski (CAMK), B. Larsson (Obs. Stockholm), B. Lefloch (Obs. Grenoble), R. Lombaert (U. Leuven), M. de Luca (Obs. Paris), Z. Makai (U. Köln), M. Marseille (SRON), Z. Nagy (Kapteyn), Y. Okada (U. Köln), S. Pacheco (Obs. Grenoble), D. Rabois (U. Toulouse), Frank Schlöder (U. Köln), S. Wang (U. Michigan), M. van der Wiel (Kapteyn/SRON), M. Yabaki (U. Köln), U. Yildiz (U. Leiden)

HIFI KP PI Representatives to the ICC/AOT Team:
E. Caux (U. Toulouse), E. van Dishoek (U. Leiden), M. Gerin (Obs. Grenoble)

15. Appendix

15.1 dumpHIFIsiam.py

```python
from herschel.pointing.siam import SiamReader

import string
import math

mySIAM = "/your/path/to/nnnn_mmmm.SIAM"
# example: mySIAM = "/home/michael/HIFI/pointing/0068_0002.SIAM"

HifiApertures = (
    "H11_0", "H12_0", "H13_0", "H14_0", "H15_0", "H16_0", "H17_0", "H18_0",
    "H21_0", "H22_0", "H23_0", "H24_0", "H25_0", "H26_0", "H27_0", "H28_0",
    "H31_0", "H32_0", "H33_0", "H34_0", "H35_0", "H36_0", "H37_0", "H38_0",
    "H41_0", "H42_0", "H43_0", "H44_0", "H45_0", "H46_0", "H47_0", "H48_0",
    "H51_0", "H52_0", "H53_0", "H54_0", "H55_0", "H56_0", "H57_0", "H58_0",
    "H61_0", "H62_0", "H63_0", "H64_0", "H65_0", "H66_0", "H67_0", "H68_0",
    "H71_0", "H72_0", "H73_0", "H74_0", "H75_0", "H76_0", "H77_0", "H78_0")

csvfile = string.replace(mySIAM, ".SIAM", ".csv")
csv = open(csvfile, "w")

sr = SiamReader(mySIAM)
print sr.siamVersion
csv.write('"instrument","aperture","X","Y","Z"\n')

R2S = 3600.0*180.0/math.pi
for aper in HifiApertures:
    siam = sr.getSiam(aper)
    theta = siam.toEulerZYX().negate()
    x = theta.x
    y = theta.y
    z = theta.z
    if z < -math.pi:
        z = z+2.0*math.pi
    x = x*R2S
    y = y*R2S
    z = z*R2S
    csv.write('"HIFI","%s",%20.15e,%20.15e,%20.15e\n' % (aper, x, y, z))
    print "HIFI  %s %20.15e %20.15e %20.15e" %  (aper, x, y, z)

csv.close()
```

END OF DOCUMENT